The Geochemical Evolution of Groundwater and Surface Water in a Small Glaciated Basin Involving Effluents from Iron Mining: Hydrologic and Geochemical Constraints

By
Eric A. Roth

A Thesis

Submitted to
Michigan State University
in partial fulfillment of the requirements
for the degree of

Masters of Science

Department of Geological Sciences

1992

Abstract

The Geochemical Evolution of Groundwater and Surface Water in a Small Glaciated Basin Involving Effluents from Iron Mining: Hydrologic and Geochemical Constraints

By

Eric Allyn Roth

The impact of iron mining on the Sands Plain aquifer in Marquette County, Michigan allows for a unique opportunity to study the geochemical evolution of a groundwater-streamflow system in a small glaciated basin. Groundwater and surface water chemistry and numerical flow modeling techniques indicate that effluent water from mining operations affect surface water and groundwater in the northwestern portion of the study area. Groundwater and surface water indicate elevated concentrations of calcium, magnesium, sulfate, iron and manganese, which may result from dolomite and gypsum dissolution, and pyrite oxidation. Water chemistries observed in the northern portion of the study area indicate a shallow component of groundwater flow exists. Water chemistry in the southern portion of the study area results from feldspar, dolomite, and calcite dissolution and kaolinite precipitation, and has not been impacted by effluent water.

Acknowledgments

I would like thank my committee members Dr. David T. Long, Dr. Graham Larson, Dr. Mike Velbel, and Norm Grannemann for their guidance and support. I would like to thank again Dave for giving me a chance to work with him, and for the use of analytical equipment and materials in the Geochemistry Laboratory at Michigan State University. I would like to extend special thanks to Norm, not only for his insights in hydrology and flow modeling, but also for his generosity. I would also like to give my deep thanks to Jerry Sun whose help in groundwater sampling was immeasurable.

I would like to thank the faculty and staff at the Department Geological Sciences at Michigan State University, and co-workers at the U.S Geological Survey in Lansing. I would finally like to acknowledge the following companies and agencies that donated equipment and funds to this project: Keck instruments, U.S. Geological Survey, Michigan Basin Society, and Chevron Oil.

Table of Contents

	page
Abstract	ii
List of Tables	v
List of Figures	vi
1. Introduction	
A. Purpose and Scope	1
B. Previous Investigations	3
C. Setting	6
1. Historical Development of Water Resources in the Sands Plain Region	6
2. Topography	7
3. Geology of the Sands Plain Region	7
4. Hydrology of the Sands Plain Region	15
a. Surface Water Hydrology	15
b. Groundwater and Hydrogeologic Units	21
2. Hydrologic Simulation of the Sands Plain Region	
A. Introduction	22
B. Conceptual Model	23
C. Mathematical Basis	25
D. Numerical Model Design	26
E. Model Calibration	29
F. Sensitivity Analysis	32
G. Potentiometric Surface	32
H. MODPATH Simulations	34
1. Mathematical Basis	34
2. Flow System Analysis	36
I. Volumetric Water Budgets	41
J. Zone Budget	41

Table of Contents (cont'd)

	page
3. Groundwater and Surface Water Chemistry	
A. Methods	49
1. Groundwater Sampling	49
2. Sediment Collection	51
3. Field Analysis	51
4. Analytical Methods	52
a. Calcium and Magnesium	52
b. Sodium and Potassium	53
c. Chloride	53
d. Sulfate	53
e. Silica	53
f. Trace metals	54
5. Pre-Treatment for Clay Mineralogy Analysis	54
6. X-Ray Diffraction Analysis	55
B. Groundwater-Surface Water Chemistry	56
1. Groundwater Isogram Maps	56
2. Piper Diagrams	76
C. Minerals and Clay Minerals	81
D. Chemical Modeling with WATEQ4F	85
E. Groundwater-Streamflow System	95
4. Discussion	104
5. Conclusion	108
6. References	110
7. Appendix	
A. XRD Figures	119

List of Tables

		page
Table 1.	Stratigraphic Column	10
Table 2.	Measured and Simulated Head Values	30
Table 3.	Measured and Simulated Streamflow Values	31
Table 4.	Interflow rates between Adjacent Zones	44
Table 5.	Groundwater Chemistry for Major Species	58
Table 6.	Groundwater Chemistry for Trace Species	60
Table 7.	Surface Water Chemistry for Major Species	61
Table 8.	Surface Water Chemistry for Trace Species	62
Table 9.	Saturation Indices for Groundwater and Surface Water Samples with Respect to Selected Mineral Phases	87
Table 10.	Equilibrium and Enthalpy Values for Selected Minerals	93

List of Figures

	page
Figure 1. Site Location Map	2
Figure 2. Areal Distribution of Bedrock	9
Figure 3. Altitude of Bedrock Top	11
Figure 4. Areal Distribution of Glacial Deposits	13
Figure 5. Glacial Deposits Thickness	14
Figure 6. Drainage Basins	16
Figure 7. Flow Duration curve Cherry and Cedar	18
Figure 8. Flow Duration Big and Silver	19
Figure 9. Flow Duration Goose Lake Outlet	20
Figure 10. Grid	27
Figure 11. Potentiometric Surface	33
Figure 12. Backwards Particle Tracking from Well Locations	37
Figure 13. Forwards Particle Tracking from Well Locations	49
Figure 14. Backwards Particle Tracking from Stream Samples Sites	40
Figure 15. Zone budget	42
Figure 16. Groundwater and Surface Water Samples Site Locations	57
Figure 17. Isogram Total Dissolved Solids in mg/L	64
Figure 18. Isogram Calcium in mg/L	66
Figure 19. Isogram Magnesium in mg/L	67
Figure 20. Isogram Sodium + Potassium in mg/L	68
Figure 21. Isogram Bicarbonate in mg/L	69
Figure 22. Isogram Sulfate in mg/L	70
Figure 23. Isogram Chloride in mg/L	72
Figure 24. Isogram Barium ug/L	73
Figure 25. Isogram Manganese in ug/L	74
Figure 26. Isogram Strontium in ug/L	75
Figure 27. Groundwater Piper	77

page
Figure 28. Surface Water Piper 79
Figure 29. Historical Data Piper 80
Figure 30. Cedar Creek headwaters X-ray diffraction 82
Figure 31. Silver Creek headwater X-ray diffraction 83
Figure 32. Calcium versus Magnesium in mg/L 96
Figure 33. Calcium versus Sulfate in mg/L 96
Figure 34. Calcium versus Bicarbonate in mg/L 99
Figure 35. Calcium versus Total Dissolved Solids in mg/L 99
Figure 36. Calcium versus Strontium in mg/L 102
Figure 37. Sulfate versus Bicarbonate in mg/L 102
Figure 38. Chloride versus Sodium in mg/L 103

Introduction

Purpose and Scope

The Sands Plain aquifer of Marquette County in the Upper Peninsula of Michigan represents a freshwater resource that displays a similar sequence of glacial deposits observed in many parts of the Great Lakes basin. The impact of iron mining on this small glaciated basin allows for a unique opportunity to study the geochemical evolution of a groundwater-streamflow system, because of its well constrained hydrogeologic setting, geochemical variability and the existence of a historical data base (see Figure 1) (Wiitala, 1969; Grannemann, 1979, 1984; Doonan and VanAlstine, 1982). The first objective of this study is to characterize the hydrogeologic setting of the Sands Plain region, and the distribution and composition of shallow groundwater and stream water within it. The construction of a finite difference flow model for the Sands Plain area proposed by Grannemann (1984) and modified for this study is used to display the potentiometric surface, groundwater flow path direction and travel time information, as well as a quantitative volumetric water budget data. Water samples from twenty two wells and fifteen stream sites were taken over a large portion of the region to define the chemical composition of these waters. Water samples were analyzed for Ca, Mg, Na, K, HCO_3, SO_4, Cl, Si, Al, Ba, Cu, Fe(II), Fe (III), Mn, Sr, and Zn, and used in conjunction with precipitation chemistry (NADP/NTN, 1992), and Lake Superior water chemistry (Water-Resource Data, 1980).

The second objective of this study is to investigate the factors which control the distribution and composition of these dilute waters. This is accomplished by relating hydrologic flow modeling, water composition data, equilibrium modeling with aid of WATEQ4F (Ball, 1991), and clay mineralogy information by X-ray diffraction.

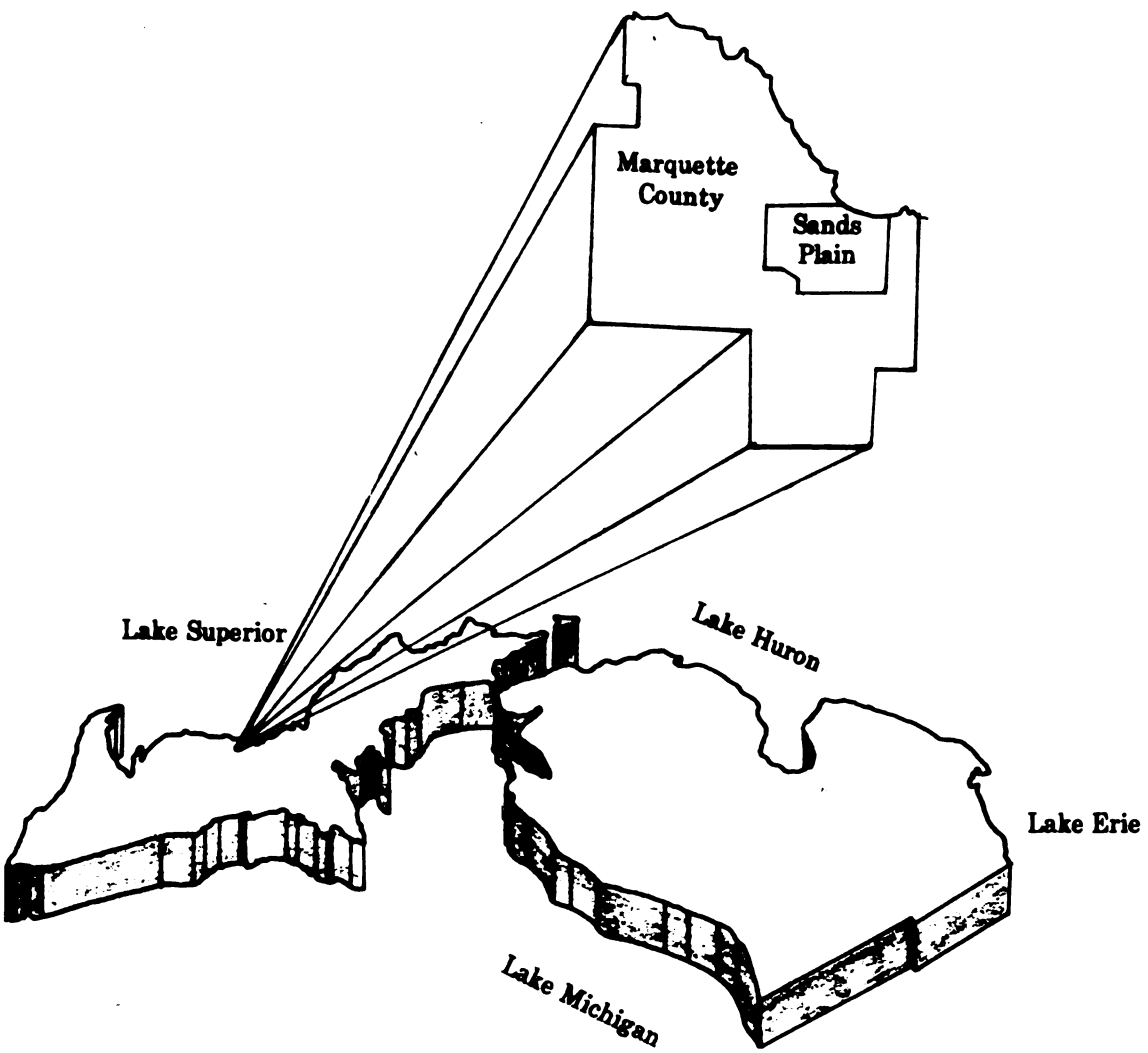
Marquette
County
Sands
Plain
Lake Superior
Lake Huron
Lake Erie
Lake Michigan

Figure 1

Previous Investigations

Combining physical flow information, aqueous chemistry, and mineralogic information is essential to the understanding of the chemical evolution of water in the hydrologic cycle. Previous studies that investigate aqueous chemistry and/or hydrogeologic models of small glaciated systems include: Newbury et al. (1971); Cherry (1972); Sklash et al. (1975); Grisak (1976); Desaulniers, Cherry and Fritz (1980); Wallick (1981); Bradbury (1984); Bottomley and Johnston (1986); Hendry et al. (1986); Anderson (1989); Ophori and Toth (1989); Kenoyer and Bowser (1992).

Early studies by Wallick (1981) and Cherry (1972) were able to characterize the chemical evolution of groundwater in glaciated drainage basins by observing the influence of water-rock interactions on major ions in groundwater. Wallick (1981) attributed a Ca-Mg-HCO_3 type water in the recharge area of a glacial-drift aquifer to the dissolution of calcite and dolomite by carbonic acid formed by atmospheric CO_2 in the soil zone. He also attributed a Ca-Mg-SO_4 type water to the dissolution and precipitation of gypsum in the presence of calcite and/or dolomite under conditions of partial saturation. In addition, he attributed a Na-HCO_3 type water from bedrock aquifers to result from the consumption of H^+ by the chemical weathering of feldspars and the dissolution of calcite and siderite minerals.

The degree to which alumino-silicate and clay minerals control groundwater chemistry is not well understood. Nordstrom et al. (1990) observe that mineral groups such as illites, smectites, and micas have never been shown to be the dominant control of water composition. This is reflected by a constant ion activity product (IAP) for a known silicate mineral composition in an aquifer where the water compositions of that aquifer varies (Nordstrom et al.,1990). The alteration of these minerals may still affect the composition of natural waters as observed by Kenoyer and Bowser (1992b), Jackson and Patterson (1982), and Garrels and Mackenzie (1969). Kenoyer and Bowser (1992) indicated that changes in groundwater chemistry along a flow path in a glacial drift aquifer which lacked carbonate minerals could be explained through the

dissolution of feldspars and clay minerals with the aid of the reaction-path model PHREEQE (Parkhurst, Thorstenson and Plummer, 1980).

Velocity and direction of groundwater flow are important factors in controlling the pattern of chemical evolution of natural waters, because they determine the sequence and duration of spatially distributed chemical and biologic processes (Schwartz and Domenico, 1973). Flow modeling requires determination of hydraulic parameters and boundary conditions, and the use of calibration techniques. Anderson (1989) proposed methods to adapt glacial and glacialfluvial sedimentological facies models for conceptualizing large scale hydrogeologic trends and delineating hydraulic conductivity for use in numerical models.

Oxidation and reduction reactions may also have an important role in dictating water chemistry in glaciated systems. Hendry et al. (1986) indicated that high sulfate concentrations in fractured weathered till in Alberta was mainly due the oxidation of organic sulfur by bacteria, along with the dissolution of minor amounts of sulfate-rich bedrock materials. Hendry (1986) was able disprove the hypothesis of glacial-load squeezing of sulfate-rich brines proposed by Cherry (1972) for the origin of sulfate-rich waters through the use of $\partial^{18}O$ and $\partial^{34}S$ data, and through geochemical modeling with aid of PHREEQE (Parkhurst, Thorstenson and Plummer, 1980). Hendry et al. concluded that concentrations of Ca^{+2} and Na^{+} were due to cation-exchange and gypsum precipitation, and that these processes were in turn governed by SO_4^{-2} concentration and charge balance of the solution.

Stable and radioactive isotopes with major and trace groundwater species have been used effectively in delineating zones of recharge and discharge, as well as the effects of mixing between two or more water bodies. The age and origin of groundwater and hydraulic characteristics and porosity of nonfractured clayey till in the St. Clairs Basin, Ontario was determined by Desaulnier et al. (1980). The groundwater of this region was characterized by a fresh water source and displayed no evaporation as indicated by the meteoric water line plot of $\partial^{18}O$ versus $\partial^{2}H$. Groundwater

movement and age were derived by $\partial^{18}O$ and Cl^- relationships, and tritium and ^{14}C water content, respectively.

The interaction between groundwater and streamflow in glaciated systems is described by Newbury et al. (1969), Pinder and Jones (1969), and Sklash et al. (1975, 1979) . The water carried by streamflow at a given instant consists of three components: direct runoff, interflow and baseflow. The relative proportions of these components largely determine the composition of streamflow (Stumm and Morgan, 1981). The concentration of dissolved solids in each is influenced in turn by the interactions of precipitation with minerals and vegetation, and by evapotranspiration.

The contributions of the groundwater component to the total streamflow have been approached by means of graphical separation of hydrographs as seen in Chow (1964). This method of separation is considered to be some what arbitrary. Pinder and Jones (1969) and Newbury et al. (1969) used groundwater chemistry to investigate the variations in composition and to determined the groundwater component of streamflow in small glaciated basins in Nova Scotia, and in Manitoba, Ontario, respectively. Both of these studies found a much higher contribution to streamflow by groundwater (over 90%) during storm events than previously calculated by stream hydrograph separation. Newbury et al. (1969) indicated that baseflow contributions to streams could be separated into transient and long-term groundwater types during a storm event.

Sklash (1975, 1979) refined the use of water chemistry in delineating groundwater contributions to streamflow in a glaciated system with the aid of ^{18}O isotopes. The use of these techniques offer advantages over those of Pinder and Jones (1969) and Newburry et al. (1969) because the content of ^{18}O isotopes is considered to be a conservative property and is not affected by chemical or biological reactions in water. The content of oxygen-18 in water can only be altered by the mixing of two or more isotopically different waters. A disadvantage to this method of streamflow separation occurs when the isotopic signature of both groundwater and surface water do not differ significantly from one another.

Historical development of water resources in Sands Plain

As the name suggests the Sands Plain is a fairly flat lying sandy plain, but the area received its name from Jacob Sands who settled in the Marquette County in 1850's. The development of natural resources in the Marquette County began with the discovery of iron ore near Lake Teal in 1884 by W.A. Burt while surveying and mapping the region (Wiitala, 1967). By the year 1886 mining for high grade ore deposits had started at the Jackson mine near Negaunee. Mining production surged in this area until the early 1930's, and then declined as high grade ore deposits were exhausted. In the early 1950's mining production resurged owing to the development of new beneficiation processes to concentrate low grade ores deposits, and because of the development of new mining techniques.

In 1977 iron mining in Marquette County produced almost 20 percent of iron ore in the United States (Grannemann, 1979). Two mines are currently (1992) operating. These are the Empire and the Tilden mines which lie to the west of the Sands Plain region.

Water is an essential resource to the iron ore industry. In 1965 the mining industry consumed over 31.5 million gallons of water per day (Wiitala, 1967). The mining of iron ore itself places only slight demands upon water resources. Beneficiation and pelletization processes place larger demands on water resources. Local streams and lakes are targeted for these processes because of their accessibility and low operational pumping cost. Water is used primarily in these processes to aid in the grinding of ore rock material for iron ore concentration, and as a medium for transporting iron ore throughout plant facilities (Wiitala, 1967). Waste rock from concentration processes is made into a slurry and transported to large settling basins. These large basins are composed of a series of smaller basins in which the effluent is continually ponded. Solids contained in the effluent are allowed to settle out of suspension over time. Clay materials are flocculated out of solution by the addition of Alum, an aluminium potassium sulfate clarifier. Excess water used in the clarifying process is

finally discharged into streams. Wiitala (1967) indicates that the overall usage of water in the clarifier process is high, but the actual consumption of water is low. Effluent is presently being discharged by the Empire mine to Warner and Schewietezer Creeks and by the Tilden mine to Goose Lake and Goose Lake Outlet.

Other natural resources developed in Marquette County include sand, gravel and dolomite, along with the production of lumber for pulpwood. Water resources are utilized by these industries, as well as for the generation of hydroelectric power and reservoir storage.

Topography

The Sands Plain region of lower Marquette county has an area of approximately 40 square miles. The western section of the study area is composed of hills and ridges of the Marquette Iron Range with an average elevation of 1,500 feet above sea level. The Marquette Iron Range (Wewe hills) lying in the western portion of the study area forms a distinct topographic high. The highest point in Marquette county is Summit Mountain 3 miles south of Negaunee. The west central section is relatively flat-lying with a mean elevation of 1,220 feet. The eastern section of the study area is composed of northwest trending moraines that display a hummocky topography. The elevation of this area decreases steadily to the east from 1200 feet to less than 700 feet.

Geology of Sands Plain area

The Marquette Iron range is underlain by Precambrian gneiss and middle Precambrian metasedimentary and metaintrusive rocks which are located in the western portion of the study area (see Figure 2). A summary of the lithologic units in the study are presented in Table 1. The major structural/stratigraphic features of the area are: 1) The Marquette synclinorium, which trends and plunges to the west and consists of the Marquette Supergroup (middle Precambrian) (Gair, 1975); 2) The Palmer basin which borders the synclinorium to the south (Gair, 1975); 3) The Palmer fault which is associated with the Marquette synclinorium, and

bounds the Palmer basin to the north (Gair, 1975); and 4) Two major and several minor buried valleys in the Sands Plain area which were carved by streams and glacial ice activity (Huges, 1978) (see Figure 3). One major buried valley trends to the northeast towards Lake Superior paralleling the Palmer fault. The second buried valley trends to northeast following Big Creek (Grannemann, 1984).

Lower Precambrian rocks of this area are comprised of the Mona Schist and the Compeau Creek Gneiss. The Mona Schist is composed of massive mafic metavolcanics and greenstones and is intruded by the Compeau Creek Gneiss (Gair and Thaden, 1968).

Unconformably overlying the Compeau Creek Gneiss is the Marquette Supergroup which is composed of the Chocolay group, Menominee group, and Baraga group, respectively. Formations of the Chocolay group consist of the Enchantment Lake Formation, the Mesnard Quartzite, the Kona Dolomite, and the Wewe Slate. The Enchantment Lake Formation is composed of a basal conglomerate and fine grained graywacke. The Kona dolomite is composed of a thinly bedded dolomite and quartzose dolomite, and containing copper bearing minerals (Gair, 1968); (Grannemann, 1984).

The Menominee group is separated from the Chocolay group by an unconformity, and consists of the Goodrich Quartzite, Ajibik Quartzite, Siamo Slate, and the Negaunee Iron Formation. Negaunee Iron Formation is composed of siderite, hematite, magnetite, pyrite, chert, K-feldspar, quartz and chlorite, and varies in mineralogy and mineral composition (Gair, 1975).

To the east of the Marquette Supergroup is the Jacobsville Sandstone which is late Precambrian. The Jacobsville is a reddish to light gray lenticular sandstone composed of quartz and variable amounts of feldspar, and is intercalated with gray conglomerate and reddish shale (Gair and Thaden, 1968).

Proterozoic deposits are in turn overlain by Pleistocene glacial deposits which cover most of the Sands Plain area (see Figure 4). The glacial history of the Sands Plain area has been described by Hughes (1978), and is briefly summarized: During the

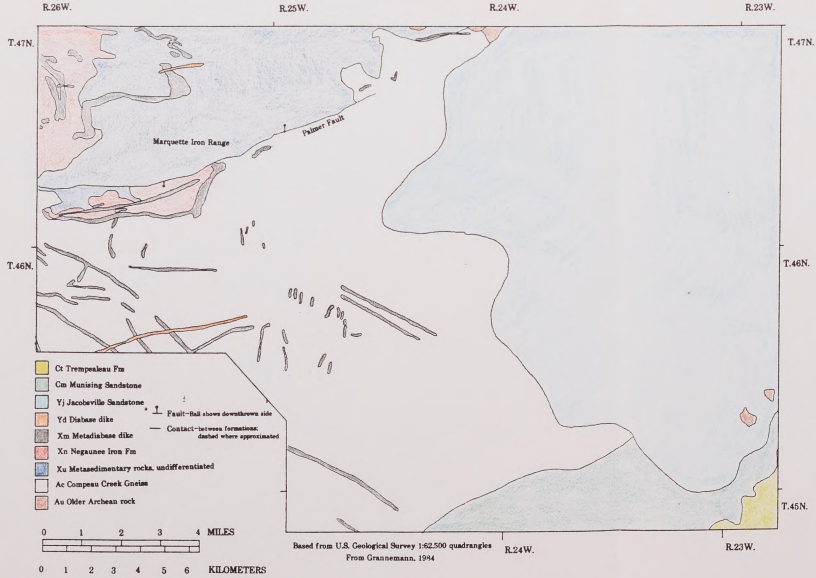

Figure 2 Areal Distribution of Bedrock

Table 1 Stratigraphic Column

Age				Geologic Unit	Lithology
Phanerozoic	Cenozoic	Quaternary	Pleistocene	Glacial deposits; till outwash and drainage deposits, and lacustrine deposits	Till is a poorly sorted, nonstratified mixture of sand, silt, clay, gravel, and boulders. Outwash and drainage channel deposits are composed of well-sorted, stratified sand and gravel with some silt. Lacustrine deposits are stratified mixtures of sand, silt, and clay with some gravel. Maximum known thickness of glacial deposits in the study area is 459 feet.
	Paleozoic	Cambrian	Late	Trempealeau Formation	Dolomitic limestone. Maximum thickness is about 300 feet.
				Munising Sandstone	Unit consist of a basal conglomerate overlain by a well-sorted, medium-grained competent sandstone and an upper poorly sorted, friable sandstone. Maximum thickness is about 100 feet.
Proterozoic	Middle			Jacobsville Sandstone	A mottled red or reddish-brown feldspatic sandstone containing lenses of red or gray conglomerate and some red shale. Four lithologic units are recognized: a basal conglomerate, a lenticular sandstone, a massive sandstone, and an upper red siltstone. Thickness varies from 1 to 100 feet.
				Intrusive rock	Mostly diabase dikes. Massive, dark gray, medium to fine grained; in places extensively argillized.
	Early			Metamorphosed dikes and sills	Mostly metadiabase dikes. Ranges from thin, fine-grained intrusions that may be greatly altered to thick, coarse grained intrusions that are relatively resistant to alteration; variable in appearance and composition.
				Negaunee Iron Formation	Iron rich metasedimentary rock in places extensively oxidized. Near Palmer, thickness ranges from 450 to 1,300 feet.
				Metasedimentary rocks, undifferentiated	Includes Goodrich Quartzite, Siamo Slate, Ajibik Quartzite, Wewe Slate, Kona Dolomite, Mesnard Quartzite, and Enchantment Lake Formation.
Archean				Compeau Creek Gneiss	Mostly gneiss composed of lightly colored, quartzite feldspar with some pegmatite, and locally, some layered rock.
				Older Archean rocks	Mostly medium grained chlorite-quartz-muscovite schist, quartz-plagioclase-chlorite schist, and actinolite schist cut by thin dikes.

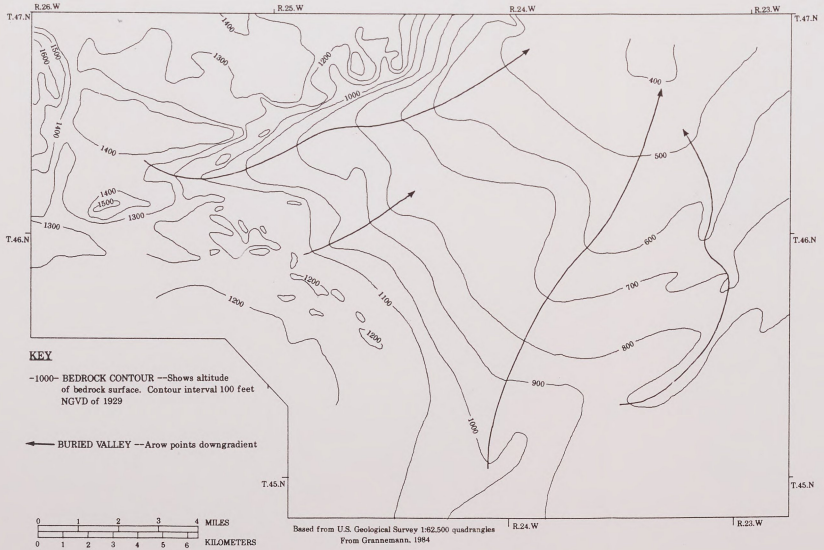

Figure 3 Altitude of Bedrock Surface

last
valle
adva
for t
Mora
depo
silt,
Marq
comp
of cl
(Gra
lobe
melt
to m
Tran
Mora
trans
depo

seco
depo
melt
rece
secti
sand
depo
burie

last Wisconsinan stage, ice advanced from the northeast along valleys covering a large portion of the Sands Plain area with ice. Ice advancement was hindered by elevation and resistant rock allowing for the formation of a till ridge known as the Outer Marquette Moraine. The Outer Marquette Moraine is composed of basal till deposits containing a mixed assortment of boulders, gravel, sand, silt, and clay. Deposits both underlying and to the rear of the Outer Marquette Moraine are composed of ablation till. Abalation till is composed of coarse grained to fine grained sand with lesser amounts of clay (approximately 11%) and is roughly 175 feet thick (Grannemann, 1984). Outwash is deposited in front of this morainal lobe to the south and to the west by stream systems associated with melt water. These outwash deposits are composed mainly of coarse to medium sand and gravel and range from 0 to 150 feet in thickness. Transitional till deposits also occur between the Outer Marquette Moraine and outwash deposits. These deposits represent the transition between unstratified ablation till and stratified outwash deposits (Grannemann, 1984).

Glacial ice readvancement from the northeast generated a second ridge of till, the Inner Marquette Moraine. Outwash was again deposited in a narrow plain between the inner and outer moraines by melt water. Ancestral lakes produced during the final glacial ice recession deposited lacustrine sediments in the northeastern section of the study area. Lacustrine deposits consist of silt, fine sand and clay (up to 17%) (Grannemann, 1984). In total, glacial deposits range roughly from 0 to 450 ft, and are thickest along buried valleys as observed in Figure 5.

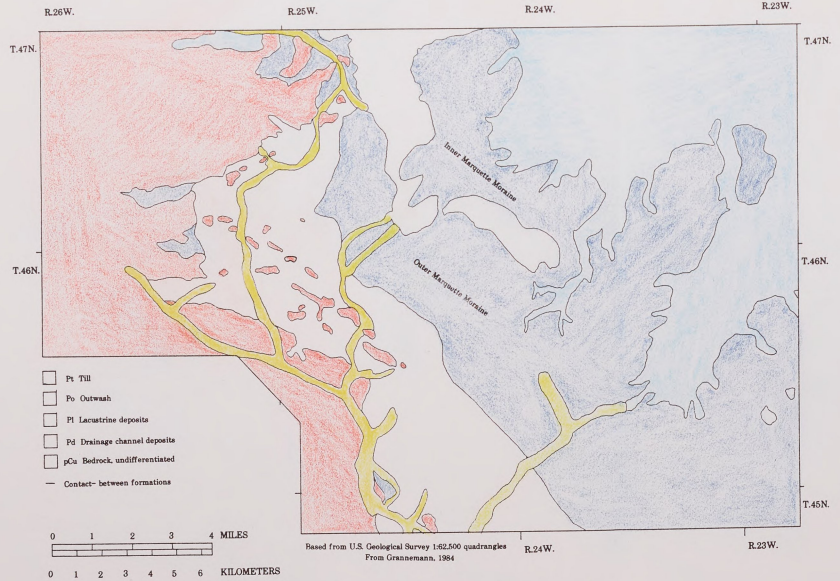

Figure 4 Areal Distribution of Glacial Deposits

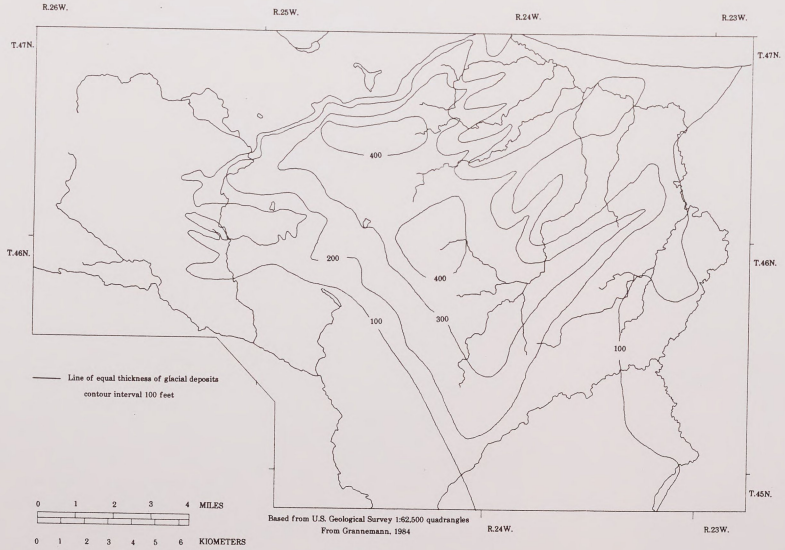

Figure 5 Glacial Deposits Thickness

Hyd

prec
grou
prim
the
Esca

Surf

Cho
Cho
disc
with
bec

Che
the
Cre
the
dir
pov
are
Sch
are

Sa
pre
dis
we
ov
are

Hydrology of the Sands Plain area

Water in the Sands Plain area is derived almost exclusively by precipitation, which is stored temporarily in streams, lakes and groundwater (Grannemann, 1984). The Sands Plain area is drained primarily by the Chocolay River basin. This basin is surrounded to the north by the Carp River basin, and to the south and west by the Escanaba River basin (see Figure 6).

Surface Water

The Sands Plain area contains three major rivers, the Chocolay, the Carp, and the East Branch Escanaba. The Carp and the Chocolay Rivers flow eastward and northeastward, respectively, and discharge to Lake Superior. The East Branch Escanaba River joins with the Middle Branch Escanaba River at the town of Gwin, to become the Escanaba River which flows south into Lake Michigan.

Tributaries of the Chocolay River are Big Creek, Silver Creek, Cherry Creek, and Cedar Creek. Headwaters of Big Creek originate in the Outer Marquette Moraine. Headwaters of Silver, Cherry and Cedar Creeks originate from springs in the outwash plain associated with the Inner Marquette Moraine (Grannemann, 1984). The Carp River directly feeds Deer Lake Reservoir and is utilized for hydroelectric power near Harvey. Tributaries of the East Branch Escanaba River are Warner Creek, Goose Lake Outlet, Powell Lake Outlet, and Schweitzer Creek. Goose Lake Outlet and its tributaries drain the area surrounding Gribben tailings basin.

Since precipitation is the main source of recharge for the Sands Plain area, seasonal variations in rate and volume of precipitation due to climatic changes have marked effects on stream discharge. Grannemann (1984) indicates that the Chocolay River as well as Cherry and Cedar Creek have only slight stage fluctuations over one seasonal cycle. Small stage fluctuations in these streams are attributed to highly permeable stream beds, and a relatively

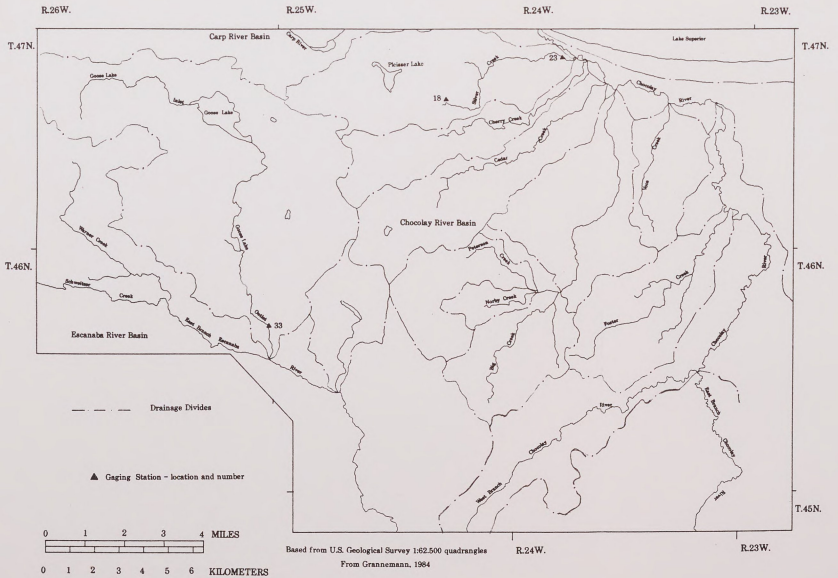

Figure 6 Drainage Divides

constant baseflow influx. This can be observed in the flow duration curve Figure 7, where the recurrence interval of equal stream discharge in one annual cycle is plotted versus discharge in cubic feet for Cherry Creek. The relatively flat slope of this curve indicates a steady baseflow component for Cherry Creek. This figure can also be used as an indicator of Cherry Creek's low-flow capacity at approximately the 90 percentile level. High flow capacity volumes indicated at the 10 and 25 percentiles for the Cherry Creek duration curve are only slightly greater than low flow capacity volumes at the 90 percentile, suggesting that runoff during flood intervals is rapidly dissipated.

Big Creek and Silver Creek have greater seasonal variability in flow than Cedar and Cherry Creeks. Variability in flow for Big Creek and Silver Creek is due to higher amounts of silt and clay in outwash or till material making up the streambed which reduce the rate of infiltration by precipitation and promotes greater stream discharge during storm events. This can be observed in the flow duration curve for Big Creek (Figure 8). The relatively steep slope of this curve indicates the creek has a higher degree of variability due to the larger component of runoff. High flow capacity volumes indicated at the 10 and 25 percentiles for the Big Creek duration curve are only slightly greater then low flow capacity volumes at the 90 percentile, suggesting once again that runoff during flood intervals is rapidly dissipated. Goose Lake Outlet has a similar seasonal variability as observed for Big and Silver Creek, but has a much higher rate of discharge (see Figure 9).

As a result of the nearly constant baseflow influx into Big Creek, Cherry Creek and Cedar Creek, discharge rates increase down stream (Grannemann, 1984). Not all streams in the Sands Plain region are effluent. Grannemann (1984) indicates that Silver Creek loses water to groundwater from gaging stations 18 to 23 downstream at rates that ranging from 0.1 to 1.2 cubic feet/second. Goose Lake Outlet loses approximately 10.3 cubic feet/second in a three-mile reach from Goose Lake to gaging site 33 (see Figure 6) (Wiitala, 1967); (Grannemann, 1984).

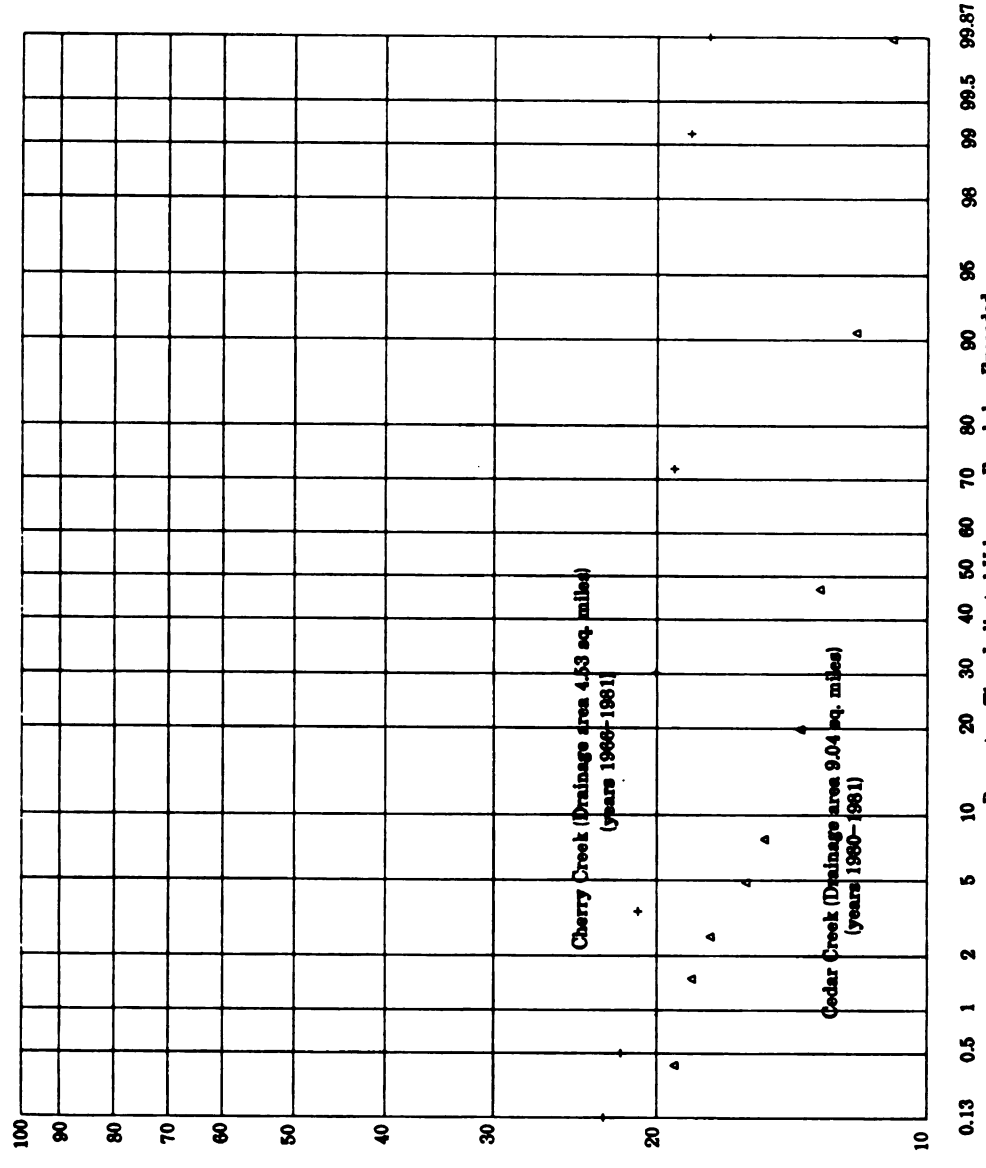

Figure 7 Stream Flow Duration Curves for Cherry and Cedar Creeks

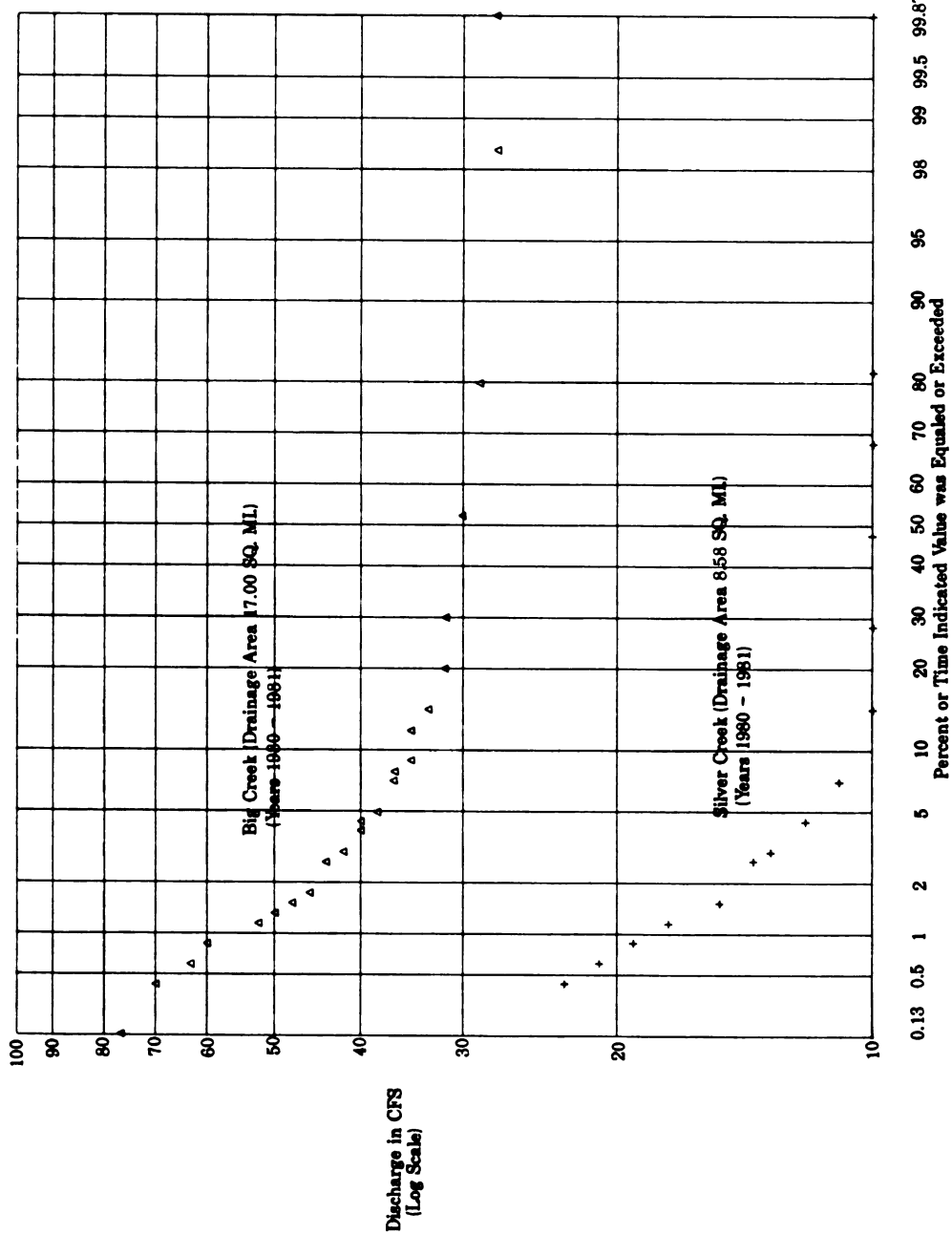

Figure 8 Stream Flow Duration Curves for Big and Silver Creeks

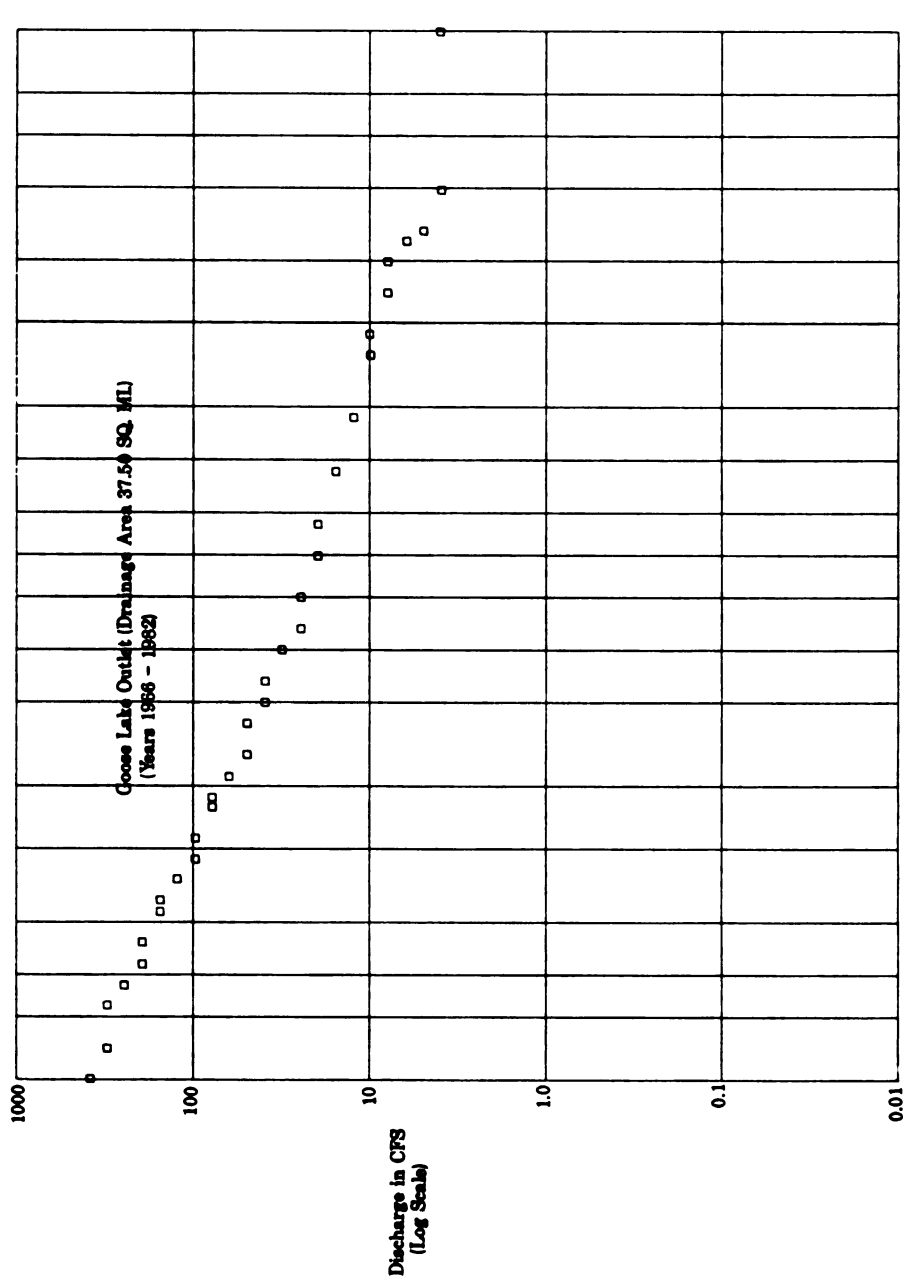

Figure 9 Stream Flow Duration Curves for Goose Lake Outlet

Groundwater

The movement and storage of groundwater in the lower Precambrian igneous and metasedimentary units are considered to be minimal compared to those of Pleistocene glacial deposits in the Sands Plain area. Hydrologic characteristics of igneous and metasedimentary units depend almost entirely on the fractures and joints in the rock (Grannemann, 1979). Upper Precambrian Jacobsville Sandstone, which covers the eastern portion of Sands Plain area, is also considered to be a poor aquifer; hydraulic conductivity values are on the order of 1 foot/day (Doonan and Van Alstine, 1982). The Munising Sandstone and the Tremaeleau Formation have higher hydraulic conductivities (on the order of 8 to 10 feet/day), but are not areally extensive (Grannemann, 1979). Bedrock units composed of low permeability materials bound the Sands Plain area to the north and west creating the basin-like structure which has an outlet towards Lake Superior.

Glacial deposits lying in this basin-like structure make up the primary aquifer material. These deposits have hydraulic conductivity (K) values ranging from 30 to 180 feet/day (Grannemann, 1984). Hydraulic conductivity values were determined by various pumping tests throughout the Sands Plain area by Wiitala (1967). Storage coefficients (S) determined by pumping tests ranged from 0.01 to 0.0001. This range in storage coefficients indicates that the Sands Plain aquifer is mainly unconfined, but may be locally confined or semiconfined in morainal areas with abundant amounts of clay and/or silt.

Groundwater contained in glacial deposits receives minimal interbasin flow from the Carp River Basin and is bounded to the south by the Silver Lead Creek and Chocolay River drainage divide. Groundwater is recharged directly by precipitation, and by a three mile stretch along Goose Lake Outlet. Groundwater is discharged to creeks and lakes contained in the Sands Plain area and to Lake Superior. Thus the hydrologic conditions of the Sands Plain area indicates a fairly isolated system which is well constrained, and thus ideal for this study.

Hydrologic Simulation of the Sands Plain Region

Sands Plain Model

A numerical model simulating steady-state hydrologic conditions in the Sands Plain area was developed to quantify water inflows and outflows, to test hypotheses involving stream and aquifer interactions, and to generate flow path direction and travel time information to help interpret concentration distribution for dissolved constituents. The Sands Plain numerical models integrates broad conceptual ideas about the aquifer's hydraulics with geologic and hydrologic data established by field measurement and observations. Aquifer characteristics and concepts are then discretized in time and space and entered into governing flow equations to which computer solution techniques are applied.

The numerical model used for the Sands Plain area is based on a previous model developed and calibrated by Grannemann (1984). The Sands Plain model presented by Grannemann (1984) was used to investigate hydrologic and geochemical effects of the Gribben Tailings Basin and hypothetical tailings basins to the Sands Plain aquifer. Modifications made to this model were primarily in updating its capability to graphically display input parameters, the potentiometric surface, and cell-by-cell flow data generated by the model. Only minor changes were made to initial input data. Post-processing techniques such as particle tracking and zone budget analysis were also linked to the Sands Plain model.

Conceptual Model

A conceptual model of the Sands Plain aquifer system is based on the geologic setting, and hydrologic parameters discussed previously. Basic assumptions of the conceptual flow model include boundary conditions, hydrologic properties, and stresses to the system which are summarized below:

1. Precambrian deposits composed of igneous and metamorphic rock types are considered to have poor conductivities for flow and little to no storage capacity, although various degrees of fracturing may occur in them. Precambrian and Paleozoic sandstones are considered to have low conductivities and/or are areally insignificant to the modeled study area.
2. Rock types ascribing the hydrologic characteristics stated above are assigned a Type 2 impermeable no-flow boundary condition. A Type 2 boundary (Neumann type) assumes that flux across the impermeable boundary is negligible (McDonald and Harbaugh, 1988; Kinzelbach, 1986). This assumption is justified by hydraulic conductivities values that are two orders of magnitude lower for these rock units than for that of the modeled system (Anderson and Woessner, 1991). Type 2 boundaries are assigned to bedrock units underlying the Sands Plain glacial package and to the Marquette Iron Range lying to the northwest.
3. A Type 1 prescribed head boundary is assigned to Lake Superior in the northeast section of the study area, to the West Branch of the Chocolay River, and to the Chocolay River in the south, south eastern section of the modeled area. A Type 1 boundary (Dirichlet type) specifies a constant head (equipotential line) and is necessary to guarantee the uniqueness of the solution (McDonald and Harbaugh, 1988; Kinzelbach, 1986; Schwartz and Domenico, 1990).
4. Interbasin flow from areas outside of the defined boundaries is negligible.
5. Proterozoic glacial deposits make up the principal hydrostratigraphic unit for the Sands Plain area.
6. Hydraulic conductivity values assigned to glacial deposits are isotropic, vertically averaged over depth, and are based on the material type and its thickness. Hydraulic conductivity values are

distributed spatially in Sands Plain area according to the glacial depositional environments described by Hughes (1978).

7. The Sands Plain aquifer is unconfined. Although this assumption seems valid, perched water tables and leaky confining layers may be present in some localities.

8. The head values can be calculated from Dupuit's flow assumptions, which states that flow lines are horizontal and equipotential lines are vertical, and that the hydraulic gradient is equal to the slope of the free surface and is invariant with depth (Freeze and Cherry, 1979; Kinzelbach, 1986; Anderson and Woessner, 1991).

9. Water levels in all streams are considered to be constant. This assumption is considered valid because the greatest measured difference in gage height over a year period at designated gaging stations on tributaries of the Chocolay River and for Goose Lake Outlet are approximately 2 feet and 4.5 feet, respectively, (Grannemann, 1984). These differences are insignificant compared to a total head difference of about 600 feet between Goose Lake Outlet and Lake Superior (Grannemann, 1984).

10. The Sands Plain area is recharged directly by precipitation, runoff from Marquette Iron Range, and by losing reaches of Goose Lake Outlet.

11. Groundwater is discharged from the Sands Plain area by leakage to Lake Superior and to tributary streams of the Chocolay River.

12. The water consumption in the Sands Plain area by domestic and industrial use is minimal.

Mathematical Basis

A two-dimensional groundwater flow equation describing the conservation of mass is given by,

$$\rho V_x + \rho V_y = \rho V_x - \partial/\partial x\,(\rho V_x) + \rho V_y - \partial/\partial y(\rho V_y) \qquad (1)$$

were V_x and V_y are the specific discharge in the x and y direction, respectively, and ρ is the density (Kinzelbach, 1986; Freeze and Cherry, 1979). The conservation of mass requires that the rate of fluid mass flow into an elemental control area is equal to the rate of the fluid mass flow out. For steady state flow with a constant fluid density the equation for flow translates into,

$$\partial(V_x)/\partial x + \partial(V_y)/\partial y = 0 \qquad (2)$$

Substitution of Darcy's Law ($V=K\partial h/\partial x$) for V_x and V_y into equation (2) gives

$$\partial/\partial x(K_x\,\partial h/\partial x) + \partial/\partial x(K_y\,\partial h/\partial y)=0 \qquad (3)$$

for steady state flow through an anisotropic saturated porous media. The flow equation for an isotropic steady state unconfined aquifer can be described by

$$(K_x b\,\partial^2 h/\partial x^2) + (K_y b\,\partial^2 h/\partial y^2)=0 \qquad (4)$$

where b is the saturated thickness of the aquifer and $K_x = K_y = C$ where is a C=constant. The equation for a isotropic steady state unconfined aquifer is used for the Sands Plain modeled area.

Numerical Model Design

The Sands Plain model is defined by a one layer grid having dimensions of 74 columns by 64 rows (see Figure Grid). Each grid-cell face has a length of 1000 feet, with the total area of the model to covering approximately 160 sq. miles. The grid was oriented 40° counter clockwise from the lower left hand origin and roughly aligns the principal directions of the hydraulic conductivity with the x and y coordinate axes. Prescribed head boundary cells were positioned such that their nodal centers lay along the boundaries, and impermeable no-flow boundaries cells were positioned such that their cell face(s) lay along the boundary (see Figure 10). The distribution of hydraulic conductivity values for grid-cells range in values from 0 to 120 feet/day.

The position of the top and the bottom of the glacial hydrostratigraphic unit is referenced to a sea level datum and entered into model grid-cell locations by use of computer program GRID.F77 (Swain, 1974). This program utilizes the spline fit method of data point interpolation to discretize topographic and bedrock top surfaces into 74x64 gridded area. Thickness data of glacial deposits for each grid-cell could then be derived by subtracting gridded glacial top data from gridded glacial bottom data.

Groundwater flow between the Sands Plain aquifer and overlying streams and lakes was simulated by the use of the River (RIV) package (McDonald and Harbaugh, 1988) (see leaky layers in Figure Grid). Streambeds and lake bottoms are assigned conductance values (CRIV). Conductance values are calculated by multiplying the vertical conductivity values (K_r) for stream sediments by the length (L) and width (W) of the stream channel and dividing by the thickness (M) of the streambed sediments, where

$$CRIV=K_r \cdot L \cdot W/M \qquad (5)$$

These values generally range from 0.36 to 1.68 square feet/day in the Sands Plain area. The rate of water leakage (QRIV) is calculated by multiplying the streambed conductance by the difference between the stream head (HRIV) and the aquifer head (h), where

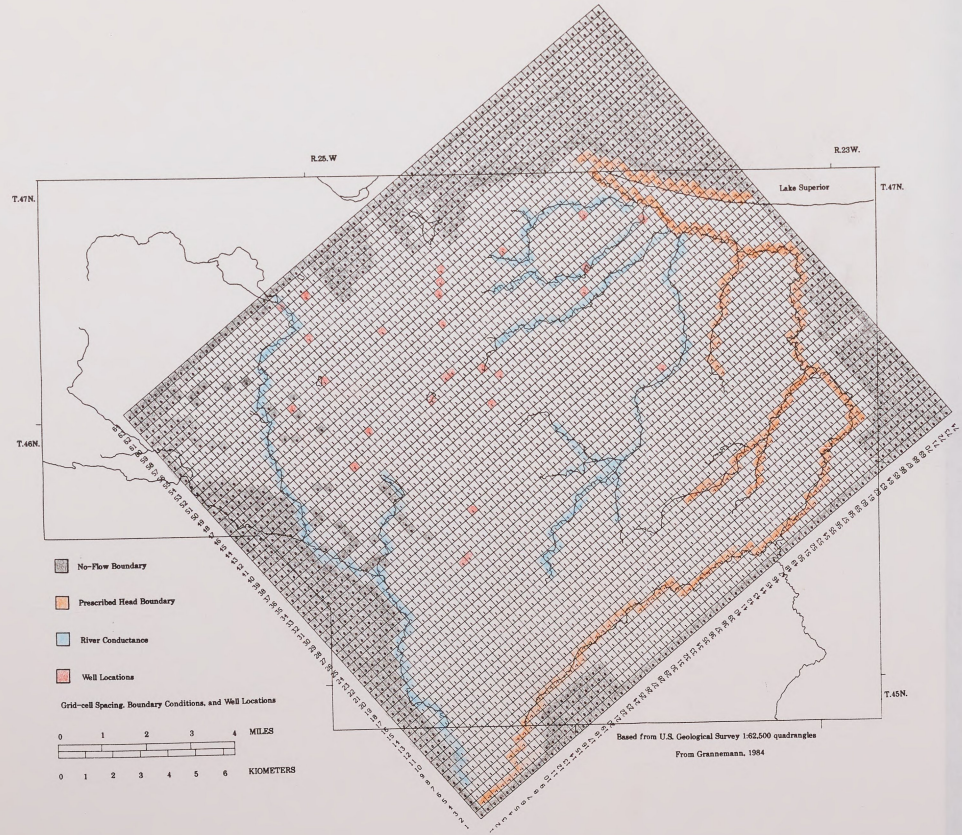
R.25.W
R.23W.
T.47N.
T.47N.
Lake Superior
T.46N.
T.45N.
No-Flow Boundary
Prescribed Head Boundary
River Conductance
Well Locations
Grid-cell Spacing, Boundary Conditions, and Well Locations
0 1 2 3 4 MILES
0 1 2 3 4 5 6 KIOMETERS
Based from U.S. Geological Survey 1:62,500 quadrangles
From Grannemann, 1984

Figure 10

$$QRIV=CRIV(HRIV-h) \qquad (6)$$

Losing reaches of streams are simulated when QRIV is a positive number and gaining reaches are simulated when QRIV is negative number.

The recharge (RCH) package is used to simulate precipitation percolating into the groundwater system (McDonald and Harbaugh, 1988). The recharge rate (QRi,j) is specified as the rate of flux ($I_{i,j}$) applied to the top cell face DELRj· DELCi, where

$$QR_{i,j} = I_{i,j} \cdot DELR_j \cdot DELC_i \qquad (7)$$

Recharge is distributed areally over the whole grid and is approximately 15.0 inches/year (Grannemann, 1984).

The well package is used to simulate pumpage from three wells having withdraw rates of approximately 1 cubic foot/sec from the southwestern region of the study area. The pumping or injection rates ($Q_{i,j,k}$) for each layer can be approximately calculated by

$$Q_{i,j,k} = T_{i,j,k}(Q_{WT}/S\ T_{i,j,k}) \qquad (8)$$

where Q_{WT} is the total pumping or injection rates for the well, $T_{i,j,k}$ is the transmissivity of a layer and $S\ T_{i,j,k}$ is the sum of the transmissivities of all layers penetrated by the well (McDonald and Harbaugh, 1988).

The evapotranspiration package was not included in the flow model because no confirmed estimates for the rates of evapotranspiration could be obtained.

Model Calibration

The ability of the Sands Plain model to simulate field measured head and flow values is demonstrated through the calibration process. The calibration process is accomplished indirectly by a series of trial and error adjustments of the model parameters. In each simulation, modeled head and flow values were compared to field measurements. In areas where poor matches between modeled and measured head existed, hydraulic conductivity values, river conductance and/or recharge values where changed until the difference between modeled and measured head values averaged no more that 1.4 feet.

The model shows no apparent bias for head values (Holtschlag, oral communication). Table 2 indicates the differences in modeled and measured head values for each well location. Differences in head values ranged from 6.0 feet in Well 21 to -5.3 feet in Well 5. The standard deviation between measured and modeled head values is 3.2 feet; the mean difference between measured and modeled head values is 1.35 feet.

The model shows no apparent bias for flow values (Holtschlag, oral communication). Measured baseflow values from gaging stations were compared to modeled stream flow values (see Table 3). Simulated flow velocities (leakage) were calculated by summing grid-cell flow values along stream reaches. Negative leakage values indicate that the stream is effluent (gaining water from baseflow), and positive leakage values indicate the stream is influent (losing water to the groundwater system). In areas where poor matches between observed and measured stream flow existed, conductance in the River Package was changed until the average difference was -1.05 cubic feet/second. The standard deviation between measured and modeled flow was 1.91 cubic feet/second; the mean difference between measured and modeled flow was 1.05 cubic feet/second.

Table 2

Measured and Modeled Head Values

Well #	I	J	Head in feet Modeled	Measured	Difference
34	43	32	1024.4	1045.6	3.2
33	56	23	1176.9	1179.6	0.3
30	52	16	1194.0	1198.4	4.4
29	42	17	1198.0	1199.0	1.0
26	52	21	1182.5	1182.7	0.2
23	44	22	1141.5	1144.1	2.6
21	52	30	1101.4	1107.4	6.0
19	60	26	1185.3	1188.9	3.6
15	55	36	1058.4	1061.6	3.2
14	54	42	998.9	994.2	-4.7
11	25	21	1148.3	1147.7	-0.6
10	29	24	1130.0	1132.9	2.9
8	36	24	1125.1	1127.0	1.9
7	37	34	1022.8	1025.2	2.4
6	34	39	939.5	953.3	-2.3
5	39	37	963.1	957.8	-5.3
1	42	56	634.8	638.2	3.4
P4	48	35	1047.5	1049.2	1.7
P1	51	37	1035.8	1038.0	2.2

* I and J values define grid-cell locations with respect to the lower left corner of the model grid

Table 3

Measured and Simulated Stream Flow Rates

		Leakage in cubic feet per second		
Location	Gaging Station	Simulated	Observed	Difference
Silver Creek	22	-6.851	-9.2	-2.3
Cherry Creek	16	-18.481	-19.2	-0.7
Cedar Creek	11	-10.742	-12.8	-2.1
Upper Reach of Goose Lake Outlet		10.841		
Lower Reach of Goose Lake Outlet		0.040		
Strawberry Lake		-9.708		
Big Creek	7	-30.285	-29.3	0.9

Sensitivity Analysis

Sensitivity analysis is performed to understand how changes in parameter values effects the model's solution. Grannemann (1984) analyzed the sensitivity of the Sands Plain model to changes in three sets of interrelated parameters: hydraulic conductivity, recharge, and stream conductance. Grannemann (1984) indicates that estimates to recharge are consistent with baseflow measurements Given this recharge information, variation in hydraulic conductivity caused greater variation in head and flow values than similar variations in stream conductance.

Potentiometric Surface

Simulated potentiometric surface for the Sands Plain aquifer is displayed graphically in Figure 11. The potentiometric surface was contour at 20 feet interval. Hydraulic-heads range from 1200 feet in the west portion of the modeled area to 610 feet near Lake Superior. The potentiometric surface in Figure 11 indicates that flow is towards Lake Superior (northeast), and that hydraulic gradients are generally highest in the central portion of the modeled area. Figure 11 also indicates discharge to groundwater from Goose Lake Outlet near Goose Lake, and that tributaries of the Chocolay River receive recharge from groundwater.

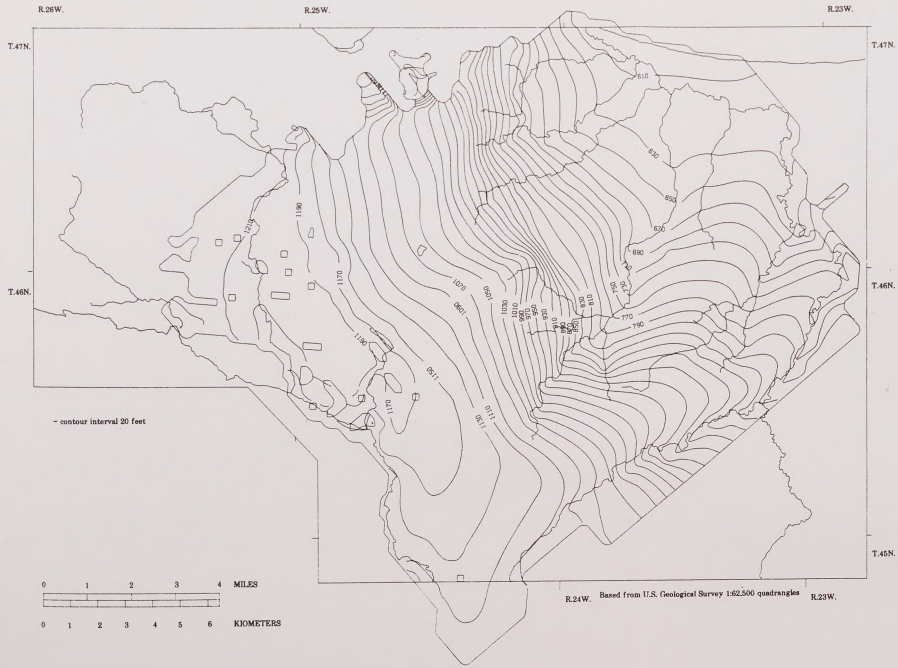

Figure 11 Potentiometric Surface

MODPATH Simulation

Mathematical Basis

Head output from the calibrated Sands Plain model are linked to the post-processing particle tracking package MODPATH and MODPATH-PLOT (Pollock, 1989) to determine path directions and residence times for solutes in the system. MODPATH utilizes advective flow transport to simulate the movement of dissolved constituents in groundwater.

Although modeling solely with advective transport does not account for effects of dispersion and chemical reactions along flow path, it provides a good first order approximation because of the uncertainties in assigning parameters for these variables. Estimates of particle-travel time in the Sands Plain region thus represent the fastest rate of particle movement along a flow line. These estimates assume that groundwater volumetric flow rates do not fluctuate rapidly over time.

MODPATH solves the advective component of transport equation by calculating average linear velocity. The average linear velocity across a face in a grid-cell is obtained by dividing the volumetric flow rate (Q_x) across the face by the cross sectional area of the face (Dx Dy) and the effective porosity (n) of the porous media as given by,

$$V_{x1} = Q_{x1}/(n.Dx\ Dy) \qquad (9)$$

in the x-direction. Effective porosity was estimated from tables in Freeze and Cherry (1979) and assigned a value of 0.20 corresponding to medium size sands.

MODPATH calculates groundwater velocity vectors by simple linear interpolation. Simple linear interpolation assumes that a component of velocity varies linearly along a principle axis direction, and that these variations are independent of the other velocity components which vary linearly along their associated principle axis. Linear interpolation for the x-direction is described by

$$V_{x2} = A_x(\Delta x) + V_{x1} \qquad (10)$$

where A_x is a constant that corresponds to the component of the velocity gradient inside the grid-cell (Pollock, 1988). Equation (10) can be rearranged into

$$A_x=(V_{x2}-V_{x1})/\Delta x \text{ or } A_x=dV_x/dx \qquad (11)$$

The rate of change in the particles velocity through the grid-cell is given by,

$$(dV_x/dt)_p = (dV_x/dx)(dx/dt)_p \qquad (12)$$

where the term $(dx/dt)_p=V_{xp}$ is the change in the particle's x-location with respect to time. Substituting into equation (12) gives,

$$(dV_x/dt)_p=A_xV_{xp} \text{ or } (1/V_{xp})dV_{xp}=A_xdt \qquad (13)$$

MODPATH uses a semianalytical method to solve the integration of equation (13) directly to give,

$$\ln[Vx_p(t_2)/Vx_p(t_1)]=A_x\Delta t \text{ where } \Delta t=t_2-t_1 \qquad (14)$$

Equation (14) finally rearranges into,

$$x_p(t_2)=x_1+(1/A_x)[V_{xp}(t1)\exp(A_x\Delta t)-v_{x1}] \qquad (15)$$

which determines the particle's new coordinate location in the x-direction at a specified time interval.

MODPATH has the ability to track particles backward in time by multiplying the velocity component by -1. This feature is useful in delineating recharge sources in the Sands Plain area by tracking particles backward from discharge sinks.

The initial starting location for particles in the grid-cell at $t_1=0$ can also be varied by MODPATH. Starting locations of particles can be generated inside a grid-cell (internally), or can be generated on a grid-cell face(s). The Sands Plain model described here utilizes this feature to reflect differences between particles which originated at streams sites and are then tracked backwards to a

groundwater source, and particles which originated at a well location and are tracked forwards to a stream sink. Particles generated at a stream or surface water site are initiated on the top face of the grid cell, while particles generated at well locations are initiated internally.

Flow System Analysis

Particle tracking techniques were first performed from select well locations to delineate their sources of recharge. Figure 12 was constructed by the backward tracking of four particles at each well location over an 80 year period. Four particles were used in tracking simulations because this number of particles could accurately depict individual flow paths while retaining the clarity of the simulation. Flow paths in Figure 12 are represented by dashes and can be traced backwards towards their recharge source. Time series data is represented as colored circles lying along a flow path, and have a constant time step of 10 years. Figure 12 indicates that flow paths traced from wells 21, 19, 15, B. McDonald, P4, and P1 in the northern region of the modeled area derive a proportion of their recharge directly from the upper reaches of Goose Lake Outlet. Time series data show that it takes a period of 10 to 30 years for a particle of water to reach these wells from their respective recharge sources. Flow paths traced from wells 34, 30, 29, 26, and 23 located in the west central part of the modeled area derive a proportion of their recharge indirectly from Goose Lake Outlet. Time series data indicates that it takes a period of 10 to 30 years for a particle of water to reach these wells from their respective recharge sources. Flow paths for wells 7, 6, and 5 located in the central region of the modeled area derive their recharge primarily from precipitation, and require a time period of 40 to 50 years. Flow paths traced from wells 8, 10, D. McDonald and 11 derive their recharge primarily from precipitation, but only in a period of 10 years or less. Well 1 located near Lake Superior derives a proportion of recharge from both the upper reaches of Goose Lake Outlet in the north and from a groundwater source in the western central region

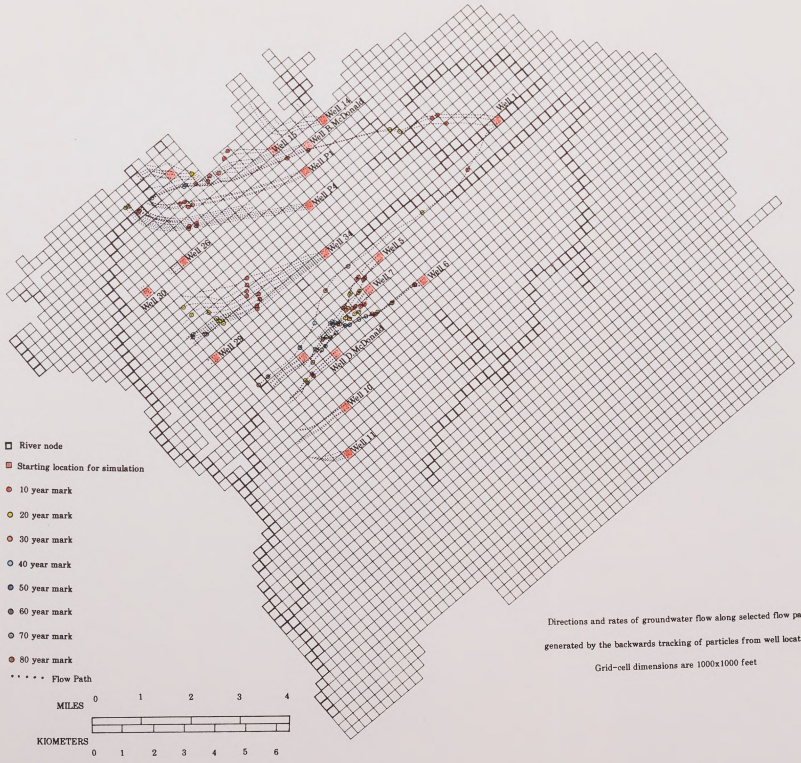
Well 14
Well 15
Well 16
Well 13
Well 1
Well 12
Well 11
Well 4
Well 3
Well 2
Well 5
Well 6
Well 7
Well 8
Well 9
Well 10
Well 23
Well 24
Well 25
Well 26
Well 27
Well 28
Well 29
Well 30
River node
Starting location for simulation
10 year mark
20 year mark
30 year mark
40 year mark
50 year mark
60 year mark
70 year mark
80 year mark
Flow Path
MILES
0 1 2 3 4
KIOMETERS
0 1 2 3 4 5 6
Directions and rates of groundwater flow along selected flow paths
generated by the backwards tracking of particles from well locations
Grid-cell dimensions are 1000x1000 feet

Figure 12

of the modeled area. Time series data indicate that it takes a period of 50 and 80 years for a particle of water to reach these wells from these recharge sources, respectively.

Particle tracking techniques were then performed from well locations to delineate their points of discharge in the modeled area. Figure 13 was constructed by the forward tracking of four particles at each well location over a 80-year period. Figure 13 indicates that flow paths traced from wells 33, 19, 15, 14, P4, P1 and Heidtman discharge into the upper and lower reaches of Silver Creek and Cherry Creek. Time series data for these wells indicate that water is discharged to Silver Creek and Cherry Creek in a period of 20 to 50 years. Flow paths can be traced from wells 34, 30, 29, 26, and 23 in Figure 13 to the headwaters of Cedar Creek in a period of 10 to 30 years. Flow paths observed for wells 8, 7, 6, and 5 can be traced into the lower reaches of Cherry Creek and Cedar Creek in a period of 30 to 80 years. Flow paths traced from wells 11, 10, 6, and D. McDonald discharge into Big Creek in a period of 30 to 70 years.

Particle tracking techniques were performed from stream sample site locations to delineate their sources of recharge in the modeled area. Figure 14 was constructed by the backward tracking of four particles at each well location over a 40-year period. Figure 14 indicates that flow path traced from Silver Creek headwaters derive a proportion of their recharge indirectly from Goose Lake Outlet in a period of 20 years. Flow path for Cedar Creek trace its source of recharge to a groundwater source in the western central region of the modeled area. Time series data indicate that it takes a 40-year period for a particle of water to recharge Cedar Creek from its source area. Flow path traced backwards from Big Creek indicate a southern groundwater source which recharge Big Creek over a 40-year period. Other stream site locations in Figure 14 are strong sinks and have no single source area in which they are recharged.

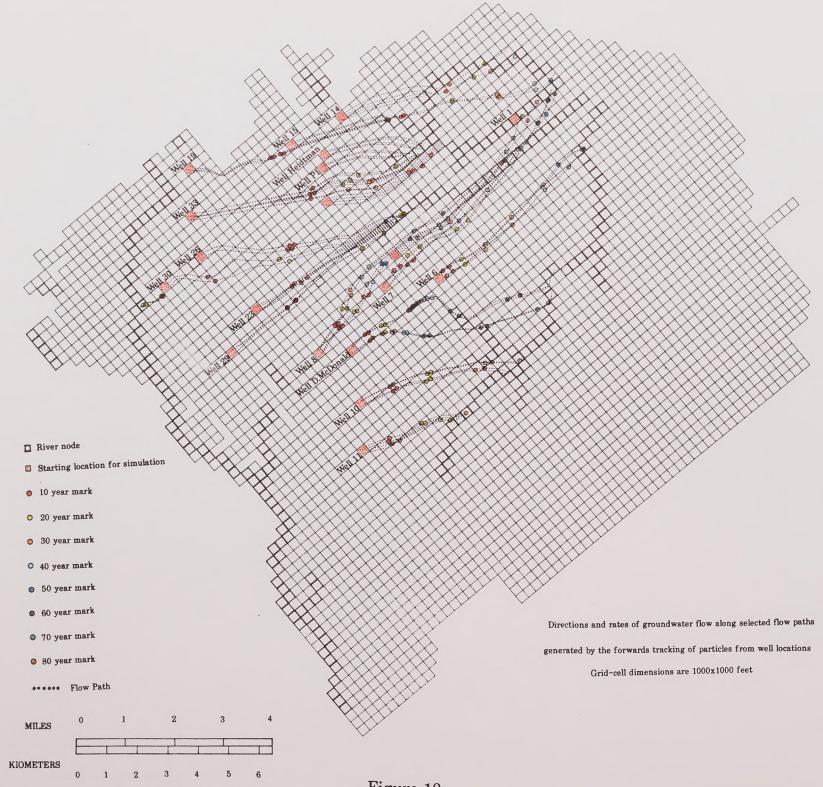
Well 12
Well 11
Well 13
Well Heptanes
Well 15
Well 14
Well 16
Well 17
Well 18
Well 19
Well 20
Well 21
Well 22
Well 23
Well 24
Well 25
Well 26
Well 27
Well 28
Well 29
Well 30
Well 31
Well 32
Well 33
Well 34
Well 35
Well 36
Well 37
Well 38
Well 39
Well 40
Well 41
Well 42
Well 43
Well 44
Well 45
Well 46
Well 47
Well 48
Well 49
Well 50
Well 51
Well 52
Well 53
Well 54
Well 55
Well 56
Well 57
Well 58
Well 59
Well 60
Well 61
Well 62
Well 63
Well 64
Well 65
Well 66
Well 67
Well 68
Well 69
Well 70
Well 71
Well 72
Well 73
Well 74
Well 75
Well 76
Well 77
Well 78
Well 79
Well 80
Well 81
Well 82
Well 83
Well 84
Well 85
Well 86
Well 87
Well 88
Well 89
Well 90
Well 91
Well 92
Well 93
Well 94
Well 95
Well 96
Well 97
Well 98
Well 99
Well 100
Well 101
Well 102
Well 103
Well 104
Well 105
Well 106
Well 107
Well 108
Well 109
Well 110
Well 111
Well 112
Well 113
Well 114
Well 115
Well 116
Well 117
Well 118
Well 119
Well 120
Well 121
Well 122
Well 123
Well 124
Well 125
Well 126
Well 127
Well 128
Well 129
Well 130
Well 131
Well 132
Well 133
Well 134
Well 135
Well 136
Well 137
Well 138
Well 139
Well 140
Well 141
Well 142
Well 143
Well 144
Well 145
Well 146
Well 147
Well 148
Well 149
Well 150
Well 151
Well 152
Well 153
Well 154
Well 155
Well 156
Well 157
Well 158
Well 159
Well 160
Well 161
Well 162
Well 163
Well 164
Well 165
Well 166
Well 167
Well 168
Well 169
Well 170
Well 171
Well 172
Well 173
Well 174
Well 175
Well 176
Well 177
Well 178
Well 179
Well 180
Well 181
Well 182
Well 183
Well 184
Well 185
Well 186
Well 187
Well 188
Well 189
Well 190
Well 191
Well 192
Well 193
Well 194
Well 195
Well 196
Well 197
Well 198
Well 199
Well 200
Well 201
Well 202
Well 203
Well 204
Well 205
Well 206
Well 207
Well 208
Well 209
Well 210
Well 211
Well 212
Well 213
Well 214
Well 215
Well 216
Well 217
Well 218
Well 219
Well 220
Well 221
Well 222
Well 223
Well 224
Well 225
Well 226
Well 227
Well 228
Well 229
Well 230
Well 231
Well 232
Well 233
Well 234
Well 235
Well 236
Well 237
Well 238
Well 239
Well 240
Well 241
Well 242
Well 243
Well 244
Well 245
Well 246
Well 247
Well 248
Well 249
Well 250
Well 251
Well 252
Well 253
Well 254
Well 255
Well 256
Well 257
Well 258
Well 259
Well 260
Well 261
Well 262
Well 263
Well 264
Well 265
Well 266
Well 267
Well 268
Well 269
Well 270
Well 271
Well 272
Well 273
Well 274
Well 275
Well 276
Well 277
Well 278
Well 279
Well 280
Well 281
Well 282
Well 283
Well 284
Well 285
Well 286
Well 287
Well 288
Well 289
Well 290
Well 291
Well 292
Well 293
Well 294
Well 295
Well 296
Well 297
Well 298
Well 299
Well 300
Well 301
Well 302
Well 303
Well 304
Well 305
Well 306
Well 307
Well 308
Well 309
Well 310
Well 311
Well 312
Well 313
Well 314
Well 315
Well 316
Well 317
Well 318
Well 319
Well 320
Well 321
Well 322
Well 323
Well 324
Well 325
Well 326
Well 327
Well 328
Well 329
Well 330
Well 331
Well 332
Well 333
Well 334
Well 335
Well 336
Well 337
Well 338
Well 339
Well 340
Well 341
Well 342
Well 343
Well 344
Well 345
Well 346
Well 347
Well 348
Well 349
Well 350
Well 351
Well 352
Well 353
Well 354
Well 355
Well 356
Well 357
Well 358
Well 359
Well 360
Well 361
Well 362
Well 363
Well 364
Well 365
Well 366
Well 367
Well 368
Well 369
Well 370
Well 371
Well 372
Well 373
Well 374
Well 375
Well 376
Well 377
Well 378
Well 379
Well 380
Well 381
Well 382
Well 383
Well 384
Well 385
Well 386
Well 387
Well 388
Well 389
Well 390
Well 391
Well 392
Well 393
Well 394
Well 395
Well 396
Well 397
Well 398
Well 399
Well 400
Well 401
Well 402
Well 403
Well 404
Well 405
Well 406
Well 407
Well 408
Well 409
Well 410
Well 411
Well 412
Well 413
Well 414
Well 415
Well 416
Well 417
Well 418
Well 419
Well 420
Well 421
Well 422
Well 423
Well 424
Well 425
Well 426
Well 427
Well 428
Well 429
Well 430
Well 431
Well 432
Well 433
Well 434
Well 435
Well 436
Well 437
Well 438
Well 439
Well 440
Well 441
Well 442
Well 443
Well 444
Well 445
Well 446
Well 447
Well 448
Well 449
Well 450
Well 451
Well 452
Well 453
Well 454
Well 455
Well 456
Well 457
Well 458
Well 459
Well 460
Well 461
Well 462
Well 463
Well 464
Well 465
Well 466
Well 467
Well 468
Well 469
Well 470
Well 471
Well 472
Well 473
Well 474
Well 475
Well 476
Well 477
Well 478
Well 479
Well 480
Well 481
Well 482
Well 483
Well 484
Well 485
Well 486
Well 487
Well 488
Well 489
Well 490
Well 491
Well 492
Well 493
Well 494
Well 495
Well 496
Well 497
Well 498
Well 499
Well 500
Well 501
Well 502
Well 503
Well 504
Well 505
Well 506
Well 507
Well 508
Well 509
Well 510
Well 511
Well 512
Well 513
Well 514
Well 515
Well 516
Well 517
Well 518
Well 519
Well 520
Well 521
Well 522
Well 523
Well 524
Well 525
Well 526
Well 527
Well 528
Well 529
Well 530
Well 531
Well 532
Well 533
Well 534
Well 535
Well 536
Well 537
Well 538
Well 539
Well 540
Well 541
Well 542
Well 543
Well 544
Well 545
Well 546
Well 547
Well 548
Well 549
Well 550
Well 551
Well 552
Well 553
Well 554
Well 555
Well 556
Well 557
Well 558
Well 559
Well 560
Well 561
Well 562
Well 563
Well 564
Well 565
Well 566
Well 567
Well 568
Well 569
Well 570
Well 571
Well 572
Well 573
Well 574
Well 575
Well 576
Well 577
Well 578
Well 579
Well 580
Well 581
Well 582
Well 583
Well 584
Well 585
Well 586
Well 587
Well 588
Well 589
Well 590
Well 591
Well 592
Well 593
Well 594
Well 595
Well 596
Well 597
Well 598
Well 599
Well 600
Well 601
Well 602
Well 603
Well 604
Well 605
Well 606
Well 607
Well 608
Well 609
Well 610
Well 611
Well 612
Well 613
Well 614
Well 615
Well 616
Well 617
Well 618
Well 619
Well 620
Well 621
Well 622
Well 623
Well 624
Well 625
Well 626
Well 627
Well 628
Well 629
Well 630
Well 631
Well 632
Well 633
Well 634
Well 635
Well 636
Well 637
Well 638
Well 639
Well 640
Well 641
Well 642
Well 643
Well 644
Well 645
Well 646
Well 647
Well 648
Well 649
Well 650
Well 651
Well 652
Well 653
Well 654
Well 655
Well 656
Well 657
Well 658
Well 659
Well 660
Well 661
Well 662
Well 663
Well 664
Well 665
Well 666
Well 667
Well 668
Well 669
Well 670
Well 671
Well 672
Well 673
Well 674
Well 675
Well 676
Well 677
Well 678
Well 679
Well 680
Well 681
Well 682
Well 683
Well 684
Well 685
Well 686
Well 687
Well 688
Well 689
Well 690
Well 691
Well 692
Well 693
Well 694
Well 695
Well 696
Well 697
Well 698
Well 699
Well 700
Well 701
Well 702
Well 703
Well 704
Well 705
Well 706
Well 707
Well 708
Well 709
Well 710
Well 711
Well 712
Well 713
Well 714
Well 715
Well 716
Well 717
Well 718
Well 719
Well 720
Well 721
Well 722
Well 723
Well 724
Well 725
Well 726
Well 727
Well 728
Well 729
Well 730
Well 731
Well 732
Well 733
Well 734
Well 735
Well 736
Well 737
Well 738
Well 739
Well 740
Well 741
Well 742
Well 743
Well 744
Well 745
Well 746
Well 747
Well 748
Well 749
Well 750
Well 751
Well 752
Well 753
Well 754
Well 755
Well 756
Well 757
Well 758
Well 759
Well 760
Well 761
Well 762
Well 763
Well 764
Well 765
Well 766
Well 767
Well 768
Well 769
Well 770
Well 771
Well 772
Well 773
Well 774
Well 775
Well 776
Well 777
Well 778
Well 779
Well 780
Well 781
Well 782
Well 783
Well 784
Well 785
Well 786
Well 787
Well 788
Well 789
Well 790
Well 791
Well 792
Well 793
Well 794
Well 795
Well 796
Well 797
Well 798
Well 799
Well 800
Well 801
Well 802
Well 803
Well 804
Well 805
Well 806
Well 807
Well 808
Well 809
Well 810
Well 811
Well 812
Well 813
Well 814
Well 815
Well 816
Well 817
Well 818
Well 819
Well 820
Well 821
Well 822
Well 823
Well 824
Well 825
Well 826
Well 827
Well 828
Well 829
Well 830
Well 831
Well 832
Well 833
Well 834
Well 835
Well 836
Well 837
Well 838
Well 839
Well 840
Well 841
Well 842
Well 843
Well 844
Well 845
Well 846
Well 847
Well 848
Well 849
Well 850
Well 851
Well 852
Well 853
Well 854
Well 855
Well 856
Well 857
Well 858
Well 859
Well 860
Well 861
Well 862
Well 863
Well 864
Well 865
Well 866
Well 867
Well 868
Well 869
Well 870
Well 871
Well 872
Well 873
Well 874
Well 875
Well 876
Well 877
Well 878
Well 879
Well 880
Well 881
Well 882
Well 883
Well 884
Well 885
Well 886
Well 887
Well 888
Well 889
Well 890
Well 891
Well 892
Well 893
Well 894
Well 895
Well 896
Well 897
Well 898
Well 899
Well 900
Well 901
Well 902
Well 903
Well 904
Well 905
Well 906
Well 907
Well 908
Well 909
Well 910
Well 911
Well 912
Well 913
Well 914
Well 915
Well 916
Well 917
Well 918
Well 919
Well 920
Well 921
Well 922
Well 923
Well 924
Well 925
Well 926
Well 927
Well 928
Well 929
Well 930
Well 931
Well 932
Well 933
Well 934
Well 935
Well 936
Well 937
Well 938
Well 939
Well 940
Well 941
Well 942
Well 943
Well 944
Well 945
Well 946
Well 947
Well 948
Well 949
Well 950
Well 951
Well 952
Well 953
Well 954
Well 955
Well 956
Well 957
Well 958
Well 959
Well 960
Well 961
Well 962
Well 963
Well 964
Well 965
Well 966
Well 967
Well 968
Well 969
Well 970
Well 971
Well 972
Well 973
Well 974
Well 975
Well 976
Well 977
Well 978
Well 979
Well 980
Well 981
Well 982
Well 983
Well 984
Well 985
Well 986
Well 987
Well 988
Well 989
Well 990
Well 991
Well 992
Well 993
Well 994
Well 995
Well 996
Well 997
Well 998
Well 999
Well 1000
River node
Starting location for simulation
10 year mark
20 year mark
30 year mark
40 year mark
50 year mark
60 year mark
70 year mark
80 year mark
Flow Path
MILES
0 1 2 3 4
KIOMETERS
0 1 2 3 4 5 6
Directions and rates of groundwater flow along selected flow paths
generated by the forwards tracking of particles from well locations
Grid-cell dimensions are 1000x1000 feet

Figure 13

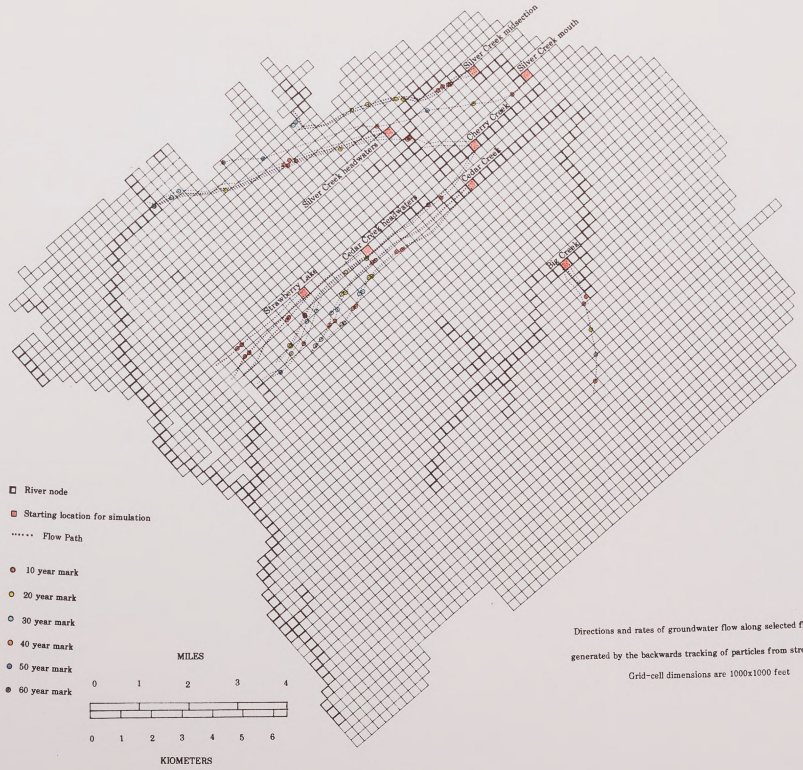
Silver Creek confluence
Silver Creek mouth
Silver Creek headwaters
Silver Creek
Coyote Creek
Coyote Creek headwaters
Coyote Creek
Big Creek
Stevens Creek
Stevens Creek
River node
Starting location for simulation
Flow Path
10 year mark
20 year mark
30 year mark
40 year mark
50 year mark
60 year mark
MILES
0 1 2 3 4
0 1 2 3 4 5 6
KIOMETERS
Directions and rates of groundwater flow along selected flow paths
generated by the backwards tracking of particles from stream sites
Grid-cell dimensions are 1000x1000 feet

Figure 14

Volumetric Water Budget

The volumetric groundwater budget for the Sands Plain area is the summary of all inflows and outflows of water to the modeled area contributed by each flow component package. The difference between these inflows and outflows should equal zero for a balanced volumetric water budget. The volumetric budget for the Sands Plain area indicates that the total inflow rate of water to the modeled area is 171.77 cubic feet/second, and the total outflow rate of water from the modeled area is 171.78 cubic feet/second, giving a difference of approximately -0.007 cubic feet/second.

Inflows of water to the Sands Plain area are composed of recharge from precipitation, specified head boundaries, and leakage from streams. The volumetric inflow rates are 10.2 cubic feet/second from specified head boundaries, 142.31 cubic feet/second from precipitation, and 19.3 cubic feet/second from river leakage. Although their is some amount inflow into specified head, it occurs primarily near the southern boundary of the modeled area and does not effect simulated head results. Recharge is fairly uniformly distributed throughout the modeled area and is the greatest contributor of water to the Sands Plain area. Outflows of water from the Sands Plain area are composed of pumping wells, specified head boundaries, and leakage to streams. The volumetric outflow rates are 48.9 cubic feet/second to constant head, 3.3 cubic feet/second to pumping wells, and 119.5 cubic feet/second to river leakage. Leakage of water to streams are the greatest means of water discharge from the modeled area.

Zone Budget

Figure 15 displays a series of ten zones which divide the Sands Plain area into distinct hydrologic areas. These zones are used to isolate individual groundwater-streamflow systems and to evaluate the interflow rates of groundwater from one zone of the modeled area to another. The boundaries of these zones are constructed along groundwater drainage divides by a series of trial and error adjustments in which head distribution, stream orientation, and

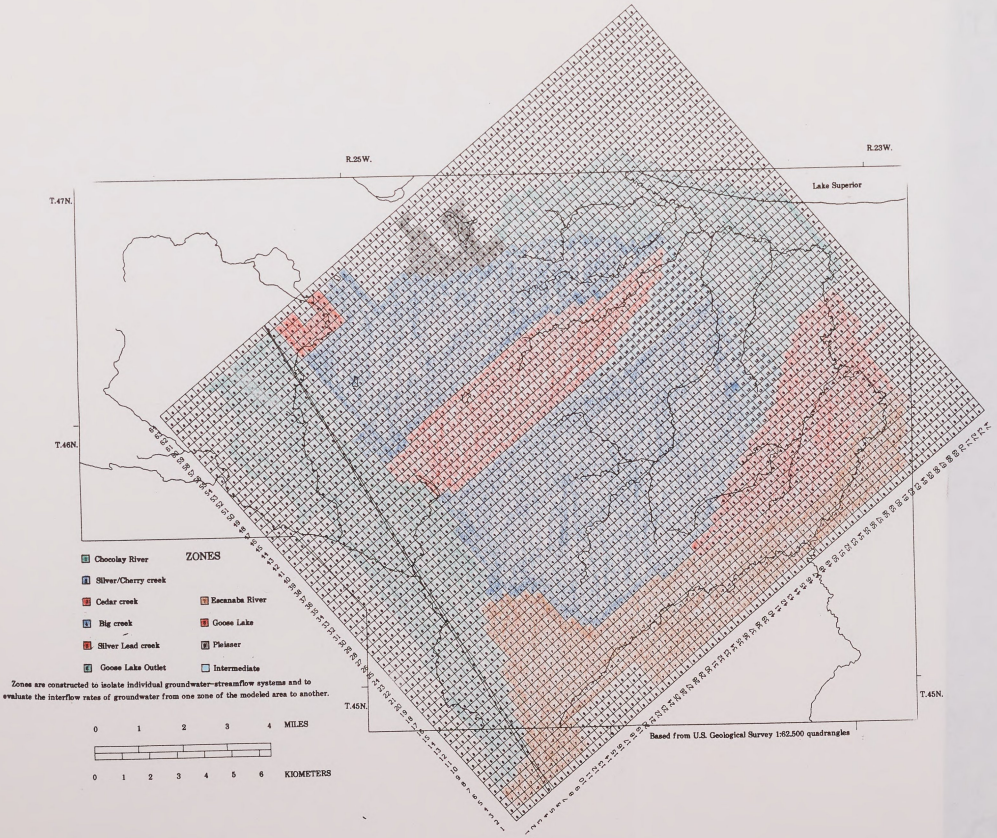
R.25W.
R.23W.
Lake Superior
T.47N.
T.46N.
T.45N.
T.45N.
ZONES
Chocolay River
Silver/Cherry creek
Cedar creek
Escanaba River
Big creek
Goose Lake
Silver Lead creek
Pleisner
Goose Lake Outlet
Intermediate
Zones are constructed to isolate individual groundwater–streamflow systems and to evaluate the interflow rates of groundwater from one zone of the modeled area to another.
0 1 2 3 4 MILES
0 1 2 3 4 5 6 KILOMETERS
Based from U.S. Geological Survey 1:62,500 quadrangles

Figure 15

groundwater flow paths generated by MODPATH (Pollock, 1989) were observed.

Cell by cell interflow datum is used by the post processing package Zonebudget (Harbaugh, 1990) to calculate groundwater interflow rates between zones. Table 4 summaries interflow rates between one particular zone, and those zones and/or to specified head boundaries which surrounding it.

Zone Goose Lake in Figure 15 represents a groundwater recharge area in which Goose Lake and the upper portion of Goose Lake Outlet discharge water into the system. Surrounding zone Goose Lake are zone Silver/Cherry Creek and zone Goose Lake Outlet. The boundaries of zone Silver/Cherry Creek were constructed to isolate a subregion of groundwater which is thought to be the source of recharge to the upper reaches of Silver and Cherry Creeks. The boundaries surrounding zone Goose Lake Outlet isolate an area which contains the lower reaches of Goose Lake Outlet and a portion of the Middle Branch of the Escanaba River. Table 4 indicates that their is no interflow from zone Silver/Cherry Creek to zone Goose Lake, and that only a small rate of interflow (1.1 cubic feet/second) from zone Goose Lake Outlet enters zone Goose Lake. Table 4 also indicates that a large rate of interflow (13.9 cubic feet/second) occurs from zone Goose Lake to zone Silver/Cherry Creek, and that only a small rate of interflow (0.17 cubic feet/second) occurs from zone Goose Lake to zone Goose Lake Outlet. This data suggests that groundwater in zone Goose Lake which is recharged from leakage by Goose Lake and Goose Lake Outlet will eventually act as a source of recharge for groundwater in zone Silver/Cherry Creek.

The boundaries surrounding zone Cedar Creek were constructed to isolate an area containing the headwaters of Cedar Creek. The boundaries surrounding zone Big Creek were constructed to isolate an area containing the headwaters of Big Creek and its tributaries. Only a small rate of interflow occurs between zone Goose Lake Outlet and zones Silver/Cherry, Cedar, and Big Creeks as indicated by Table 4.

A significant rate of interflow occurs between zone Silver/Cherry Creek and zone Cedar Creek. Attempts to redraw

Table 4

Zone Budget

Interflow rates in cubic feet per second

zone 1= zone Chocolay River
zone 2= zone Silver/Cherry Creek
zone 3= zone Cedar Creek
zone 4 = zone Big Creek
zone 5 = zone West Branch of the of Chocolay
zone 6= zone Goose Lake Outlet
zone 7 = zone Escanaba
zone 8 = zone Goose Lake
zone 9 = zone Pleisser Lake
zone 10 = Intermediate zone
zone 12 = Intermediate zone

Flow Budget for zone 1

In:		Out:	
Constant Head	=4.96	Constant Head	=17.20
Zone 2 to 1	= 7.67	Zone 1 to 2	= 6.07
Zone 4 to 1	= 0.86	Zone 1 to 4	= 0.99
Zone 5 to 1	= 0.65	Zone 1 to 5	= 0.45
Zone 9 to 1	= 2.98	Zone 1 to 9	= 0.00
Zone 10 to 1	= 1.98	Zone 1 to 10	= 0.03
Zone 12 to 1	= 1.84	Zone 1 to 12	= 1.07
Total in	**=20.94**	**Total out**	**= 25.81**

In - Out = -4.87

Flow Budget for Zone 2

In:		Out:	
Constant Head	=0.00	Constant Head	= 0.00
Zone 1 to 2	= 6.07	Zone 2 to 1	= 7.67
Zone 3 to 2	= 5.97	Zone 2 to 3	=10.20
Zone 6 to 2	= 1.15	Zone 2 to 6	= 0.00
Zone 8 to 2	=13.98	Zone 2 to 8	= 0.00
Zone 9 to 2	= 7.73	Zone 2 to 9	= 6.73
Zone 10 to 2	= 0.10	Zone 2 to 10	= 0.00
Total in	**= 35.00**	**Total out**	**= 24.60**

In-Out =10.40

Table 4 (cont'd)

Flow Budget for Zone 3

In:		Out:	
Constant Head	=0.00	Constant Head	= 0.00
Zone 2 to 3	=10.21	Zone 3 to 2	= 5.97
Zone 4 to 3	= 0.68	Zone 3 to 4	= 0.89
Zone 6 to 3	= 0.33	Zone 3 to 6	= 0.00
Zone 10 to 3	= 1.88	Zone 3 to 10	= 3.22
Total in	=13.10	Total out	= 10.08

In-Out =3.02

Flow Budget for Zone 4

In:		Out:	
Constant Head	=0.00	Constant Head	= 0.00
Zone 1 to 4	= 0.99	Zone 4 to 1	= 0.86
Zone 3 to 4	= 0.88	Zone 4 to 3	= 0.68
Zone 5 to 4	= 1.61	Zone 4 to 5	= 0.93
Zone 6 to 4	= 0.72	Zone 4 to 6	= 0.08
Zone 7 to 4	= 1.66	Zone 4 to 7	= 1.49
Zone 10 to 4	= 0.08	Zone 4 to 10	= 1.22
Zone 12 to 4	= 2.10	Zone 4 to 12	= 1.14
Total in	= 7.98	Total out	= 6.40

In-Out =1.49

Flow Budget for Zone 5

In:		Out:	
Constant Head	=0.99	Constant Head	= 9.81
Zone 1 to 5	= 0.45	Zone 5 to 1	= 0.64
Zone 4 to 5	= 0.92	Zone 5 to 4	= 1.61
Zone 7 to 5	= 0.66	Zone 5 to 7	= 0.65
Zone 12 to 5	= 0.53	Zone 5 to 12	= 0.61
Total in	= 3.55	Total out	= 13.32

In-Out =-9.77

Table 4 (cont'd)

Flow Budget for Zone 6

In:		Out:	
Constant Head	=0.00	Constant Head	= 0.00
Zone 2 to 6	= 0.00	Zone 6 to 2	= 1.10
Zone 3 to 6	= 0.00	Zone 6 to 3	= 0.33
Zone 4 to 6	= 0.00	Zone 6 to 4	= 0.72
Zone 7 to 6	= 0.20	Zone 6 to 7	= 0.74
Zone 8 to 6	= 0.17	Zone 6 to 8	= 1.10
Total in	= 0.37	Total out	= 3.99

In-Out =-3.62

Flow Budget for Zone 7

In:		Out:	
Constant Head	=0.25	Constant Head	=18.24
Zone 4 to 7	= 1.49	Zone 7 to 3	= 1.66
Zone 5 to 7	= 0.65	Zone 7 to 5	= 0.66
Zone 6 to 7	= 0.74	Zone 7 to 6	= 0.20
Total in	= 3.13	Total out	= 20.76

In-Out =-17.63

Flow Budget for Zone 8

In:		Out:	
Constant Head	=0.00	Constant Head	= 0.00
Zone 2 to 8	= 0.00	Zone 8 to 2	=13.94
Zone 6 to 8	= 1.10	Zone 8 to 6	= 0.17
Total in	= 1.10	Total out	=14.11

In-Out =-13.01

Table 4 (cont'd)

Flow Budget for Zone 9

In:		Out:	
Constant Head	=0.00	Constant Head	= 0.00
Zone 1 to 9	= 0.00	Zone 9 to 1	= 2.98
Zone 2 to 9	= 6.73	Zone 9 to 2	= 7.74
Total in	**= 6.73**	**Total out**	**=10.72**

In-Out =-3.99

Flow Budget for Zone 10

In:		Out:	
Constant Head	=0.00	Constant Head	= 0.00
Zone 1 to 10	= 0.04	Zone 10 to 1	= 1.98
Zone 2 to 10	= 0.00	Zone 10 to 2	= 0.10
Zone 3 to 10	= 3.22	Zone 10 to 3	= 1.88
Zone 4 to 10	= 1.22	Zone 10 to 4	= 0.08
Total in	**= 4.48**	**Total out**	**= 4.04**

In-Out = 0.44

Flow Budget for Zone 12

In:		Out:	
Constant Head	=0.00	Constant Head	= 0.00
Zone 1 to 12	= 1.07	Zone 12 to 1	= 1.84
Zone 4 to 12	= 1.14	Zone 12 to 4	= 2.10
Zone 5 to 12	= 0.61	Zone 12 to 5	= 0.53
Total in	**= 2.82**	**Total out**	**= 4.47**

In-Out =-1.65

these boundary lines to reduce the rate of interflow between these two zones failed, and suggest that these two zones could not be hydrologically separated. Small rates of interflow exist between zone Cedar Creek and zone Big Creek, allowing zone Silver/Cherry Creek and zone Cedar Creek to be partially hydrologically separated from zone Big Creek (see Figure 15). This suggests that groundwater recharged from Goose Lake lying in the northern region of the modeled area in zones Silver/Cherry and Cedar Creeks is hydrologically distinct from groundwater in the southern region of the modeled area in zone Big Creek.

The boundaries surrounding zone Chocolay were constructed to isolate an area of groundwater discharge, and area where stream water tributaries converge on the Chocolay River. The boundaries surrounding zone Pleisser were constructed to isolate the Pleisser Lake area. Zones Chocolay, Silver/Cherry Creek and Pleisser display high rates of interflow between each other, suggesting that groundwater in this area may be mixing.

Groundwater and Surface Water Chemistry

METHODS SECTION

Groundwater Sampling

Groundwater samples were collected from twenty-two shallow water wells distributed throughout the Sands Plain area in September, 1990 (see Figure 16). These wells consisted of fifteen U.S.G.S installed 4" monitoring wells, five domestic wells, and two irrigation wells. Water levels and total depth were measured and recorded at each monitoring well with a water level indicator. Monitoring wells were then purged for half an hour to forty-five minutes with a Grumpus 4" submersible pump rated at 10 gal/min, or for forty-five minutes to one hour with a Keck 2" submersible pump rated at 2 gal/min. Because of its size and mobility the Keck 2" submersible pump was prefered over the Grumpus 4" submersible pump, but was limited in use because of its low pumping rate, and periodic clogging due to silt and sand. Domestic wells were purged for over one hour to clear their twenty gallon storage tanks, with resident pumps that were rated between 25 to 60 gal/min. Irrigation wells discharged water continuously at high outputs of 100 to 250 gal/min and could be sampled directly.

When purge time for each well was completed, an in-line 45 micron filter pack was attached to the submersible pump outlet nozzle to remove silt and clay size particles from the discharging well water. The filter pack was allowed to discharge water for a few minutes before water samples were collected.

Surface water samples were taken in August 1991, from creeks, rivers, and a lake. Water samples were initially collected in a 500 ml Nalgene beaker a few feet from the waters edge at depths of approximately half a foot. Water samples were then filtered through a 45 micron filter pack with the aid of a peristaltic pump.

After filtering was completed calcium, magnesium, potassium, and sodium samples were collected in a 125 ml Nalgene bottles and acidified with 2 ml of analytical grade nitric acid. Samples for sulfate analysis were collected in 250 ml Nalgene

bottles and were preserved with 2 ml of formaldehyde. Samples for silica and chloride analyses were collected in 125 ml Nalgene bottles with no preservative. Samples for trace metals and aluminum analyses were collected in 50 ml Nalgene bottles and acidified with 1 ml of distilled Ultrex nitric acid.

Samples for isotopic analyses of ^{18}O, ^{16}O, hydrogen and deuterium were collected with no filtering device and were stored in 1 Liter glass bottles and sealed with tape.

Monomeric aluminum was extracted through a procedure modified from Barnes (1976). Well water was prefiltered through a 45 micron filter. This water was then refiltered through an acid rinsed 0.2 micron polycarbonate filter into an acid rinsed 200 ml Erlenmeyer flask with the aid of a peristaltic pump. A 50 ml sample volume was then collected using an acid rinsed pipet and dispensed into an acid rinsed 200 ml beaker. An additional 50 ml of distilled deionized water was added to the beaker and the two aliquots mixed. To this was added 2 ml of 8-hydroxyquinoline solution, followed by 5 ml of an ammonium hydroxide buffer. This produced a solution having a pH of 8.3. The water solution was then transfered to an acid rinsed 250 ml volumetric flask. 10 ml of methyl isobutyl ketone (MIBK) was then pipeted into the volumetric flask and mixed for exactly 10 seconds. At the end of the 10 second time period two immiscible layers formed. The upper MIBK layer containing the monomeric aluminum species was then extracted by carefully adding distilled deionized water into the volumetric flask until the MIBK layer moved up the neck of the volumetric flask. The MIBK layer could then be removed using an acid rinsed 1 ml Eppendorf pipet and stored in a 30 ml Nalgene bottle.

All water samples were iced down and stored in a coolers after field collection. Samples were then transfered and stored at 4 °C.

Sediment Collection

Sediment samples for clay analysis were collected at each creek, lake, and river locality where water samples were collected. Sediment samples were stored in freezer bags and kept on ice in coolers in the field and were then later dried in preparation for clay analysis.

Field Analysis

Field analysis consisted of pH, alkalinity, temperature and reduced iron measurements. Water temperature was measured using a standard mercury laboratory thermometer. pH was measured with an Orion model 399A pH meter equipped with an Orion 91-05 combination electrode. Reference standards of pH 7 and 10 were brought to the same temperature as the water sample by placing them in the discharge bucket during the purging process or stream collection. This allowed the reference standards to equilibrate to the temperature of the discharging well water. The pH meter was then calibrated with these reference standards. Unfiltered water samples were collected in a beaker and measured for pH.

Alkalinity measurements were performed by placing 2 ml of unfiltered water into a glass vessel equipped with magnetic stir bar. Water samples were then titrated using a Brinkman micropipet filled with 0.01639N Sulfuric acid solution following a procedure similar to that of U.S.G.S method I-2030-85 (1989). Sulfuric acid solutions were standardized against a 1000 mg/L Na_2CO_3 solution daily before field measurements began.

Reduced iron species were measured using a method similar to that described by Muray and Gill (1978). Water samples were filtered with a 45 micron filter pack and were discharged into a 125 ml Nalgene bottle that was placed inside a 500 ml Nalgene beaker. The 125 ml Nalgene bottle was then allowed to overflow into the 500 ml Nalgene beaker, which in turn was allowed to overflow. Using this procedure the water sample being collected inside the 125 ml Nalgene bottle was completely cut off from contact with ambient air. After letting the containers overflow for a few

minutes, a 1 ml Ependorf pipet was inserted into the 125 ml Nalgene bottle. A 2 ml of sample was then extracted from the container and pipeted into a glass couvet. 2 ml of 0.05 ug/L, 1.0 ug/L and 2.0 ug/L iron standards and a blank were in turn pipeted into individual couvets. Two ml of ferrozine was then pipeted into each couvet. A light purple color quickly developed in samples and standards bearing reduced iron. Absorbance was measured within 30 seconds using a Bausch and Lomb 121 spectrophotmeter at a wavelength of 562 nm.

Analytical Methods

Cation concentrations in the collected groundwater and surface water samples were measured by atomic absorption and graphite furnace atomic absorption spectroscopy using a Perkin-Elmer 5100 A.A.S instrument with a HGA 5100 Controller and AS Autosampler. Standards for cation analysis were made by the dilution of 1000 mg/L stock solutions. Anion concentrations were measured through colorimetric and turbidimetric techniques using a Milton Roy 5000 spectrophotometer.

Calcium and Magnesium

Groundwater and surface water samples were analyzed for calcium and magnesium (in mg/L) using the methods for determination described in U.S.G.S (1989) method I-1152-85 and I-1447-85, respectively, and Perkin-Elmer (1982). To suppress phosphate, sulfate, or aluminum interference, 0.2 ml of $LaCl_3$ was added to standards and samples. Water samples outside the recommended linear range were diluted 1:25, 2:25, or 5:25 depending on the initial concentrations of these cations.

Sodium and Potassium

Ground water and surface water samples were analyzed for sodium and potassium (in mg/L) using the methods for determination described in U.S.G.S (1989) method I-1735-85 and I-1630-85 , respectively, and Perkin-Elmer (1982). Water samples outside the recommended linear range were diluted 1:25, 2:25, or 5:25, depending on the initial concentrations.

Chloride

Chloride was measured in (mg/L) using a ferric thiocyanate colorimetric, automated-discrete method of determination (U.S.G.S I-2188-85, 1985). This method has a detection range from 0.10 to 500.00 mg/L, and indicates that the sample retains a constant absorbance reading for over an 1 hour. The absorbance measurements for standards and samples, although initially stable for the first few minutes of analysis, declined over time. To achieve reproducible, accurate, results chloride measurements on standards and samples were performed on three separate runs. Since absorbance through time for each run varied, an average absorbance for the three runs was taken at the end of the first minute of analysis. A calibration curve of concentration versus absorbance was constructed and sample concentrations were determined correcting for the time variation.

Sulfate

Sulfate was measured (in mg/L) using the barium sulfate turbidimetric method outlined in Standard Methods for the Examination of Water and Waste Water (1971).

Silica

Silica was measured (in mg/L) using the molybdosilicate colorimetric method outlined in Standard Methods for the Examination of Water and Waste Water (1971).

Trace Metals

Iron, manganese, nickel, copper, zinc, barium, and strontium were measured in concentrations of ug/L by methods outlined in Perkin-Elmer (1985) using a HGA Zeeman/5000 Graphite Furnace and AS Autosampler. Iron, manganese and zinc were measured using recommended HGA conditions by the atomization of sample solutions off a L'vov Platform in a pyrolytically coated tube, with a $Mg(NO_3)_2$ matrix modifier. Water samples were diluted using an AS-40 autosampler or using acid washed volumetric flasks depending on the samples concentration. Ramping time and temperature were altered in pretreatment and atomization steps to optimize absorbance.

Copper and nickel were measured using methods similar to that outlined above but with no addition of a matrix modifier. Barium and strontium were analyzed by the atomization of sample solution off the wall of a pyrolytic tube, with no addition of a matrix modifier.

Pre-treatment for Clay Mineralogy Analysis

Sediment samples were prepared for clay determination using procedures outlined by Jackson (1969) with modifications described by S. Anderson (oral communication). Carbonates and soluble salts were first removed from sediment samples. Sediment samples were placed in a Pyrex beaker, wetted with distilled water and heated to 75°C. To this was added a 1 molar sodium acetate solution, adjusted to a pH of 5.0 with acetic acid was added until effervescing ceased. Supernate was then siphoned off and discarded.

Organic matter was removed by the addition of approximately 30 ml of hydrogen peroxide over a 5 day period while sediment samples were maintained at 75°C. Clay was then separated from the sediment sample by allowing the sand and silt size particles to settle out from flocculatent material through the addition of water

and NaCl in 5 liter beakers over time periods based on Stokes' Law. Supernate was then siphoned off and discarded.

The clay samples were then divided into two subsets and saturated with potassium chloride and magnesium chloride, respectively. In addition to this division, clay samples from Goose Lake Inlet, Goose Lake Outlet, Goose Lake Tel, and Warner Creek were further split into two other subsets for iron oxide removal. Iron oxides were removed using the sodium dithionite-citrate-bicarbonate to allow for better clay orientation during preparation of slide mount (Aguilera and Jackson, 1953). After iron was removed, the clay samples were then divide into another set of sub samples and saturated with potassium chloride and magnesium chloride. Chloride was then removed from all clay samples through a series of washes with ethanol. Glycol was added to magnesium saturated samples which were then heated at 80°C in an oven overnight. Clay fractions were mounted on glass slides with pasture pipets.

X-Ray Analysis

Determination of clays were made using a Philips 3100 X-Ray Generator with copper tube. Goniometer measurements were made at scanning speed of 5° / 5.00 seconds, rotating from 2° to 30° (2œ). Potassium saturated slides were analyzed in a series of 25°C, 100°C, 300°C and 550°C heat treatments. Magnesium glycol saturated slides were analyzed at 25°C.

Groundwater and Surface Water Chemistry

Groundwater analyses for major and trace elements, and additional monitoring well data from William and Works (1988) are presented in Tables 5 and Table 6. Analyses of surface water, precipitation (NAPD/NTN, 1992), and Lake Superior (Water-Resource Data, 1980) for major elements are presented in Table 7. Surface water analyses for trace elements are presented in Table 8.

Groundwater Isogram Maps

The spatial distribution of groundwater constituents in the Sands Plain study area is displayed by a series of isogram maps. The Sands Plain study area is defined by sample site location, and differs from the Sands Plain modeled area which was defined by the model-grid. Isogram maps display lines of equal concentration for individual ion species and/or concentrations of dissolved solids, in the glacial aquifer. These maps assume homogeneity in the composition of groundwater in the vertical direction. Two wells (MQT dump and Gravel Well) in the northern section of the study area are shown on the isogram map series but do not reflect water of the glacial aquifer. These wells are completed in Siamo Slate and Kona Dolomite, respectively, and are included in the map series to characterize water quality in the north where uncertainty remains in the hydraulic interconnections between fractured bedrock associated with the Palmer fault and glacial deposits.

An isogram map of total dissolved solids is displayed in Figure 17. Total dissolved solids concentrations above 150 mg/L for water from wells 19, ETW-2, 21, 15, and Gravel are observed to form an elliptical pattern in the north west section of the modeled area. Total dissolved solids less than 150 mg/L but greater than 100 mg/L encircle this area of elevated concentrations to the south and east. Total dissolved solids less than 100 mg/L are observed in the remaining wells and surround both these areas to the south and east. Well 11 (the southern most well) displays a concentrations slightly above 100 mg/L.

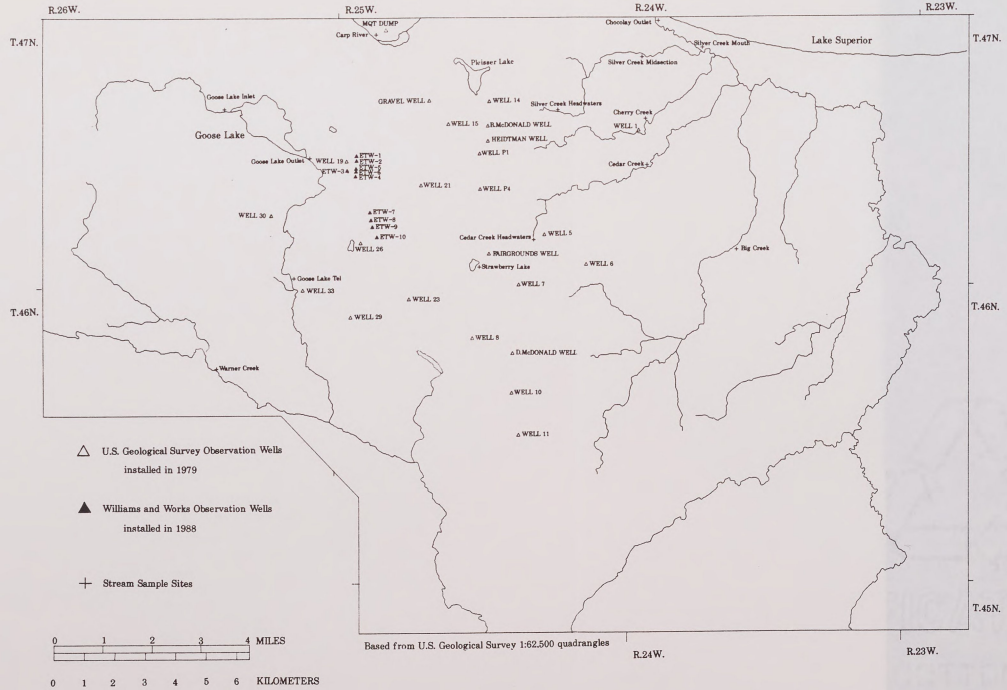

Figure 16 Groundwater and Surface Water Sample Site Locations

Table 5 Groundwater Major Species in mg/L

WELL	Temp	pH	Ca^{+2}	Mg^{+2}	Na^{+}	K^{+}	$HCO3^{-}$	$SO4^{-2}$	Cl^{-}	Si	TDS
Well 30	8.0	8.65	7.62	2.06	1.84	0.42	24.37	3.33	5.87	3.98	49.59
Well 29	8.0	8.35	12.41	1.87	1.49	0.52	36.33	3.92	6.05	3.14	65.73
Well 26	8.0	8.31	16.94	2.65	1.45	0.36	55.16	3.75	5.49	2.81	88.61
Well 23	8.0	8.03	7.96	2.23	1.09	0.94	26.99	3.17	5.05	3.80	51.23
Well 19	9.0	7.02	32.00	7.74	3.49	1.01	76.41	39.33	8.54	3.68	172.20
Well 15	8.0	6.97	57.82	14.97	4.20	1.85	203.31	12.75	27.03	4.85	326.78
Well 11	7.0	8.51	19.77	3.55	1.12	0.31	64.03	7.92	4.01	3.50	104.21
Well 10	8.0	8.70	9.93	2.00	0.88	1.00	37.84	3.67	1.00	3.02	59.34
Well 8	9.0	7.40	7.99	1.77	1.06	1.05	31.51	3.33	1.12	3.41	51.24
Well 7	9.0	8.21	15.40	3.47	1.57	0.70	65.67	2.75	0.52	4.04	94.12
Well 5	8.0	8.02	21.00	5.22	1.63	0.65	87.61	5.00	1.13	5.16	127.40
Well 1	7.5	8.41	15.03	3.61	1.36	0.71	62.15	3.17	1.64	4.46	92.13
Well P4	8.0	7.87	21.98	4.85	0.94	0.59	84.73	5.83	1.67	4.49	125.08
Fairgrounds	8.0	8.60	15.05	2.69	1.12	0.49	54.50	5.08	1.18	3.99	84.10
Gravel Well	8.0	7.51	52.20	14.06	5.86	3.70	221.85	10.17	10.34	4.13	322.31
Heidtman	9.0	8.28	20.70	4.55	1.99	0.99	68.62	14.33	2.53	3.92	117.63
B. McDonald	9.0	8.17	20.70	4.22	1.84	0.53	80.39	5.00	1.99	4.87	119.54
D. McDonald	9.0	8.53	8.19	2.39	1.39	0.47	35.88	3.42	0.58	3.89	56.21
MQT Dump	9.5	7.84	25.80	9.32	2.17	1.03	123.73	5.92	1.91	7.13	177.01
Field B I	-	-	0.00	0.00	0.00	0.00	-	0.00	0.00	0.00	0.0
Field B II	-	-	0.00	0.00	0.00	0.00	-	0.00	0.00	0.00	0.0

Table 5 (cont'd)

WELL	Temp	pH	Ca^{+2}	Mg^{+2}	Na^{+}	K^{+}	$HCO3^{-}$	$SO4^{-2}$	Cl^{-}	Si	TDS
* ETW-2	-	8.38	40.1	8.8	4.2	0.7	119.9	38.8	6.0	5.0	222.8
* ETW-3	-	7.01	42.0	9.7	-	-	78.0	26.0	3.4	5.0	-
△ Well 21	-	-	47.0	10.0	3.0	-	140.0	48.0	5.6	5.0	-

* Water samples collected and analyzed by Williams and Works, 1988

△ Water sample collected and analyzed by Grannemann, 1984

Table 6 **Groundwater Trace Species in μg/L**

Site	Al	Ba	Cu	Fe(III)	Fe(II)	Mn	Ni	Sr	Zn
Well 30	21.00	70.62	0.22	0.00	36.38	0.72	2.10	34.25	197.45
Well 29	33.68	21.25	0.80	18.90	4.85	1.27	0.00	31.00	139.78
Well 26	51.15	37.80	1.29	85.63	11.12	39.45	0.08	26.25	198.78
Well 23	49.25	10.63	0.50	15.86	24.89	0.96	0.08	25.25	359.45
Well 19	52.06	56.25	6.21	50.63	0.00	7.02	2.42	140.75	89.45
Well 15	27.71	71.25	1.05	23.17	4.33	2.81	1.01	79.25	219.45
Well 11	62.18	21.25	0.22	10.36	13.14	1.14	0.20	23.00	99.78
Well 10	111.15	11.88	0.00	12.93	21.70	0.34	0.39	14.75	189.78
Well 8	112.35	10.00	0.90	6.75	0.00	0.68	0.29	10.75	219.45
Well 7	67.13	20.00	2.40	26.48	3.15	34.70	1.98	33.50	189.45
Well 5	68.67	28.75	2.47	0.00	8.50	1.82	1.00	30.25	99.45
Well 1	55.17	43.33	1.47	5.78	0.00	0.83	0.38	39.00	119.45
Well P4	50.25	27.50	3.68	15.51	48.74	1.14	0.96	28.25	229.45
Fairgrounds	46.92	17.50	0.96	46.25	0.00	1.70	0.80	18.75	359.45
Gravel Well	44.17	94.16	2.22	0.00	40.88	1.66	0.84	80.00	229.45
Heidtman	113.84	22.50	14.12	147.55	12.20	2.93	0.60	29.25	149.45
B McDonald	109.16	32.92	2.44	54.63	0.00	1.28	0.93	27.00	109.45
D McDonald	48.38	12.50	0.39	49.71	13.79	0.50	0.51	55.00	319.45
MQT Dump	56.67	510.00	8.95	32.88	0.00	2.71	0.83	472.50	629.45
Blank I	0.00	0.0	0.00	0.00	0.00	0.00	0.46	0.00	0.00
Blank II	0.00	0.0	0.00	0.00	0.00	0.00	0.33	0.00	0.00

Table 7 Stream and Lake Major Species in mg/L

Site	Temp	pH	Ca^{+2}	Mg^{+2}	Na^{+}	K^{+}	$HCO3^{-}$	$SO4^{-2}$	Cl^{-}	Si	TDS
Big Creek	10.0	8.33	24.25	5.50	1.56	0.80	94.20	6.05	3.10	4.53	139.9
Carp River	16.0	8.01	23.00	6.61	8.25	1.41	98.39	8.30	10.20	22.57	178.73
Cedar Creek Headwaters	10.0	7.61	21.75	4.36	4.20	0.75	75.48	4.52	11.13	3.31	125.50
Cedar Creek	10.0	7.70	20.88	4.36	1.80	0.59	80.76	4.11	3.26	3.83	119.59
Chocolay Outlet	14.0	7.80	24.50	5.61	4.40	0.93	99.19	5.81	5.48	3.77	149.69
Fish Hatchery	8.0	8.00	27.25	6.05	3.40	0.72	97.59	10.56	6.87	4.22	156.66
Goose Lake Inlet	14.0	8.27	48.25	26.33	42.50	7.25	313.43	49.79	10.42	2.94	500.66
Goose Lake Outlet	22.0	8.53	32.75	7.38	30.50	4.38	117.77	62.35	8.58	6.09	269.80
Goose Lake Tel	11.0	7.50	19.00	6.38	11.63	1.53	91.42	12.93	7.58	4.22	154.69
Silver Creek Headwaters	10.0	8.00	29.63	6.36	1.96	0.65	113.10	5.81	4.95	3.85	166.31
Silver Creek Midsection	11.0	8.00	31.63	7.35	1.84	0.81	123.28	5.77	5.58	4.30	180.56
Silver Creek Mouth	9.0	7.91	26.75	5.87	3.75	0.80	106.93	9.59	1.53	4.09	159.31
Strawberry Lake	21.0	8.30	6.66	1.39	0.48	0.37	26.37	2.19	0.00	0.15	37.61
Warner Creek	9.0	7.40	38.25	20.70	29.50	4.38	257.22	17.23	13.95	3.10	384.33
Field Blank	-	-	0.00	0.00	0.00	0.00	-	0.00	0.00	0.00	0.0
* Rain and Snow at Chessel 9/24/91	-	5.2	0.43	0.05	0.02	0.04	1.05	1.00	0.05	0.2	3.2
* Rain and Snow at Chessel 9/24/90	-	4.9	0.22	0.02	0.04	0.01	0.93	0.5	0.05	0.2	2.0
Î Lake Superior	19.0	7.7	14.0	2.8	1.5	0.6	49.9	7.6	71.2	5.0	82.6

* Water sample collected and analyzed by NADP/NTN, 1992; Î Water sample from Water-Resource Data, 1980

Table 8 Stream and Lake Trace Species in μg/L

Sample	Al	Ba	Cu	Fe total	Mn	Ni	Sr	Zn
Big Creek	42.81	28.04	1.49	94.35	1.60	0.67	46.50	210.00
Carp River	85.00	11.72	0.81	229.35	116.75	0.81	153.00	110.00
Cedar Creek Headwaters	47.56	15.98	0.11	18.98	0.74	0.31	34.0	180.00
Cedar Creek	45.06	21.92	0.31	9.54	0.58	0.10	24.00	80.00
Chocolay Outlet	59.94	33.23	0.53	224.35	13.13	0.16	45.50	140.00
Fish Hatchery	52.38	30.80	0.41	19.79	2.36	2.88	43.50	230.00
Goose Lake Inlet	39.83	26.70	0.99	128.35	47.38	0.33	685.00	70.00
Goose Lake Outlet	37.38	20.78	0.45	22.35	14.44	0.00	570.00	100.00
Goose Lake Tel	98.25	16.14	0.51	1706.85	33.88	0.57	148.50	130.00

Table 8 (cont'd)

Sample	Al	Ba	Cu	Fe total	Mn	Ni	Sr	Zn
Silver Creek Headwaters	79.75	23.82	0.29	23.41	2.78	0.20	38.50	70.00
Silver Creek Midsection	110.38	25.56	0.24	25.04	1.24	0.00	38.50	90.00
Silver Creek Mouth	108.13	29.84	0.40	23.35	4.95	0.00	44.00	80.00
Strawberry Lake	114.75	9.36	0.30	60.03	0.43	0.00	12.00	60.00
Warner Creek	155.00	13.60	0.63	459.35	225.00	2.78	180.00	70.00
Field Blank	0.00	0.00	0.00	0.00	0.00	0.00	0.00	0.00
*Lake Superior	-	20.0	5.0	10.0	-	-	20.0	20.0

* Water sample from Water-Resource Data, 1980

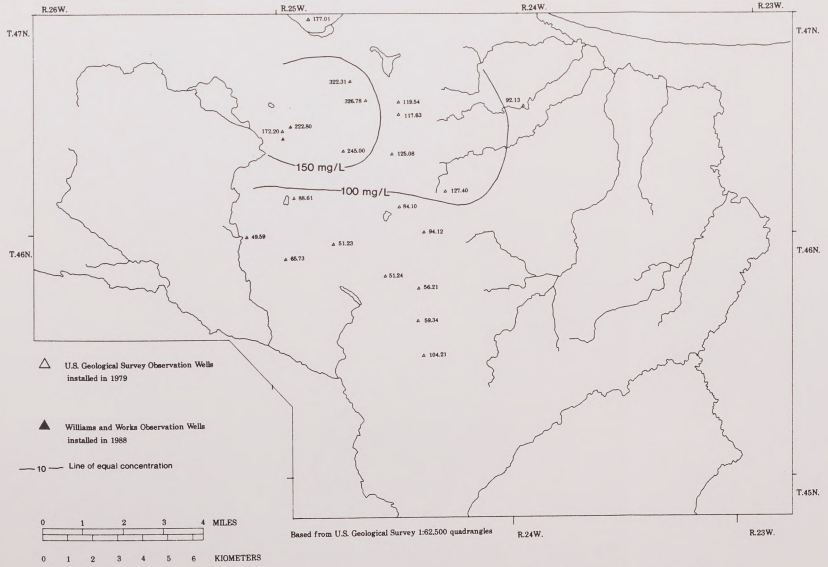

Figure 17 Distribution of Total Dissolved Solids in mg/L

Similar trends in cation distribution for the Sands Plain study area are observed. Figure 18 displays the distribution of calcium in mg/L in the Sands Plain area. Calcium concentrations above 35 mg/L occur in wells 19, 21, 15, ETW-2, and Gravel, and form a elliptical pattern near Goose Lake Outlet in the northwestern section of the study area. Concentration of calcium between 35 mg/L and 15 mg/L encircle this area of elevated concentrations to the south and east. Calcium concentrations less than 15 mg/L form a broad band in the southern most region of the modeled area. Well 11 (the southern most well) displays a concentration slightly above 15 mg/L.

Figure 19 displays the distribution of magnesium in mg/L. Magnesium concentrations above 7 mg/l occur near Goose Lake Outlet in wells 19, 21, 15, ETW-3, and Gravel. Concentrations for magnesium are less than 7 mg/L in the remaining wells.

Figure 20 displays the distribution of sodium and potassium in mg/L. Sodium and potassium concentrations above 3 mg/L occur in wells 19, 21, 15, ETW-2, and Gravel near Goose Lake Outlet. Concentrations lower than 3 mg/L characterize the remaining wells of the modeled area.

The distribution of anions in the modeled area is spatially similar to that of cations. Figure 21 displays the distribution of bicarbonate in mg/L. Wells 15 and Gravel have concentrations of bicarbonate greater than 200 mg/L. Lower concentrations of bicarbonate occur in a broad band lying south of these wells ranging between 200 and 50 mg/L. The lowest concentrations of bicarbonate (50 mg/L) occur to the south. Well 11 (the southern most well) displays a concentration slightly above 50 mg/L.

Figure 22 displays the distribution of sulfate in mg/L as a bull's eye pattern. Sulfate concentrations greater than 20 mg/L occur in wells 19, ETW-2, and 21 near Goose Lake outlet. Lower concentrations from 20 to 5 mg/L occur surrounding this area

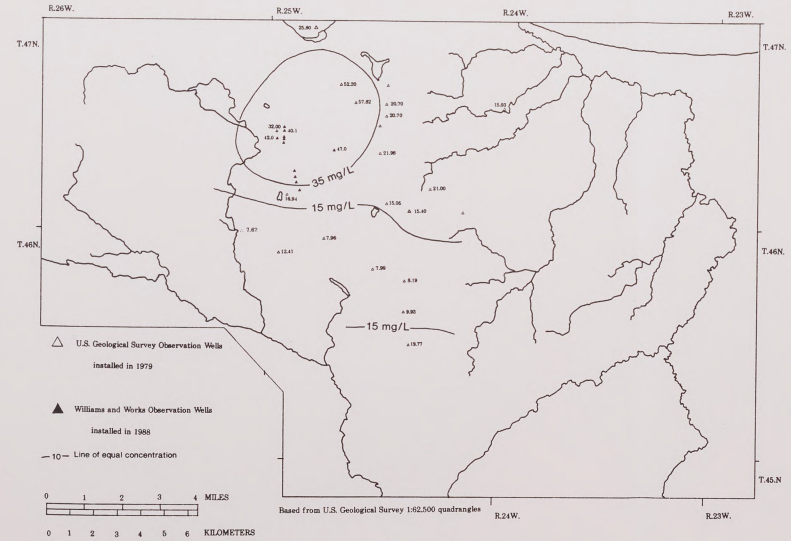

Figure 18 Distribution of Calcium in mg/L

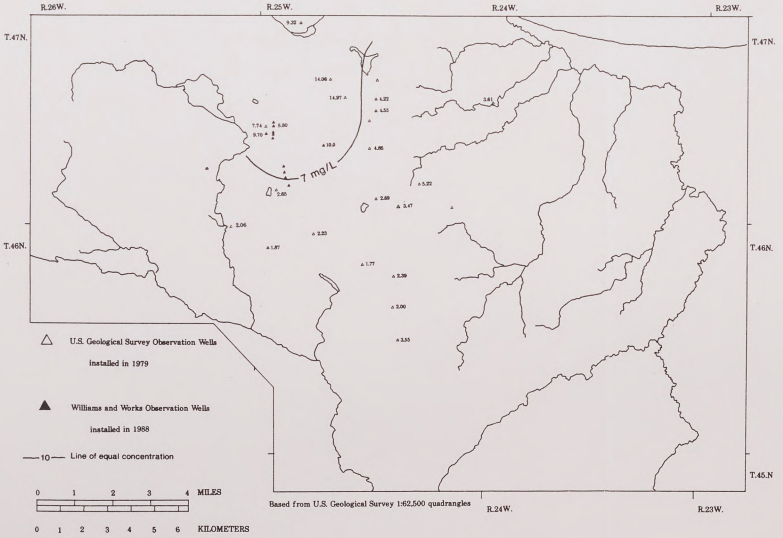

Figure 19 Distribution of Magnesium in mg/L

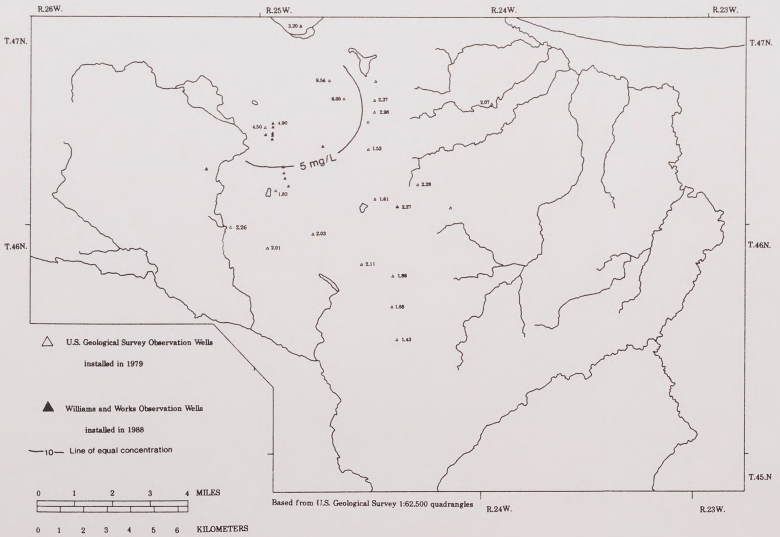

Figure 20 Distribution of Sodium + Potassium in mg/L

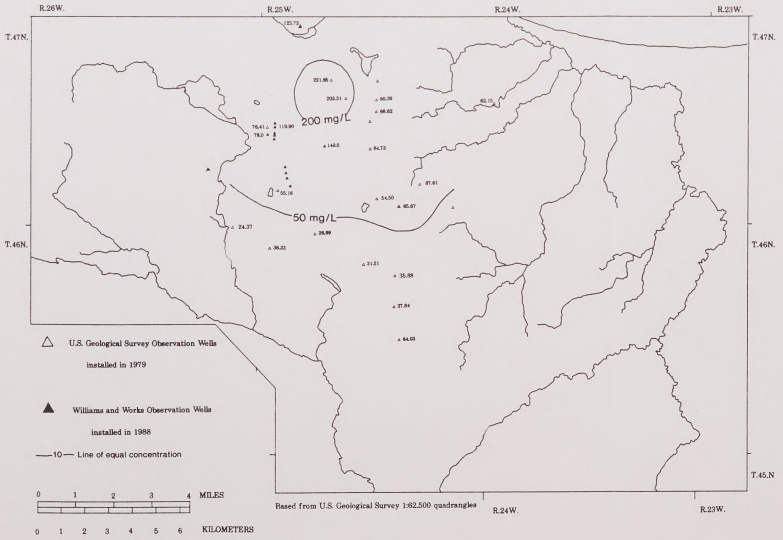

Figure 21 Distribution of Bicarbonate in mg/L

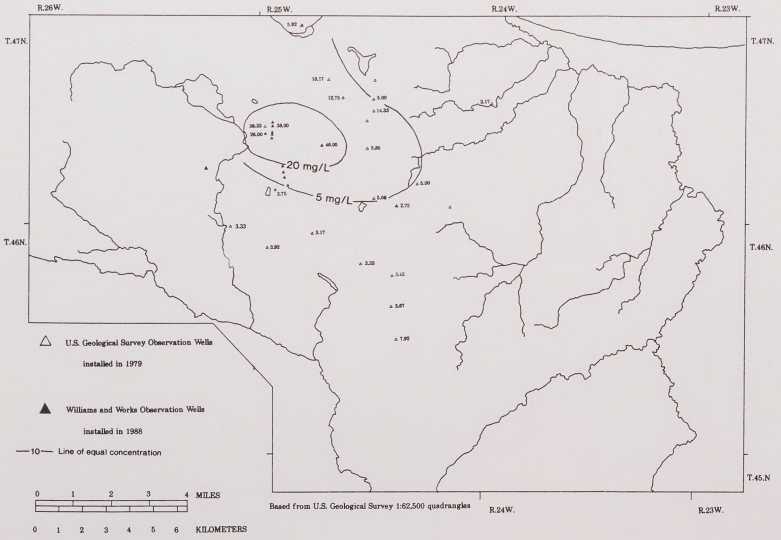

Figure 22 Distribution of Sulfate in mg/L

of elevated concentrations to the south and east. Concentrations of sulfate less than 5 mg/L occur to around both these areas.

Figure 23 displays the distribution of chloride in mg/L. Chloride concentrations above 5 mg/L occur in the western section of the study area. Concentrations of chloride less than 5 mg/L occur to the south and east.

Trace elements in the Sands Plain area have distributions that are either similar to that of cations, or display no distribution trends at all. Figure 24 displays the distribution of barium in μg/L. Barium concentrations above 50 μg/L occur in wells 19, ETW-2, 21, 15 and Gravel near Goose Lake Outlet. Concentration less than 50 μg/L occur in the remaining wells surrounding this area of elevated concentrations.

The distribution of manganese in μg/L is displayed in Figure 25. Manganese concentrations above 10 μg/L occur in wells 19, ETW-2, 21, and 26 near Goose Lake Outlet. Well 7 also shows elevated concentrations of manganese above 10 μg/L. Concentrations less than 10 μg/L are observed in the remaining wells in the study area.

Figure 26 displays the distribution of strontium in μg/L. Concentration of strontium above 60 μg/L occur in wells 19, ETW-2, 21, 15 and Gravel near Goose Lake Outlet. Concentrations of strontium less than 60 μg/L occur in remaining wells surrounding this area of elevated concentrations.

Isogram maps indicate an area of relatively high concentrations of dissolved constituents near Goose Lake in the northern portion of Sands Plain study area. Isogram maps also indicate that the southern region of the Sands Plain study area has relatively low concentrations of dissolved constituents. Distribution of water chemistries presented in isogram maps are consistent with hydrologic zone information, in which flow the northern portion of the Sands Plain area can be distinguished from flow in the southern portion.

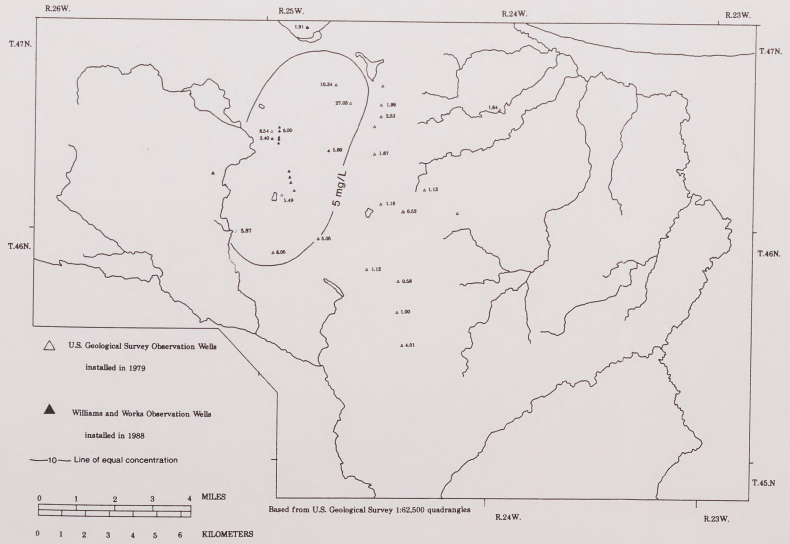

Figure 23 Distribution of Chloride in mg/L

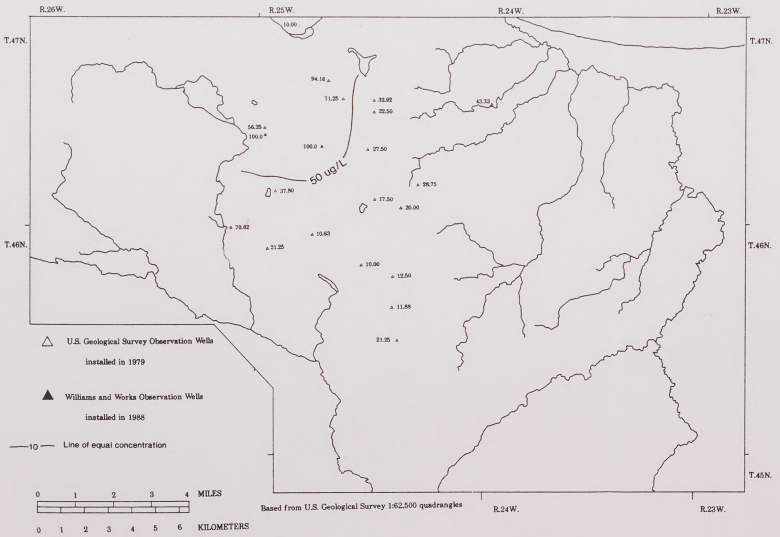

Figure 24 Distribution of Barium in ug/L

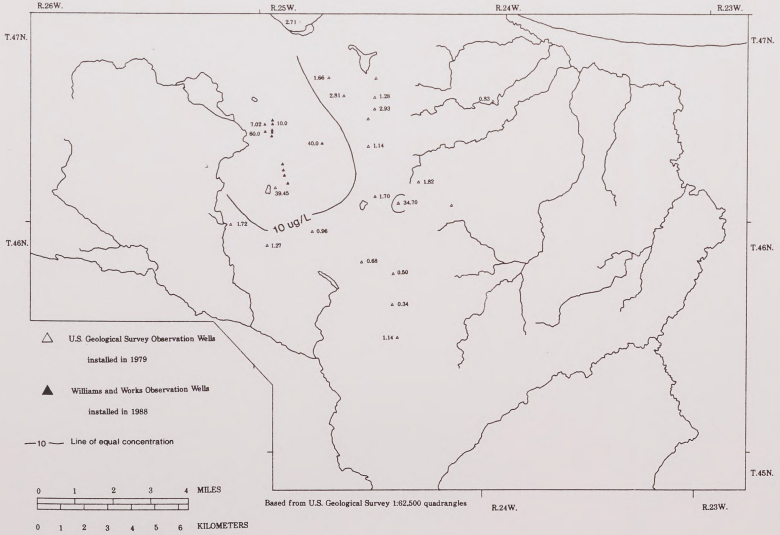

Figure 25 Distribution of Manganese in ug/L

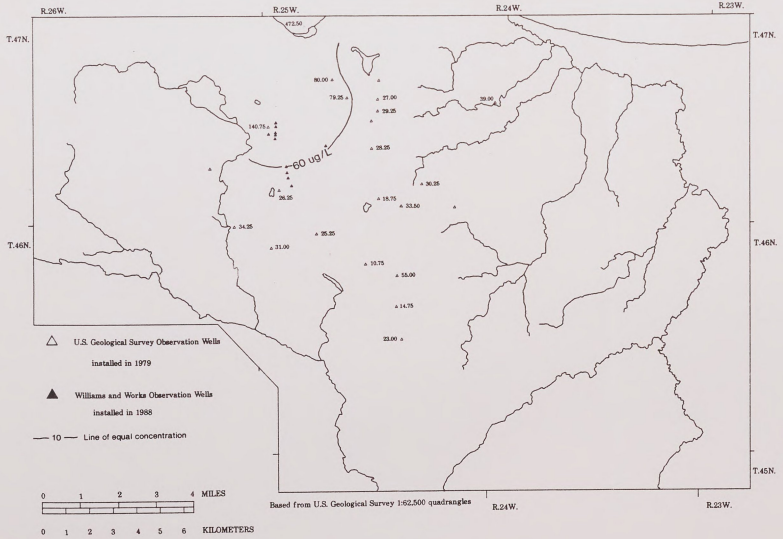

Figure 26 Distribution of Strontium in ug/L

Piper Diagrams

Piper diagrams (Piper, 1944) are used to display major-ion composition for groundwater, streamflow, Lake Superior water and precipitation data for the Sands Plain study area. These diagrams are constructed by plotting the relative abundance of cations (Ca^{+2}, Mg^{+2}, Na^{+}+ K^{+}) in %meq/L and anions ($HCO3^{-}$, $SO4^{-2}$ and Cl^{-}) in %meq/L on to cation and anion triangles, respectively. Straight lines are then projected from both cation and anion triangles on to a quadrilateral field to represent the overall major-ion composition of a single water sample.

Figure 27 displays the major-ion composition of groundwater observed in the Sands Plain area. The cation triangle in the lower left of this figure indicates that all groundwater samples have approximately the same percentage ratio 65: 35: 5 of Ca: Mg: Na+K, respectively.

The anion triangle in the lower right of Figure 27 indicates that the bicarbonate anion is over 50% of the total anion composition for all groundwater samples. A closer look at the anion triangle displays a "V" shaped distribution in anion abundance. The apex of this "V" shaped distribution is centered near the 90% bicarbonate mark with the limbs of the "V" extending towards the sulfate and chloride boundaries. Groundwaters which have high sulfate abundance and plot along the outer portion of the sulfate limb are from wells 19, 21, and Heidtman. These wells are located in the northern section of the study area and are down flow of Goose Lake Outlet (see Figure 16). Groundwaters which have a higher chloride abundance and plot along the outer portion of the chloride limb are from wells 30, 29, and 23. These wells are located to the south of Goose Lake Outlet in the western portion of the study area.

Groundwater samples plotted in the quadrilateral field fall into a general Ca-Mg-HCO3 facies category described by Back (1961). Groundwater samples are located along a narrow compositional band in the quadrilateral field, with those samples plotting on the outer portion of the sulfate and chloride limbs at one end of the band and those samples plotting near the apex at the other.

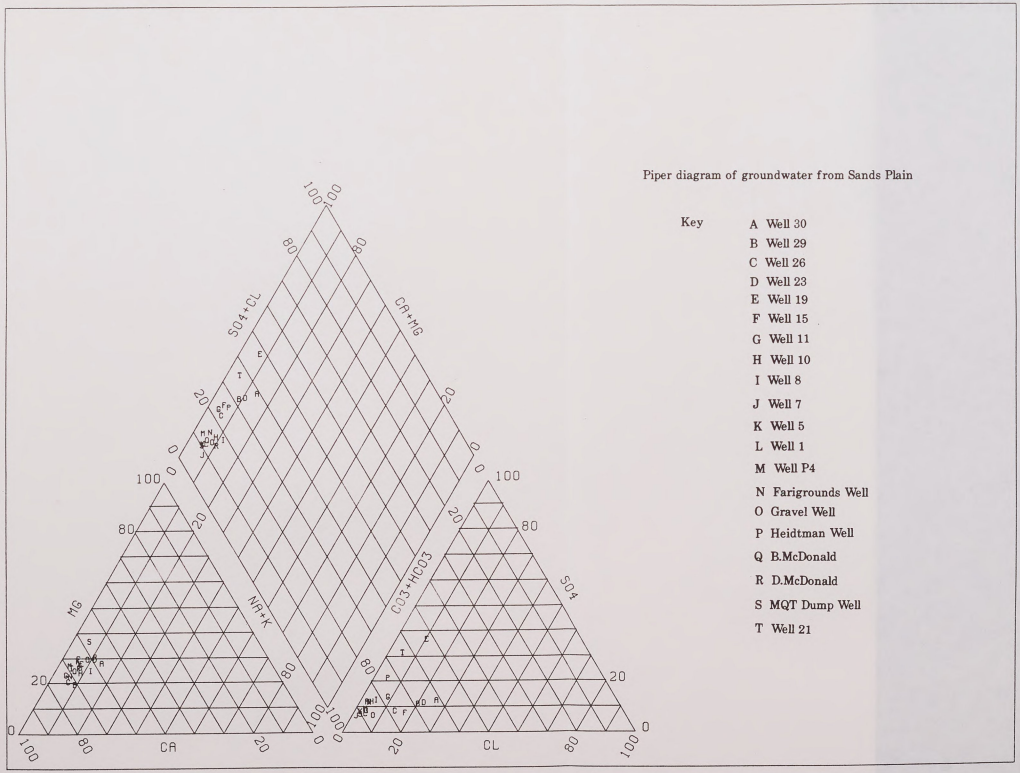

Piper diagram of groundwater from Sands Plain

Key

A Well 30
B Well 29
C Well 26
D Well 23
E Well 19
F Well 15
G Well 11
H Well 10
I Well 8
J Well 7
K Well 5
L Well 1
M Well P4
N Farigrounds Well
O Gravel Well
P Heidtman Well
Q B.McDonald
R D.McDonald
S MQT Dump Well
T Well 21

Figure 27

Major-ion compositions for surface water samples, Lake Superior (Water-Resource Data, 1980) and precipitation (NAPD/NTN, 1992) are plotted in Figure 28. The cation triangle in the lower left of this figure displays three populations of cation abundances. Samples plotting in the center of the triangle are Goose Lake Inlet, Goose Lake Outlet, Warner Creek, Carp River and Goose Lake Tel. These samples represent surface waters that are located outside of or along the boundaries of the Sands Plain study area. Lake Superior water and surface water samples inside the study area have approximately the same cation percentage ratio 65: 35: 5 of Ca: Mg: Na+K. It should be noted that the cation abundance ratios for both streamflow water found inside the study area and for groundwater samples are similar. Precipitation data for the Sands Plain has approximately a cation percentage ratio 75: 25: 10 of Ca: Mg: Na+K, respectively.

The anion triangle in the lower right of Figure 28 displays two populations. Lake Superior water and almost all of the surface water samples have over 72% $HCO3^-$ as their total anion composition. The second population observed in this figure is made up of precipitation and Goose Lake Outlet which have higher abundances of sulfate.

Surface water samples plotted in the quadrilateral field fall into a general Ca-Mg-HCO3 facies category described by Back (1961). Lake Superior, precipitation and surface water samples located inside the Sands Plain study area plot along a narrow band similar to that observed for groundwater. Surface water samples located outside or along the northern boundaries of the study area fall outside this narrow band.

Surface water from lakes and streams, and groundwater from a bedrock well previously sampled by Grannemann (1979, 1984) are displayed in Figure 29. The cation triangle in this figure shows a cation ratio of 65: 35: 5 for Ca: Mg: Na+K similar to that of surface and groundwater described above. Groundwater from bedrock well 14 and surface water samples from Harvey Lake and Pleisser Lakes fall outside this composition range. The anion triangle in the lower

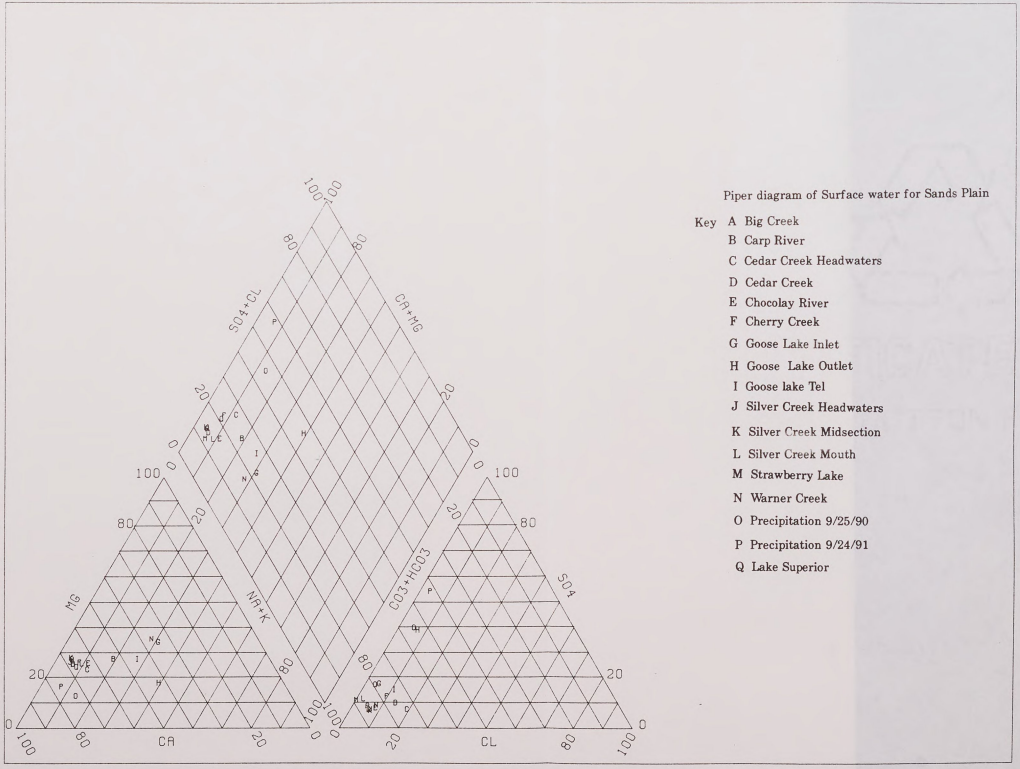

Piper diagram of Surface water for Sands Plain

Key
- A Big Creek
- B Carp River
- C Cedar Creek Headwaters
- D Cedar Creek
- E Chocolay River
- F Cherry Creek
- G Goose Lake Inlet
- H Goose Lake Outlet
- I Goose lake Tel
- J Silver Creek Headwaters
- K Silver Creek Midsection
- L Silver Creek Mouth
- M Strawberry Lake
- N Warner Creek
- O Precipitation 9/25/90
- P Precipitation 9/24/91
- Q Lake Superior

Figure 28

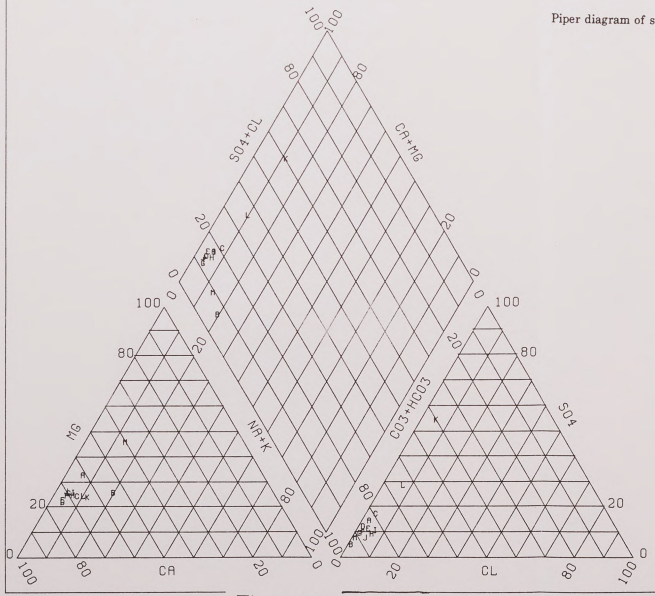

Piper diagram of surface water from Sands Plain, U.S. Geological Survey data

Key
- A Plessier Lake
- B Harvey Lake
- C Lake Superior
- D Norby Lake
- E Peterson Creek site 2
- F Big Creek site 5
- G Big Creek site 7
- H Cedar Creek site 10
- I Cherry Creek site 16
- J Silver Creek site 18
- K Goose Lake Inlet
- L Goose Lake Outlet
- M Bedrock Observation Well 14

Figure 29

right of Figure 29 indicates that the bicarbonate anion is over 80% of the total anion composition for almost all surface water samples, except for Goose Lake Inlet and Goose Lake Outlet. Goose Lake Inlet and Outlet have higher sulfate compositions and plot along a similar sulfate limb as describe above. Water compositions plotted on the quadrilateral field are again located along a narrow composition band and range from calcium-bicarbonate to calcium-sulfate ion dominant waters.

Minerals and Clay Minerals

Clay mineralogy was determined at stream sampling sites (see Figure 16) to produce a set of plausible phases which are encountered by stream water in the Sands Plain modeled area. Clay minerals from stream sediments were identified by their characteristic basal reflections from various chemical and thermal treatments, as described previously. Relative abundances of clay minerals were not determined, but are only a small percentage of the bulk sediment sample. Clay minerals identified from different stream site locations include chlorite, illite, and kaolinite. Other minerals in the sediment sample include calcite, quartz, iron oxides and manganese oxides which were identified qualitatively during clay preparation. The presence of calcite was indicated by its reaction to a pH 5 sodium acetate solution, and was observed in all sediment samples. Iron and manganese oxides were identified by the apparent color of the sediment sample before and after the addition of sodium dithionite-citrate-bicarbonate. Iron and manganese oxides occur in sediment samples of Goose Lake Inlet, Goose Lake Outlet and Warner Creek. Figure 30 and 31 show typical X-ray diffraction traces for stream sediment samples. X-ray traces displaying poor peak heights are related to the clay thickness covering a sample slide.

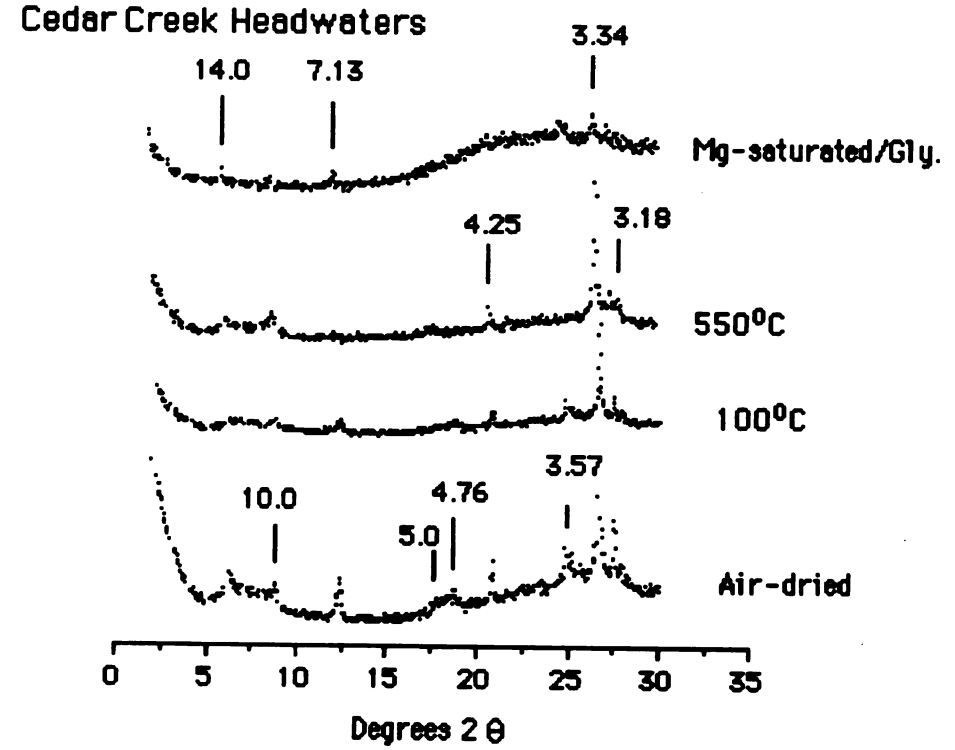

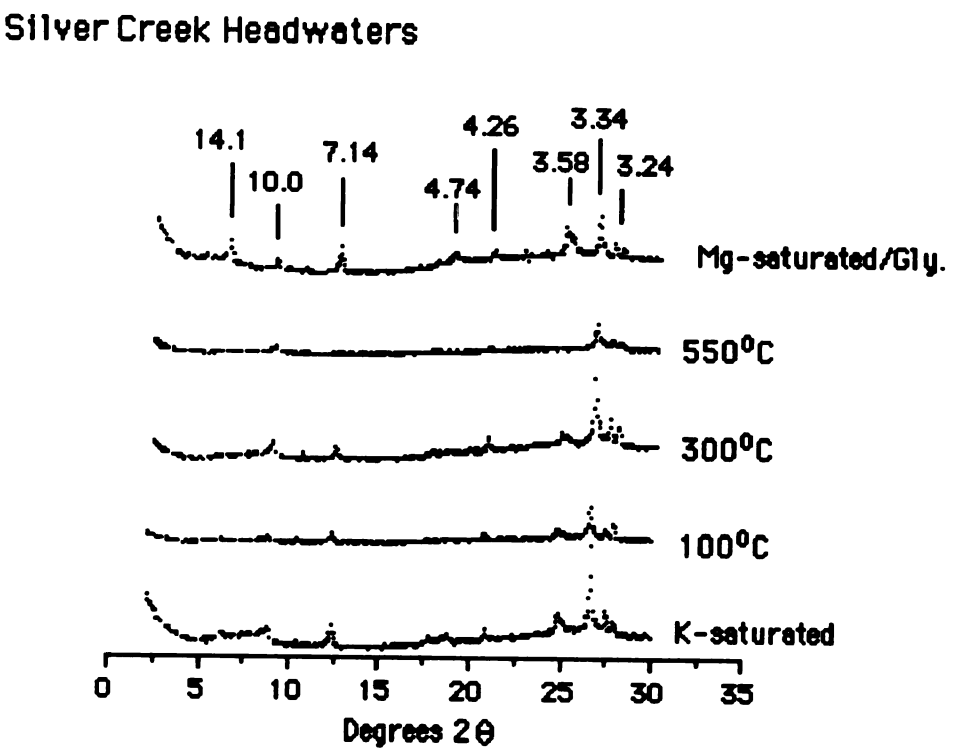

Figure 30 Cedar Creek and Silver Creek Headwaters

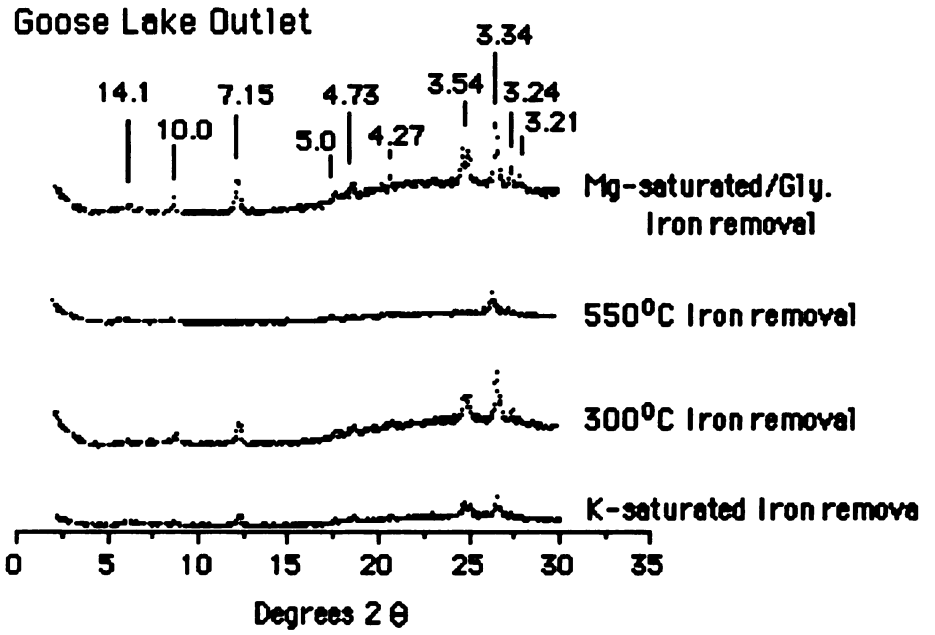

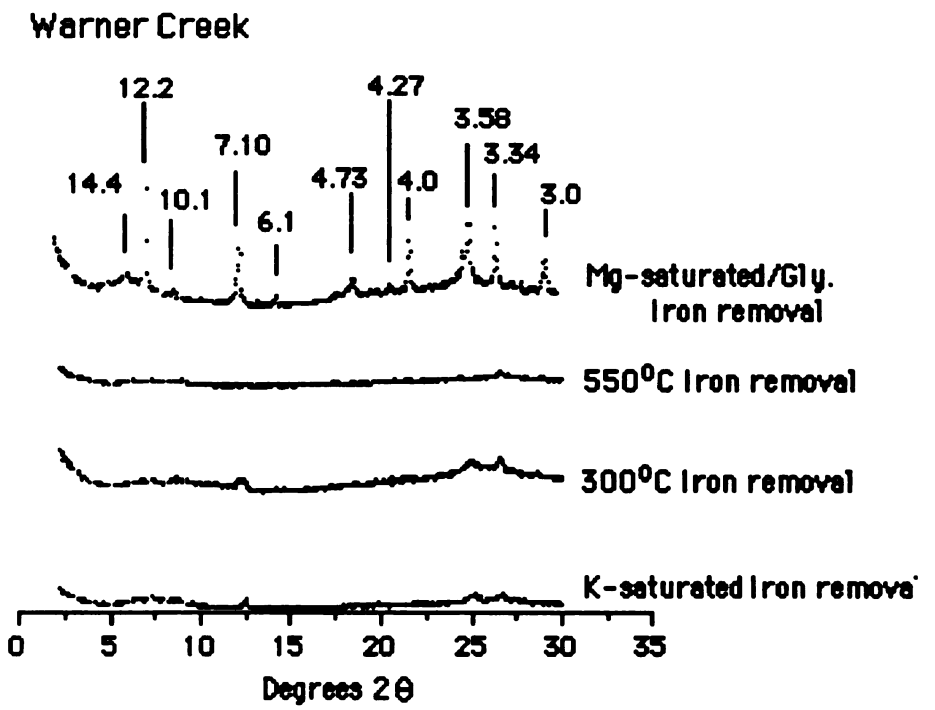

Figure 31 **Goose Lake Outlet and Warner Creek with Iron oxide removal**

Kalolinite Kalolinite was identified from first and second order basal reflections at 7.15 Å and 3.58 Å for K-saturated treatment at 25°C. First and second order kaolinite peaks lose their pronounced basal reflections at temperatures of 550°C or greater, and are distinguished from second and third order chlorite peaks by heating samples to 550°C for an 8 hour period. Kaolinite occurs in all stream samples.

Illite Illite was identified from the first, second, and third order basal reflections at 10.00 Å, 5.00 Å, and 3.33 Å, for K-saturation treatments at 25°C. Illite interlayers do not contract or swell with Mg-saturated/ glycerol treatment, and are not affected by 550°C heat treatment. Illite occurs in all stream samples.

Chlorite Chlorite was identified by from the first, second, third, and fourth order basal reflections at 14.2 Å, 7.12 Å, 4.74 Å, and 3.52 Å, respectively. Chlorite interlayers do not contract or swell with Mg-saturated /glycerol treatment, and do not dehydrate at temperatures equal to or greater than 550°C. Chlorite is distinguished from vermiculite and kaolinite by heating samples for an 8 hour period. Basal reflections at the 12.0 Å, 6.0 Å, and 3.0 Å peaks correspond to dissolution of chlorite interlayers from iron removal treatments and do not represent mixed-interlayer clays (S. Anderson, oral communication). Chlorite occurs in all stream samples.

Chemical Modeling with WATEQ4F

Water chemistries of the Sands Plain area were chemical modeling with the aid of the computer program WATEQ4F (Ball, 1991). This modeling assists in the identification of possible mineral dissolution and precipitation reactions that naturally occur in groundwater and surface water in the southern portion of the study area. It also helps characterize the effects of effluent water from Goose Lake on the equilibria of groundwater and stream water in the northern portion of the study area.

The computer program WATEQ4F (Ball, 1991) uses water analysis (temperature, pH, pe, and concentrations of dissolved species) for the calculation of elemental speciation, activities and activity coefficients of dissolved species, and saturation indices with respect to a mineral phase. WATEQ4F (Ball, 1991) achieves this by iteratively solving a series of simultaneous equations which determine equilibrium constants, and mass balance equations for each component in the system.

For a given reaction, such as

$$aA + bB = cC + dD \qquad (16)$$

the activity product (AP) is defined

$$AP = [A]^a [B]^b / [C]^c [D]^d \qquad (17)$$

where [ ] is the activity or the effective molality of that species. If the reaction is in equilibrium then

$$K_{eq} = [A]^a [B]^b / [C]^c [D]^d \qquad (18)$$

where K_{eq} is equal to AP. A equilibrium constant can be determined thermodynamically over range of temperature conditions by the van't Hoff equation

$$d\ln K_{eq} / dT = -DH^o / RT^2 \qquad (19)$$

where DH^o the change in standard enthalpy of reaction, R is the gas constant (8.314 J/ ^oK mol) and T is the temperature in degrees Kelvin.

Once the activity product and equilibrium constant are defined by WATEQ4F the saturation index (SI) can then be calculated by

$$SI = \log AP/ K_{eq} \qquad (20)$$

Tables 9 display saturation indices (SI) for groundwater and surface water samples with respect to selected mineral phases which are present or are thought to be present in Sands Plain study area. A saturation indice having a value equal to or near zero indicates that the solution is in equilibrium with respect to the specific mineral phase. A saturation indice having a negative value indicates that the solution is undersaturated with respect to the specific mineral phase. A solution which is undersaturated with respect to a specific mineral phase suggests that the mineral phase is either is not present, or will undergo dissolution under these present conditions, unless the reaction is inhibited by kinetic effects. A saturation indice having a positive value indicates that the solution is supersaturated with respect to the specific mineral phase. A solution which is supersaturated with respect to a specific mineral phase suggests that this mineral phase will precipitate under these conditions unless the reaction is inhibited by kinetic effects.

Two problems are associated with chemical modeling with WATEQ4F. The first stems from the fact that water chemistries are entered into the WATEQ4F program as molalities and not as activities. Molalities can be related to activities by

$$a_i = \gamma_i m_i \qquad (21)$$

where a_i is the activity of species (i), m_i is the molality of species (i), and γ_i is the activity coefficient of species (i). The activity

Table 9 Saturation Indices for Groundwater and Surface Water with respect to selected mineral phases

Mineral	Well 30 Log AP/K	Well 29 Log AP/K	Well 26 Log AP/K	Well 23 Log AP/K	Well 19 Log AP/K	Well 15 Log AP/K	Well 11 Log AP/K
Albite	-3.667	-3.845	-3.823	-3.554	-3.243	-3.054	-3.056
Anhydrite	-3.979	-3.719	-3.630	-3.983	-2.433	-2.741	-3.256
Anorthite	-4.193	-3.776	-3.389	-3.457	-3.128	-3.255	-2.950
Aragonite	-0.838	-0.753	-0.491	-1.380	-1.391	-0.809	-0.193
Barite	-0.599	-1.073	-0.868	-1.445	0.177	-0.243	-0.794
Calcite	-0.681	-0.597	-0.334	-1.223	-1.235	-0.652	-0.036
Dolomite	-2.471	-2.556	-2.015	-3.373	-3.726	-2.433	-1.381
Gibbsite	0.655	1.158	1.377	1.643	2.519	2.308	1.316
Goethite	5.119	8.116	8.772	8.028	8.124	7.802	7.917
Gypsum	-3.723	-3.463	-3.373	-3.726	-2.176	-2.485	-2.999
Halite	-9.449	-9.532	-9.591	-9.742	-9.037	-8.470	-9.840
Halloysite	45.975	46.789	47.132	47.931	49.415	49.482	47.444
Hematite	10.878	16.873	18.186	16.698	16.974	16.245	16.389
Kaolinite	2.1 65	2.797	3.222	4.122	5.826	5.672	3.412
Laumonite	-0.092	0.133	0.425	0.627	0.857	1.048	1.126
Magnesite	-1.679	-1.848	-1.570	-2.207	-2.267	-1.670	-1.225
Montmoillonite BF	-0.832	-0.062	0.223	0.734	1.744	1.840	0.426
Quartz	0.052	-0.044	0.091	0.043	0.016	0.153	0.017
Siderite	-1.165	-2.157	-1.687	-1.855		-2.966	-1.409

Table 9 (cont'd)

Mineral	Well 10 Log AP/K	Well 8 Log AP/K	Well 7 Log AP/K	Well 5 Log AP/K	Well 1 Log AP/K	Well P4 Log AP/K	Fairgrounds Log AP/K
Albite	-3.631	-3.429	-3.266	-2.850	-3.185	-3.404	-3.534
Anhydrite	-3.835	-3.957	3.808	-3.445	-2.961	-3.358	-3.544
Anorthite	-2.883	-2.892	-2.911	-2.529	-0.401	-2.901	-3.222
Aragonite	-0.492	-1.918	-0.537	-0.489	-0.868	-0.641	-0.266
Barite	-1.342	-2.892	-1.300	-0.896	-5.170	-0.850	-1.065
Calcite	-0.336	-1.762	-0.381	-0.341	-0.244	-0.485	-0.109
Dolomite	-1.908	-4.697	-1.927	-1.829	-1.660	-2.167	-1.507
Gibbsite	1.328	2.559	1.539	1.790	1.338	1.803	1.050
Goethite	7.922	7.448	8.194		7.634	7.997	8.488
Gypsum	-3.578	-3.701	-3.551	-3.188	-3.496	-3.102	-3.288
Halite	-10.540	-10.410	-10.582	-10.233	-10.142	-10.302	-10.396
Halloysite	47.076	49.426	47.525	48.492	47.576	48.399	46.770
Hematite	16.485	15.622	17.114		15.886	16.635	17.617
Kaolinite	3.267	5.837	3.935	4.683	3.656	4.590	2.960
Laumonite	0.974	1.026	1.145	1.821	1.290	1.329	0.884
Magnesite	-1.461	-2.834	-1.455	-1.376	-1.300	-1.572	-1.286
Montmoillonite BF	0.309	1.380	1.066		0.791	1.121	0.416
Quartz	-0.070	-0.018	0.051	0.176	0.116	0.117	0.055
Siderite	-1.190		-2.247	-1.908	-4.306	-1.301	-3.792

Table 9 (cont'd)

Mineral	Gravel Well Log AP/K	Heidtman Log AP/K	B.McDonald Log AP/K	D.McDonald Log AP/K	Well MQT Log AP/K	Superior Log AP/K	Precipitation Log AP/K
Albite	-2.803	-2.982	-2.746	-3.508	-2.501		
Anhydrite	-2.872	-2.998	-3.447	-3.944	-3.326	-3.400	-5.624
Anorthite	-2.804	-2.375	-2.213	-3.479	-2.398		
Aragonite	-0.273	-0.343	-0.375	-0.915	-0.434	-1.035	-6.547
Barite	-0.206	-0.578	-0.853	-1.367	0.351		
Calcite	-0.116	-0.187	-0.219	-0.759	-0.279	-0.887	-6.403
Dolomite	-1.344	-1.549	-1.646	-2.571	-1.505	-2.780	-13.949
Gibbsite	2.085	1.696	1.788	1.262	1.799		
Goethite	5.013	8.940	8.507	8.468	8.221		
Gypsum	-2.615	-2.742	-3.191	-3.687	-3.070	-3.160	-5.404
Halite	-8.740	-9.798	-9.935	-10.579	-9.892		
Halloysite	48.894	47.810	48.186	46.933	48.420		
Hematite	10.668	18.606	17.740	17.661	17.209		
Kaolinite	5.085	4.220	4.596	3.344	4.940		
Laumonite	1.358	1.652	2.006	0.539	2.119		
Magnesite	-1.117	-1.261	-1.326	-1.711	-1.131		
Montmoillonite BF	1.194	1.613	1.866	0.642	2.411		
Quartz	0.083	0.037	0.133	0.033	0.293	-0.012	-1.497
Siderite	-1.431	-1.599					

Table 9 (cont'd)

Mineral	Big Creek Log AP/K	Carp River Log AP/K	Cedar Creek Log AP/K	Cedar Head Log AP/K	Chocolay Log AP/K	Cherry Creek Log AP/K	Goose Inlet Log AP/K
Albite	-3.401	-0.697	-3.320	-3.519	-3.311	-2.916	-2.874
Anhydrite	-3.320	-3.222	-3.477	-0.507	-3.530	-3.037	0.629
Anorthite	-3.070	-1.294	-3.291	-3.220	-3.057	-2.844	-3.466
Aragonite	-0.077	-0.307	-0.920	-0.815	-0.507	-0.375	0.629
Barite	-0.884	-1.294	-1.240	-1.137	-0.918	-0.576	-0.289
Calcite	0.078	-0.156	-0.765	-0.660	-0.355	-0.219	0.781
Dolomite	-0.981	-1.218	-2.722	-2.494	-1.756	-1.632	0.899
Gibbsite	1.165	1.462	1.924	1.814	1.623	1.689	0.962
Goethite	8.677	8.665	7.902	7.625	8.190	8.120	8.542
Gypsum	-3.064	-2.974	-3.222	-3.274	-3.090	-2.781	-2.058
Halite	-9.821	-8.599	-8.834	-9.733	-9.135	-9.135	-7.906
Halloysite	46.625	47.175	47.883	47.788	46.421	48.117	44.874
Hematite	18.165	18.633	16.614	16.061	17.521	16.881	18.226
Kaolinite	3.255	5.085	4.512	4.418	3.911	4.307	2.363
Laumonite	1.004	3.731	0.523	0.720	0.566	1.331	-0.069
Leonhardite							
Magnesite	-0.969	-1.026	-1.867	-1.348	-1.744	-1.302	0.717
Montmoillonite BF	1.024	5.021	1.165	0.979	1.531	1.391	1.505
Quartz	0.082	0.687	-0.47	0.016	-0.56	0.089	-0.169

Table 9 (cont'd)

Mineral	Goose Outlet Log AP/K	Goose Tel Log AP/K	Silver Head Log AP/K	Silver Mid Log AP/K	Silver Mouth Log AP/K	Strawberry Log AP/K	Warner Creek Log AP/K
Albite	-2.650	-2.324	-3.236	-3.051	-2.670	-8.661	-2.011
Anhydrite	-2.275	-3.103	-3.271	-3.258	-3.088	-4.200	-2.796
Anorthite	-3.270	-2.565	-2.589	-2.221	-2.282	-6.007	-2.157
Aragonite	0.451	-1.005	-0.243	-0.167	-0.415	-0.986	-0.450
Barite	-0.369	-0.830	-0.993	-0.999	-0.652	-1.899	-0.860
Calcite	0.597	-0.850	-0.088	-0.013	-0.259	-0.893	-0.294
Dolomite	0.297	-2.646	-1.338	-1.130	-1.693	-2.628	-1.373
Gibbsite	0.278	2.289	1.762	1.848	2.038	1.063	2.677
Goethite	7.226	9.762	8.061	8.025	8.115	7.757	9.272
Gypsum	-2.044	-2.848	-3.015	-3.003	-2.831	-3.965	-2.540
Halite	-8.135	-8.566	-9.523	-9.503	-9.747		-7.915
Halloysite	42.251	48.579	47.686	47.709	48.540	40.848	49.581
Hematite	16.230	20.418	16.932	16.943	16.956	17.214	19.270
Kaolinite	1.390	5.426	4.316	4.555	4.950	-0.214	5.992
Laumonite	0.156	1.385	1.352	1.740	1.790	-5.709	1.679
Magnesite	-0.311	-1.714	-1.159	-1.036	-1.334	-1.793	-0.978
Montmoillonite BF	1.920	2.973	1.337	1.750	1.929	-4.840	3.152
Quartz		0.042	0.016	0.048	0.060	-1.574	-0.058

coefficient is the ratio of activity of a species to is molality, and nears unity as the solution approach infinite dilution. The activity coefficient is calculated by WATEQ4F by the extended Debye-Huckel equation, given as

$$\log \gamma = (-A \mid z^{+}=z^{-} \mid I^{1/2}) / (1 + B\, a)\, I^{1/2}) \qquad (22)$$

where A and B are constants and characteristics of the solvent (water) and the temperature, a' is the hydrated size of the ion, z+ and z- are the ionic charge of the species, and I is the ionic strength of a solution defined by

$$I = \tfrac{1}{2} S\, m_i\, z_i \qquad (23)$$

The extended Debye-Huckel can be effectively used for solutions with ionic strength less than 0.1 . Waters modeled in the Sands Plain study have ionic strength up to 0.087 and can be accurately modeled by WATEQ4F.

The second problem is attributed to the lack of an accurate and an consistent thermodynamic data base for the use in computer models of this type. The most complete and consistent data base available is presented by Nordstrom et al. (1990). Equilibrium constants and enthalpy values selected from Nordstrum et. al were used in WATEQ4F and are presented in Table 10. Values for certain clay minerals (illite and chlorites) are not presented in this table because the chemical composition of clays in the Sands Plain study area are unknown, and the thermodynamic data base needed to model these clay types is far from complete.

Table 9 indicates that all water samples are undersaturated with respect to feldspars minerals which are presented as albite and anorthite. Feldspar minerals are known to compose a relatively small percentage of the sediments found in the Sands Plain area, but the relative amount and compositions of these minerals are unknown. Quartz is saturated with respect to all mineral compositions, and is the primary mineral composing sediments in the Sands Plain area.

Table 10 Selected Thermodynamic data used in WATEQ4F Calculations of Saturation Indices

Mineral Name	ΔH (kcal/mol)	log K	References
Albite	25.896	-18.002	WATEQ2; Ball et al. [1980]
Anhydrite	-1.71	-4.36	Langmuir and Melchior [1985]
Anorthite	11.580	-19.714	WATEQ2; Ball et al. [1980]
Aragonite	-2.589	-8.336	Plummer and Busenberg [1982]
Barite	6.35	-9.97	Langmuir and Melchior [1985]
Calcite	-2.297	-8.480	Plummer and Busenberg [1982]
Dolomite	-11.09	-16.54	Wagman et al. [1982]
Gibbsite	-22.8	8.11	May, Helmke and Jackson [1979]
Goethite		-1.0	Langmuir er al. [1971]
Gypsum	-0.109	-4.58	Langmuir and Melchior [1985]
Halite	0.918	1.582	WATEQ2; Ball et al. [1980]
Halloysite	44.680	-32.830	WATEQ2; Ball et al. [1980]
Hematite	-30.845	-4.008	WATEQ2; Ball et al. [1980]
Kaolinite	-35.3	7.434	log k from May et al. [1986]
			ΔH from Robie et al. [1979]
Laumonite	39.610	-30.96	WATEQ2; Ball et al. [1980]
Leonhardite	90.070	-69.756	WATEQ2; Ball et al. [1980]
Magnesite		25.34	Baes and Mesmer [1976]
Montmorillonite BF		-34.913	WATEQ2; Ball et al. [1980]
Quartz	5.99	-3.98	Fournier [1985]
Siderite		-10.45	log K from Smith [1984]
			ΔH from Robie et al. [1985]

All solutions are slightly undersaturated to undersaturated with respect calcite in the Sands Plain area except Big Creek, Goose Lake Inlet, and Goose Lake Outlet. All solutions are slightly undersaturated to undersaturated with respect to dolomite except Goose Lake Inlet and Goose Lake Outlet. All solutions are slightly undersaturated to undersaturated with respect barite. Groundwater samples which were analyzed for Fe (II) and Fe (III) are undersaturated with respect to siderite.

All solutions are supersaturated with respect to kaolinite and Belle Fourche montmorillonite. Kaolinite is known to occur in this area, where as smectites have never been documented.

Chemical modeling suggests that groundwaters composition in the southern portion of the study area may be attributed to feldspar and carbonate mineral dissolution and kaolinite precipitation. Clay minerals such as illite, chlorite and smectites may also affect water composition, but to what degree is uncertain. Modeling also suggests that effluent water derived from Goose Lake does not promote the precipitation or the dissolution of selected mineral phases relative to waters that receive recharge from this area. Goose Lake Inlet and Outlet are undersaturated with respect to gypsum, which would promotes gypsum dissolution and may account for the relatively high sulfate concentrations observed. Since sulfide concentrations were not measured saturation indices for solutions with respect to pyrite could not be evaluated.

Groundwater-Streamflow System

Chemical data for groundwater, surface water, Lake Superior water (Water-Resource Data, 1980), and precipitation (NADP/NTN, 1992) were plotted in a series of x-y diagrams, to observe composition trends and/or possible effects of mineral precipitation-dissolution in groundwater and surface water from the Sands Plain area. Lake Superior and precipitation waters are not included in trace elemental diagrams since no data could be obtained for them at this present time (1992).

In Figure 32 calcium in mg/L is plotted versus magnesium in mg/L. The dissolution of pure dolomite ($CaMg(CO3)_2$)in pure water produces a 1:1 stoichiometric ratio of calcium to magnesium. This relationship is displayed in Figure 32 as the dolomite line. Outcrops of Kona Dolomite are observed throughout the Goose Lake area, and chemical modeling indicates that most of groundwater and surface water are undersaturated with respect to dolomite. Figure 32 indicates that a water compositions from Sands Plain plot below the dolomite line along a linear trend having a positive slope. This linear trend exists between calcium and magnesium for water compositions ranging from 0 to 32 mg/L and from 0 to 7 mg/L, respectively. Along this linear trend, precipitation composes a lower endmember composition, and groundwater from well 19 and surface water from Goose Lake Outlet compose an upper endmember composition. Precipitation is chosen as a lower endmember composition because it constitutes a dilute source of water which recharges the study area. Water from Goose Lake Outlet and from well 19 are chosen as an upper endmember composition because they reflect the composition of effluent water being recharged into the system from Goose Lake. The compositions of this upper endmember should influence the composition of other waters which also receive recharge from Goose Lake.

Plotted above the precipitation endmember are groundwater from wells 8, 10, 23, 30 and D.McDonald, and surface water from Strawberry Lake. These wells are located in the southern region of the study area.

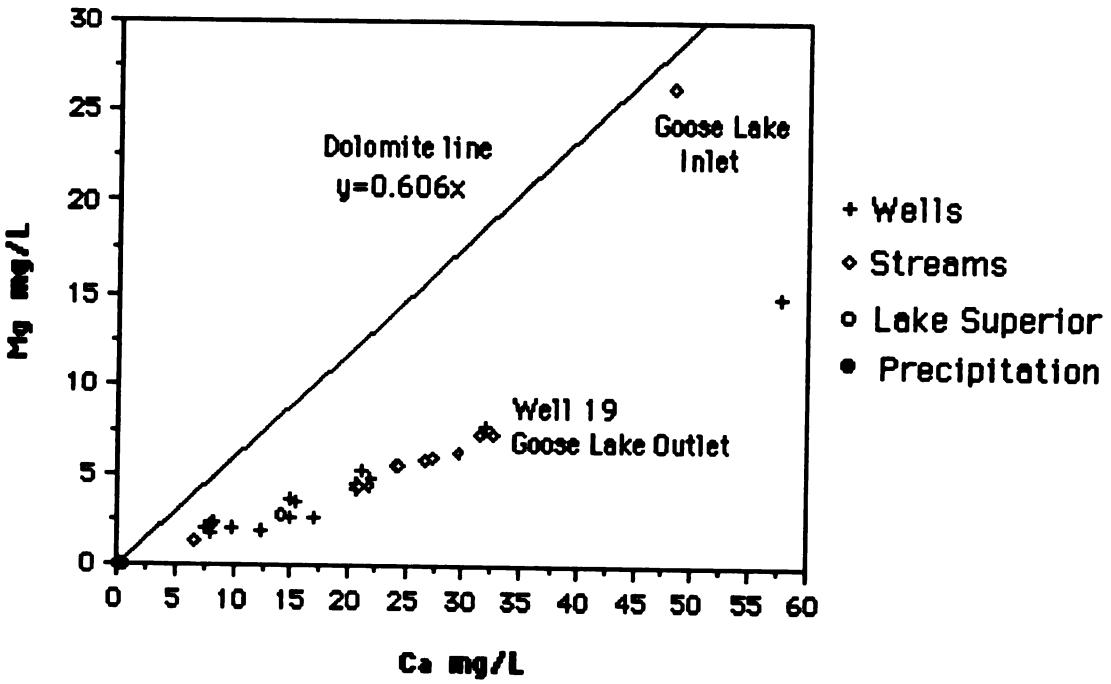

Figure 32 Calcium versus Magnesium

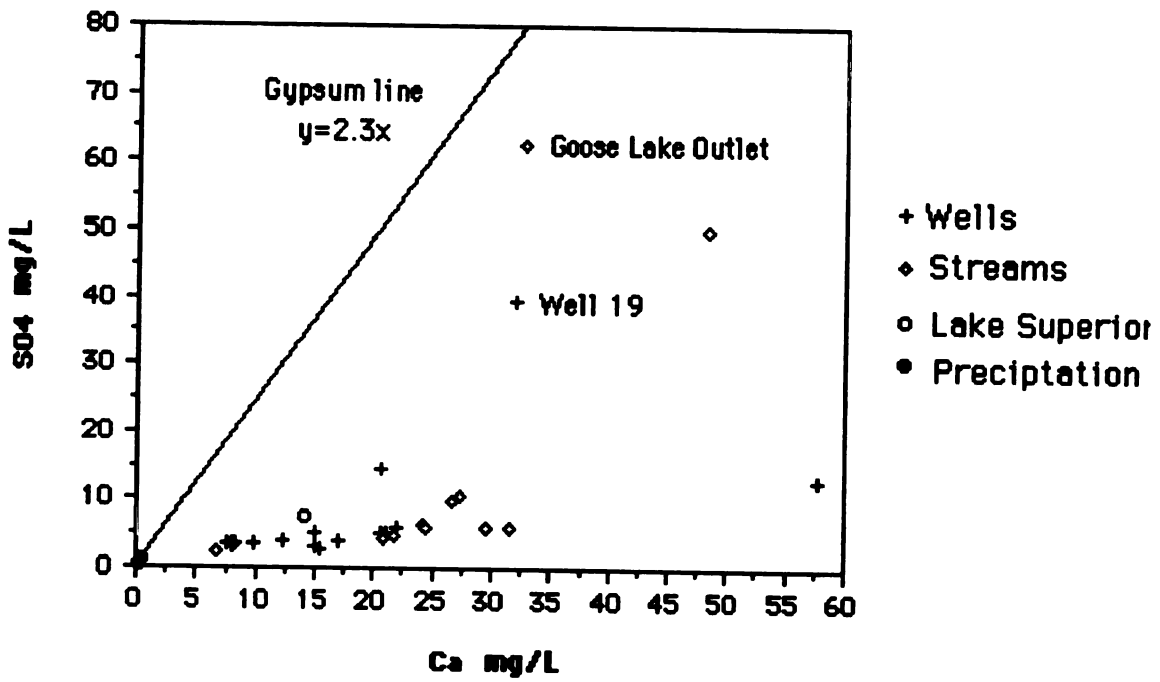

Figure 33 Calcium versus Sulfate

Above these waters and roughly at the midway point along this trend line are groundwaters from wells 1, 7, 26, 29, and Fairgrounds, and surface water from Lake Superior. It should be noted that water from well 1 and Lake Superior have similar calcium and magnesium concentrations, and that well 1 represents the closest groundwater observation to Lake Superior. Groundwaters from wells 5, P4, B.McDonald, and Heidtman plot above the midway point at approximately 21 mg/L calcium and 5 mg/L magnesium. Plotted between this compositional point and the upper endmember composition are samples of stream water from the Chocolay River and its tributaries. Stream water from Silver Creek has the highest concentrations of calcium and magnesium observed; stream water from Cedar Creek has the lowest. Stream waters from Cherry Creek, Big Creek, and Chocolay River, have concentrations of calcium and magnesium which fall in between Cedar and Silver Creeks. Calcium and magnesium concentrations decrease from tributaries in the northern region to those in the southern region.

Groundwater from well 15 also follows this linear trend, but has relatively high concentrations of calcium and magnesium and exceeds the upper endmember composition. High calcium and magnesium concentrations indicated by groundwater from well 15 may be due to the presence of Kona Dolomite near the well location although it does not plot near the dolomite line. Explanation of why this linear relation exists for calcium and magnesium concentrations from groundwater and surface water samples can not be provided at this point in time.

Surface water from Goose Lake Inlet has the highest concentrations of calcium and magnesium observed and does not follow this linear trend. Calcium and magnesium concentrations from Goose Lake Inlet plot on the dolomite line, and suggest that this water is related to dolomite dissolution. Chemical modeling also indicates that surface water from Goose Lake Inlet is saturated with respect to dolomite. High concentrations of calcium and magnesium observed in surface water from Goose Lake Inlet are dramatically reduced in Goose Lake before being discharged to Goose Lake Outlet.

In Figure 33 calcium in mg/L is plotted versus sulfate in mg/L. The dissolution of pure gypsum ($CaSO_4$)in pure water has a 1:1 stoichiometric ratio of calcium to sulfate. This relationship is displayed in Figure 33 as the gypsum line. Gypsum deposits were observed in soft ore deposits at Tracy mine (Palmer) by Wiittala (1967) and Gair (1975). Mine water from Tracy mine is discharged into Partridge Creek, a tributary of Goose Lake Inlet. This figure again displays a range of calcium concentrations for the majority of water samples, but shows little variation in sulfate concentrations. All water compositions plot below the gypsum line. Most water samples have a sulfate concentration between 0 and 15 mg/L. Surface waters from the Chocolay tributaries and groundwater from wells located in the northern portion of the study area are observed to have sulfate concentrations that are slightly higher than groundwaters from wells located in the southern portion of the study area. Water from well 1 indicates a relatively lower sulfate concentration compared to that observed from Lake Superior. Water containing higher concentrations of sulfate occurs in well 19, Goose Lake Outlet and Goose Lake Inlet. The presence of elevated sulfate concentrations by these waters may be due to the oxidation of pyrite during iron ore benification processing and/or hydrogen sulfide gas. Hydrogen sulfide gas is detected at Schweitzer Creek Reservoir and at the ore processing plant at Empire mine and are thought to be generated by sulfur bacteria acting on sulfurous material under anaerobic conditions (Wiitala, 1967).

In Figure 34 calcium in mg/L is plotted versus bicarbonate in mg/L. The dissolution of pure calcite ($CaCO_3$) in pure water has a 1:1 stoichiometric ratio of calcium to carbonate. This relationship is displayed in Figure 34 as the calcite line. The presence of calcite was observed in sediment samples, and chemical modeling indicates that groundwater and surface water are saturated to slightly undersaturated with respect to calcite. Figure 34 indicates that a water compositions from Sands Plain plot just above the calcite line

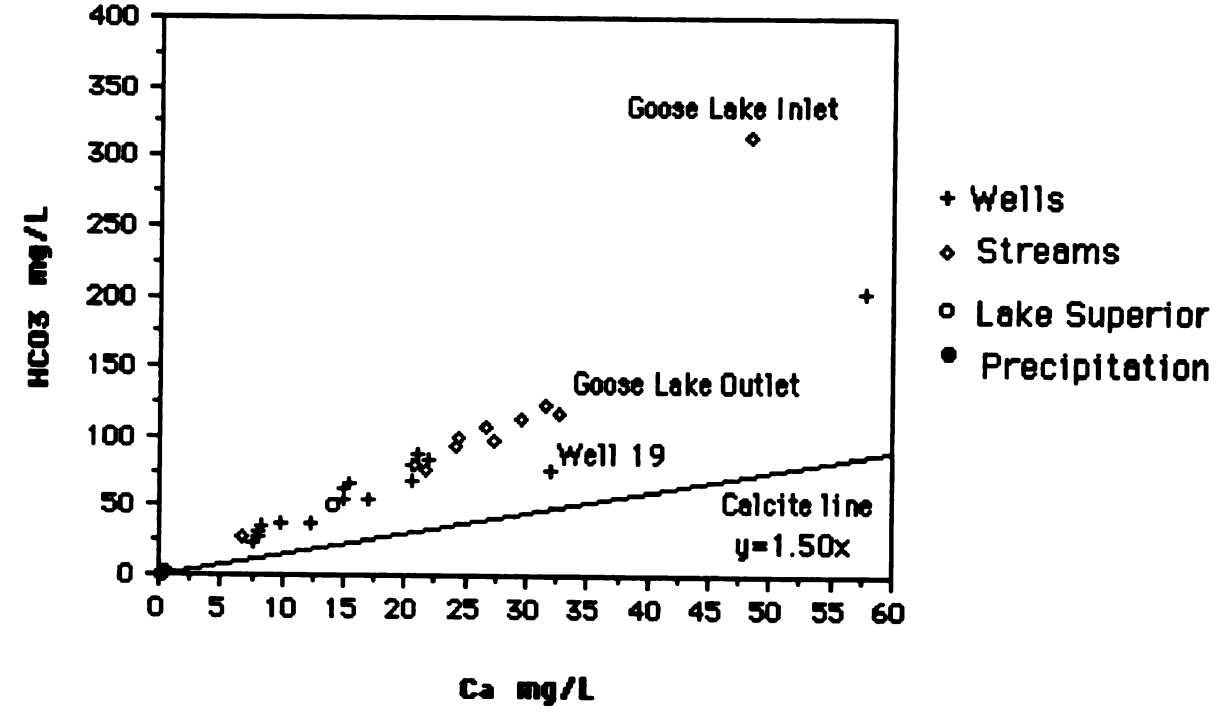

Figure 34 Calcium versus Bicarbonate

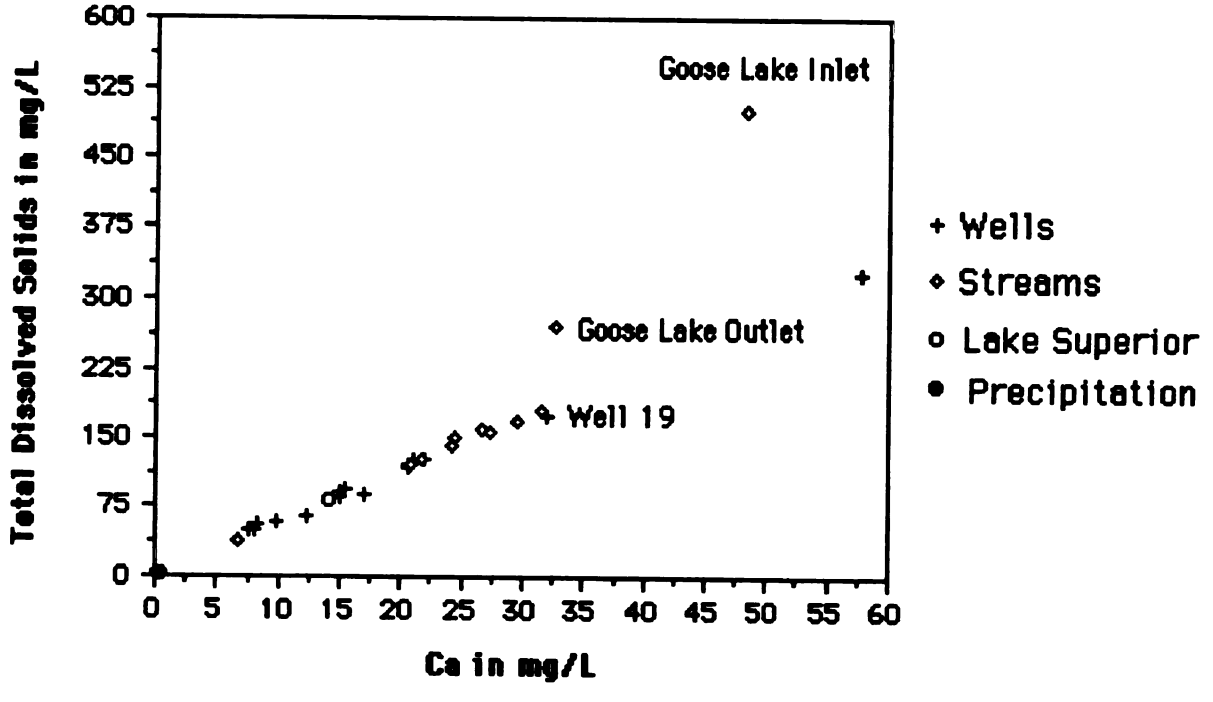

Figure 35 Calcium versus Total Dissolved Solids

along a linear trend having a positive slope. This figure indicates that water compositions range from 0 to 32 mg/L and from 0 to 125 mg/L, respectively. Figure 34 displays a similar order in sample site location along this linear trend as those observed in Figures 32. This linear relationship displays precipitation constituting a lower endmember composition, and surface water from Goose Lake Outlet constituting an upper endmember composition. Groundwater from well 19 has a lower concentration of bicarbonate than Goose Lake Outlet and plots directly underneath the linear trend. Groundwater from well 19 plots on the calcite line, and suggests that this water is related to calcite dissolution.

A lower bicarbonate concentration indicated by groundwater may be due to decreasing partial pressure of CO_2 with depth. Groundwater from well 15 also follows this linear trend, but has a higher concentration of calcium and bicarbonate than the upper endmenber composition. Surface water from Goose Lake Inlet has higher concentrations of calcium and bicarbonate than the other water samples and does not follow this linear trend.

In Figure 35 calcium in mg/L is plotted versus total dissolved solids (TDS) in mg/L. This figure indicates that a linear trend having a positive slope exists between calcium and TDS, for water compositions ranging from 0 to 32 mg/L and from 0 to 175 mg/L, respectively. This linear relationship again displays precipitation constituting a lower endmember composition, and groundwater from well 19 constituting the upper endmember composition. Figure 35 displays a similar order in water sample locations plotted along this trend line, as was observed along the linear trends in Figures 32 and 34. Surface water from Goose Lake Outlet has a higher TDS concentration than groundwater from well 19, and plots to the right of it. Groundwater from well 15 also follows this linear trend, but plots above the upper endmember composition. Surface water from Goose Lake Inlet indicates concentrations high in both calcium and TDS and does not follow this linear trend.

In Figure 36 calcium in mg/L is plotted versus strontium in μg/L. The majority of water samples displayed in this figure show little variation in strontium concentrations. Groundwater obtained

from well 19 has a slightly higher concentration of strontium. Surface waters from Goose Lake Inlet and Goose Lake Outlet have relatively high concentrations of strontium. It is interesting to note that even though calcium and strontium have similar ionic radius and charge that no trends exists between elemental concentrations and sample site locations.

In Figure 37 bicarbonate in mg/L is plotted versus sulfate in mg/L. The majority of water samples displayed in this figure range from 0 and 120 mg/L bicarbonate and from 0 and 15 mg/L sulfate. Water samples plotted outside of these ranges are groundwater from wells 19 and 15, and surface water from Goose Lake Inlet and Outlet. Groundwater from well 19 and surface water from Goose Lake Outlet have bicarbonate concentrations that fall inside the range for the majority of water samples, but have concentrations which are higher in sulfate. Groundwater from well 15 has a similar range in sulfate concentration as observed in the majority of water samples, but higher bicarbonate concentrations. Surface water from Goose Lake Outlet has relatively high concentrations of both sulfate and bicarbonate.

In Figure 38 chloride in mg/L is plotted versus sodium in mg/L. The dissolution of pure halite (NaCl) in pure water has a 1:1 stoichiometric ratio of sodium to chloride. This relationship is displayed in Figure 38 as the Halite line. This figure displays a range in chloride concentrations from 0 to 12 mg/L and sodium concentrations from 0 to 5 mg/L for the majority of water samples. Groundwater from well 15 ,and surface water from Goose Lake Inlet and Outlet have a relatively high concentration of chloride and sodium. Water from from well 15, Goose Lake Inlet, and Outlet do not plot along the halite line, this suggests that road salt is not a likely source for the elevated chloride concentrations in groundwater.

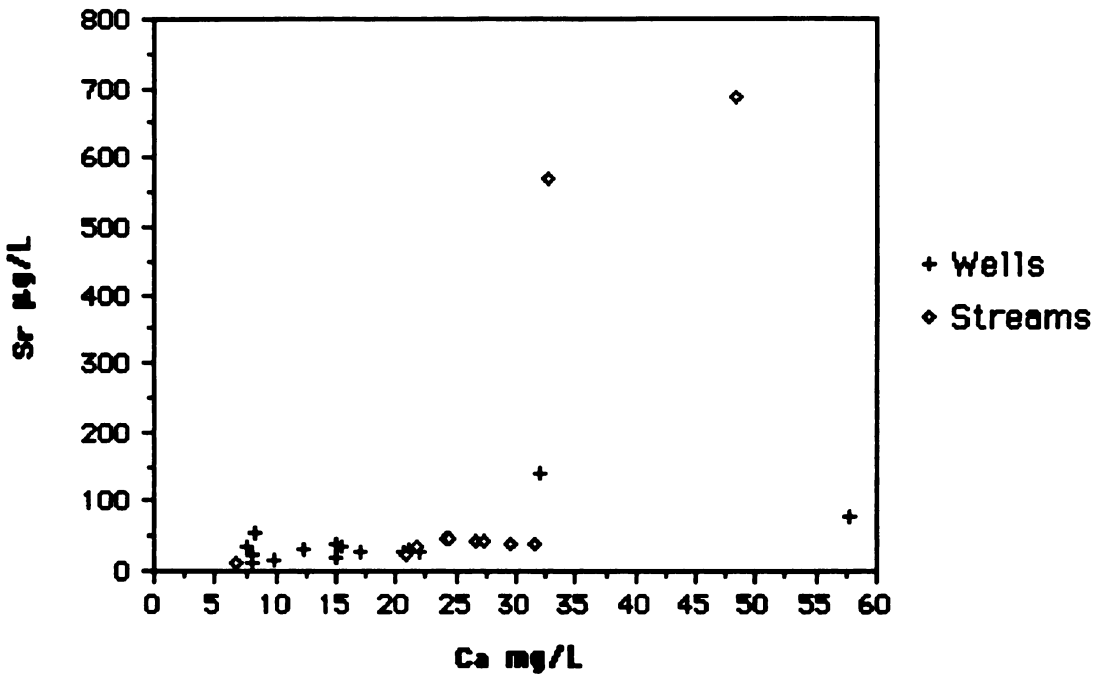

Figure 36 Calcium versus Strontium

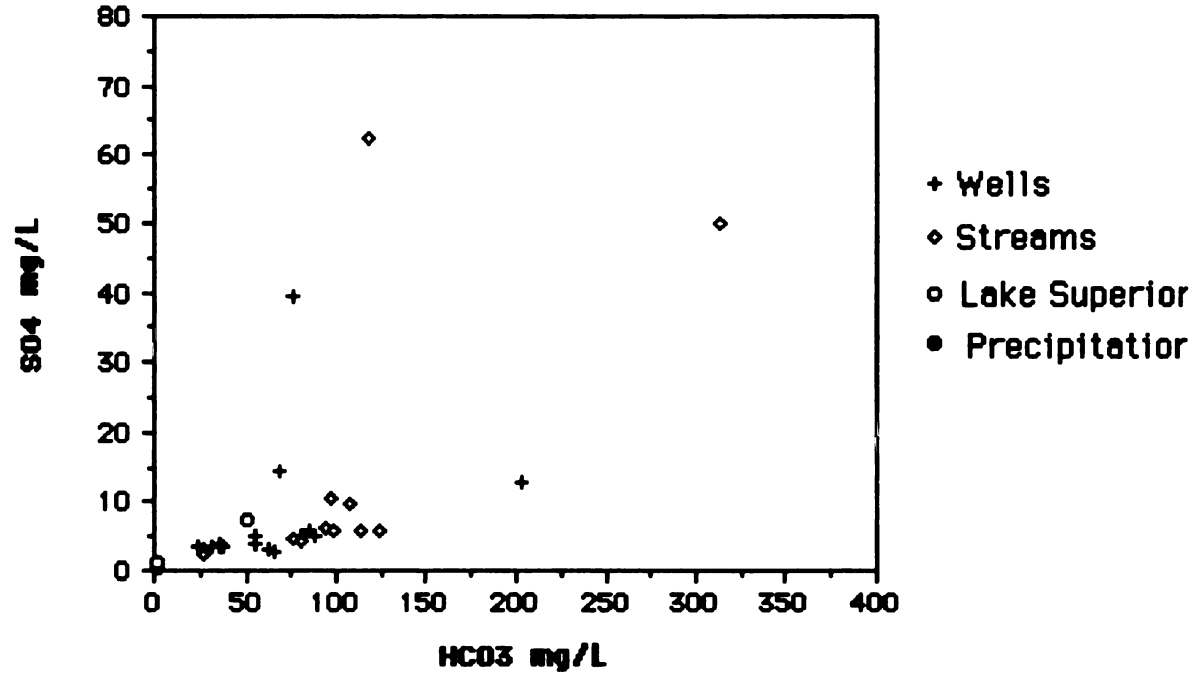

Figure 37 Bicarbonate versus Sulfate

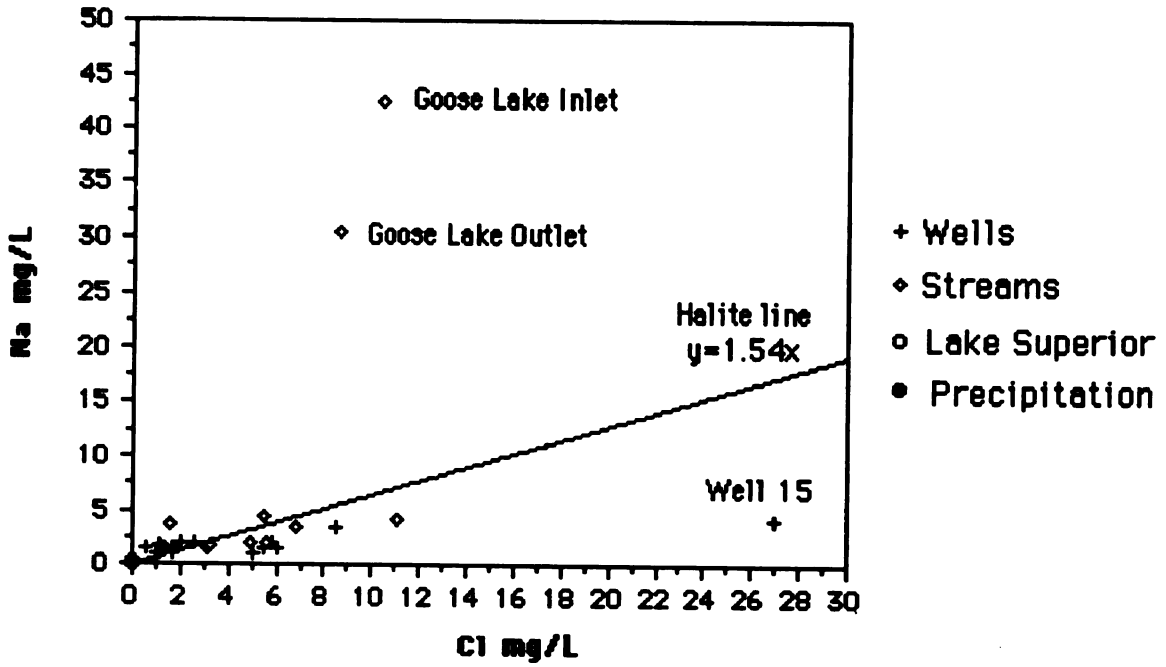

Figure 38 Chloride versus Sodium

Discussion

The Sands Plain area offers a unique opportunity to study the geochemical evolution of a groundwater-streamflow system in a glaciated environment because of its well constrained hydrogeologic setting and geochemical variability in both surface water and groundwater. A numerical model that simulates the Sands Plain hydrologic system is based on geologic setting, field measurements, and assumptions about boundary conditions, hydrologic parameters, and stresses on the system. The Sands Plain numerical model is useful for understanding groundwater flow-path direction and for estimating travel time information. The model also delineates areas of recharge and discharge, and was used to calculate volumetric inflow and outflow budgets. Samples of groundwater and surface water in the Sands Plain area were collected to characterize compositional inputs and outputs to the system, and to observe variations in water chemistry along flow paths. Water chemistry of these samples reflect physical, chemical and biological processes which have occurred. Numerical flow modeling was used in conjunction with water chemistry to understand the geochemical evolution of the Sands Plain system.

The Sands Plain model was divided into three main zones consisting of Goose Lake, Silver/Cherry Creek, and Big Creek. These zones were constructed to isolate and evaluate the major groundwater-streamflow systems. Volumetric budget information indicates that the Goose Lake zone discharges almost exclusively to the Silver/Cherry Creek zone, and the rate of interflow between these two zones is relatively high. Volumetric budgets also indicate that the Big Creek zone in the southern portion of the study area could be hydrologically separated from the two other zones in the northern portion of the study area. Hydrologic separation among these zones is probably due to the range and distribution of hydraulic conductivity values, and the location of the streams. High hydraulic conductivity values observed in the Sands Plain study area may allow the rate of advective flow in the longitudinal direction to be much greater than the rate of advective flow in the transverse

direction, and allow little interaction between northern and southern regions.

Groundwater chemistry displayed by isogram maps and in x-y plots also indicates that these zones are hydrologically separate. Water in the northern portion of the study area (including Lake Superior) displays higher concentrations of major ions than water in the southern portion of the study area. Water chemistries observed in the southern portion are thought to result from interaction between precipitation and mineral phases composing these glacial deposits. Glacial deposits are primarily composed of quartz, but are known to contain feldspar minerals, carbonates, opaque minerals, and clay minerals such as illite, chlorite, and kaolinite. Saturation indices calculated through chemical modeling suggest that groundwater in the southern portion of the study area is undersaturated with respect to feldspar minerals and calcite, and supersaturated with respect kaolinite.

Water chemistry information is consistent with groundwater and surface water flow data in the northwestern portion of the study area. Effluent waters having relatively high concentrations of dissolved constituents are discharged at Goose Lake Inlet, and then discharged to Goose Lake Outlet. Concentrations of major and trace elements, with the exception of sulfate, are observed to be generally higher in Goose Lake Inlet than in Goose Lake Outlet, which suggest that Goose Lake must be a sink for these constituents. Gypsum deposits occur in soft iron ore at Tracy mine which lies north of Goose Lake, and may be the source of sulfate.

Streamflow measurements indicate that a 3-mile reach of Goose Lake Outlet loses water at a rate if approximately 10 cubic feet per second. Water from well 19, located near Goose Lake, has similar concentrations of calcium, magnesium, sodium, potassium and chloride as Goose Lake Outlet, but has a lower concentration of sulfate. Concentrations of major and trace elements in groundwater generally decrease along flow paths from well 19 towards Lake Superior. Model simulations with particle tracking indicate that it takes approximately 50 years for groundwater to travel from Goose Lake to Lake Superior. Wiitala (1967) indicated that effluent water

from iron ore beneficiation processes and underground mine pumpage was initially discharged to Goose Lake Inlet and Partridge Creek in the 1950's. No estimates on the quantity and compositions of these effluent waters over this time period can be given at the present (1992), but flow data suggest that water initially entering the system at Goose Lake in the 1950's should now be reaching a position near Lake Superior.

Well 1 represents the furthest groundwater observation along a flow path which originates near Goose Lake. Water from well 1 has similar concentrations of calcium, magnesium, sodium, potassium and chloride to that of Lake Superior, but indicates a lower concentration of sulfate. Higher concentrations of sulfate in water from Lake Superior might be due to the discharge of stream and River water into Lake Superior and/or the influence of air pollution. Grannemann (1984) documents concentrations of mean sulfate fallout from rain and snow on the order of 17.4 lb/acre/year. Correlation between water chemistry from well 1 and Lake Superior and the proximity of their sample sites suggest that waters from well 1 and from Lake Superior are directly related. If these two water types are related then it is evident that effluent water from Goose Lake has not influenced the chemistry of water from well 1 which is approximately 160 feet deep. This implies that if flow path direction and travel time information from particle tracking techniques are accurate, most water that originates from Goose Lake remains in the upper part of the aquifer and discharges to tributaries streams of the Chocolay River.

This argument is reinforced by the observation that stream waters from the tributaries of the Chocolay River generally have higher concentrations of major dissolved species than groundwater samples in the northern portion of the study area, excluding water from well 19. Stream hydrographs indicate that baseflow to Cedar, Cherry and Silver Creeks is over 90% and water samples from these creeks should generally reflect groundwater compositions. Plots of calcium versus magnesium; bicarbonate; and total dissolved solids display a positive linear relationship for groundwater and stream water samples where upper and lower endmember compositions

were defined by water from well 19 and precipitation, respectively. Stream water composition for the tributaries of the Chocolay River consistently plot underneath upper endmember compositions along these linear trends.

Thus a higher rate of horizontal flow compared to vertical flow for groundwater receiving recharge from Goose Lake would produce a higher concentration of dissolved species in shallow groundwaters and streams down the flow path gradient compared to deeper groundwaters in the northern section of the Sands Plain area.

Conclusions

1. The Sands Plain area represents a well constrained hydrologic system, with glacial deposits composing the primary hydrostratigraphic unit. Groundwater is recharged mainly by precipitation but also receives recharge from surface water at Goose Lake and Goose Lake Outlet. Groundwater discharges mainly to Lake Superior and to tributary streams of the Chocolay River. Numerical flow modeling indicates that groundwater flows under a high hydraulic gradient towards the northeast, and that the northern portion of Sands Plain area can be hydrologically separated the southern portion. Particle tracking techniques indicate residence time (for a particle of water to enter and leave the system) is approximately 50 to 80 years.

2. Water chemistry in the northern region of the Sands Plain study area is impacted by a relatively high concentration of sulfate, iron and manganese from effluent water discharged to Goose Lake Inlet and Partridge Creek. Effluent waters result from iron ore and beneficiation and pelletization processes, and underground mine drainage. Groundwater chemistries in the northern portion of the study area may be attributed to gypsum, and dolomite dissolution, and pyrite oxidation.

3. Distribution of water chemistry in the Sands Plain area reinforces hydrologic flow modeling information and indicates that groundwater flow regimes in the northern region of the Sands Plain study area are distinct from those in the southern. Groundwater chemistries in the southern portion of the study area are relatively dilute and may be attributed to feldspar, dolomite and calcite dissolution, and kaolinite precipitation.

4. Waters from Silver, Cherry and Cedar Creeks are composed of a high percentage of baseflow and are thought to reflect groundwater compositions. Surface water chemistries from Silver, Cherry and Cedar Creeks display concentrations of dissolved constituents that are generally higher than those observed for the majority of groundwater in the northern portion of the study area.

5. Water chemistries observed for both surface water and groundwater down flow path from Goose Lake to Lake Superior indicate that a shallow component of groundwater flow exists.

References

Atkins, P.W., 1990, *Physical Chemistry 4th ed.*, W.H. Freeman and Company, N.Y. pp. 995.

American Public Health Association, American Water Works Association, Water Pollution Control Federation, 1971, *Standard Methods for the Examination of Water and Waste Water*, American Public Health Association, Wash., D.C. .

Anderson, M. P., 1989, Aquifer heterogeneity- a geological perspective, In: Parameter identification and Estimation for Aquifer and Reservoir Characteristics, Nat'l. Water Well Assoc., Columbus, Ohio, pp. 3-22.

Anderson, M.P., and Woessner, W.W., 1992, *Applied Groundwater Modeling Simulation of Flow and Advective Transport*, Academic Press, Inc, 381p.

Aquilara, N. H., and Jackson, M. L., 1953, Iron oxide removal from soils and clays. Soil Sci. Soc. Amer. Proc, 17, pp. 359-364.

Back, W., 1961, Techniques for mapping of hydrochemical facies. U.S. Geological Surv. Prof.Paper 424-D, pp. 380-382.

Ball, J.W., 1and Nordstrom, 1991, Users manual for WATEQ4F with revised thermodynamic data base and test cases for calculating speciation for major and trace and redox elements in natural waters, Open-file report 9183, pp. 189.

Ball, J.W., Jenne, E.A., and Nordstrom, D.K., 1979, WATEQ2-a computerized chemical model for trace and major element speciation and mineral equilibria of natural waters. In Chemical Modeling in Aqueous Systems. ed E.A. Jenne, ACS Symposium Series 93, pp. 815-835.

Basset, R.L., and Melchoir, D.C., *Chemical modeling of aqueous systems. In Chemical Modeling of Aqueous Systems*, ed Melchoir D.C., and Basset, R.L., ASC Symposium Series, **416**, pp. 1-14.

Bhattacharya, N., 1962, Weathering of glacial till in Indiana I. Clay Minerals, GSA Bulletin, **73** pp. 1007-1020.

Bottomley, D. J., Craig, D., and Johnston, L. M., 1984, Neutralization of acid runoff by groundwater discharge to streams in canadian precambrian shield watersheds, J. Hydrol., **75**, pp. 1-26.

Bradbury, K. R., 1984, Major ion and isotope geochemistry of ground water in clayey till, northwestern Wisconsin , USA, in Practical applications of ground water geochemistry: Dublin, Ohio, Nat'l. Water Well Association, pp. 284-289.

Cherry, J. A., 1972, Geochemical processes in shallow groundwater flow system in five areas in souther Manitoba, Canada, Proc 24th Intern. Geol. Congr., Montreal Sec, **11**, pp. 208-221.

Chow, V. T., 1964, *Handbook of Applied Hydrology*, McGraw-Hill, New York.

Cleaves, E. T., Godfrey, A. E., and Bricker, O. P., 1970, Geochemical balance of a small watershed and its geomorphic implications, GSA Bulletin, **81**, pp. 3015-3032.

Desaulniers, D. E., Cherry, J. A., and Fritz, P., 1981, Origin, age and movement of porewater in argillaceous quaternary deposits at four sites in southwestern Ontario, J. Hydrol., **50**, pp. 231-257.

Doonan, C.J., and Van Alstine, J.L., 1982, Geology of the Marquette and Sands Quadrangles, Marquette County, Michigan: U.S. Geological Survey Open-File Report 82-501, pp. 53.

Drever, J.I., 1988, *The geochemistry of natural waters* , Englewood Cliffs, N.J., Prentice-Hall, 388 pp.

Fishman M. J., Friedman L. C., 1989. *Techniques of Water-Resources Investigation of the United States Geological Survey, Chapter A1, Methods of Determination of Inorganic Substances in Water and Fluvial Sediments,* U.S. Govt. Print Off., Wash., D.C..

Freeze, R.A., and Cherry, J.A., 1979, *Groundwater*, Prentice-Hall, pp. 604.

Gair, J.E., 1975, Bedrock geology and ore deposits of the Palmer Quadrangles, Marquette County, Michigan: U.S. Geological Survey Professional Paper 769, pp. 159.

Gair, J.E. and Thaden, R.E., 1968, Geology of the Marquette Iron Range area, Marquette County, Michigan: U.S. Geological Survey Professional Paper 397, pp. 77.

Garrels, R. M., 1967, Genesis of some ground waters from igneous rocks, Researches in Geochemistry, 2, ed. P. H. Abelson. John Wiley and Sons, New York, pp. 663.

Garrels, R. M., and Mackenzie, F. T., 1967, Origin of the Chemical composition of some springs and lakes, Equilibrium Concepts in Natural Water System, 67, ed. R. F. Gould. American Chemical Society Publications, Washington, D. C., pp. 222.

Grannemann, N.G., 1979, Water resources of the Marquette Iron Range area, Marquette County, Michigan: U.S. Geological Survey Open-File Report 79-1339, pp. 77.

Grannemann, N.G., 1984, Hydrogeology and effects of tailings basins on the hydrology of Sands Plain, Marquette County, Michigan, USGS, Water-Resources Investigations Report 84-3113, pp. 98.

Grisak, G. E., Cherry, J. A., Vonhof, J. A., and Blumele, J. P., 1976, Hydrogeologic and hydrochemical properties of fractured till in the interior plains region, Glacial Till, ed. R. F. Legget. Spec. Publ. Roy. Soc. Can., pp. 304-335.

Harbaugh, A. W., 1990, A computer program for calculation subregional water budgets using results from the U.S. Geological Survey Modular Three-Dimensional Finite-Difference Ground-Water Flow Model 90-392, USGS, pp.46.

Hem, J.D., 1989, Study and interpretation of the chemical characteristics of natural water: U.S. Geological Survey Water Suply Paper, 2254, pp. 263.

Hendry, J. M., Cherry, J. A., and Wallick, E. I., 1986, Origin and distribution of sulfate in a fractured till in southern Alberta, Canada, Water Resources Res, 22, pp. 45-61.

Hitchon, B., and Friedman, I., 1968, Geochemistry and origin of formation waters in the western Canada sedimentary basin-I. Stable isotopes of hydrology and oxygen, Geochim. Cosmochim. Acta, 35, pp. 1321-1349.

Hughes, J.D., 1978, Post Two creeks buried forest near Marquette, Michigan: presentation for 24th Annual Institute on Lake Superior Geology.

Jackson, M. L., 1969, Soil Chemical analysis. Advanced Course. Pub. by the author, Dept. of Soils, Univ of Wis., Madison 6, Wisconsin.

Jackson, R. E. and Patterson, R. J., 1982, Interpretation of pH and Eh trends in a fluvial-sand aquifer system, Water Resources Res, 18, pp. 1255-1268.

Kennedy, V. C., and Zellweger, G. W., 1974, Comparison of observed and calculated concentrations of dissolved Al and Fe in stream water, Water Resources Res, 10, pp. 791-793.

Kennedy, V.C., Jones, B.F., and Zellwenger, G.W., 1974, Filter pore-size effects on the analysis of Al, Fe, Mn and Ti in water. Water Resources Res, 10, pp. 785-790.

Kenoyer, G. J., and Bowser C. J., 1992a, Groundwater chemical evolution in a sandy silicate aquifer in northern Wisconsin, 1, patterns and rates of change, Water Resources Res , 28, pp. 579- 589.

Kenoyer, G. J., and Bowser C. J., 1992b, Groundwater chemical evolution in a sandy silicate aquifer in northern Wisconsin, 2, Reaction modeling. Water Resources Res, 28, pp. 591-600.

Kinzelbach, W.,1986, *Groundwater Modeling: An Introduction with Sample Programs in Basic*, Developments in Water Science, 25, Elsevier, 334p.

Mandle, R.J. and Kontis, A.L., 1986, Directions and rates of groundwater movement in the vicinity of Kesterson Reservoir, San Joaquin Valley, California: U.S. Geological Survey Water-Resources Investigations Report 86-4196, 57 p.

McDonald, M.G., and Harbaugh A.W., 1988, A modular three-dimensional finite-difference ground-water flow model, Techniques of Water Resources Investigations 06-A1, USGS, pp. 567.

Murray, J. W., and Gill, G., 1978, The geochemistry of iron in Puget Sound, Geochimica et Cosmochimica Acta, 42, pp. 9-19.

National Atmospheric Depositional Program, 1992. NADP/NTN data base, Natural Resource Ecology Lab, Colorado State Unv, Fort Collins, CO.

Newburry, R.W., Cherry, J.A. and Cox, R.A., 1969, Groundwater-streamflow systems in the Wilson Creek Experimental Watershed, Manitoba, Can J. Earth Sci, **11**, pp. 964-975.

Nordstrom, D. K., Jenne, E. A., and Ball, J. W., 1979, Redox equilibria of Iron in Acid Mine Water, Chemical Modeling in Aqueous Systems ASC Symposium Series, American Chemical Society, Washington, D. C. pp. 51-79.

Nordstrom, D.K., Plummer, N.L., Langmuir, D., Busenberg, E., May, H.M., Jones, B.F., and Parkhurst D.L., 1990, Revised chemical equilibrium data for major water-mineral reactions and their limitations. *In Chemical Modeling of Aqueous Systems*, Melchoir D.C., and Basset, R.L., ed. ACS Symposium Series, 1990, **416**, pp 399-413.

Ophori, D. U., and Toth, J., 1989, Characterization of ground-water flow by field mapping and numerical simulation, Ross Creek basin, Alberta, Canada, Groundwater, 27, pp. 193-201.

Perkin-Elmer Corp., Part Number 0993-8150, 1985, Techniques in Graphite Furnace Atomic Absorption Spectrophotometry, Ridgefield, CT.

Perkin-Elmer, Part #0303-0152, 1982, Analytical Methods for Atomic Absorption Spectrophotometry, Norwalk, CT.

Piper, A. M., 1944, A graphical procedure in the geochemical interpretation of water analyses. Trans. Amer. Geophys. Union, 25, pp. 914-923.

Plummer, L.N. and Back W., 1980, The mass balance approach: Application to interpreting the chemical evolution of hydrologic systems, American Journal of Science, **280**, pp. 130-142.

Plummer, L.N., Parkhurst, D.L., and Thorstenson, D.G., Development of reaction models for groundwater systems. Geochimica et Cosmochimica Acta, **47**, pp. 665-686.

Pinder, G. F., and Jones, J. F., 1969, Determination of groundwater component of peak discharge from chemistry of total runoff, Water Resources Res, **5**, pp. 438-445.

Pollock, D.W., 1988, Semianalytical computation of path lines for finite-difference models, Ground Water **26(6)**, pp. 743-750.

Pollock, D.W., 1989, Documentation of computer programs to complete and display pathlines using results from U.S. Geological Survey modular three-dimensional finite-difference ground-water model, USGS, Open File Report 89-381, 81p.

Schwartz, F. W., and Domenico, P. A., 1973, Simulation of hydrochemical patterns in regional groundwater flow, Water Resources Res, **9**, pp. 707-720.

Schwartz, F. W., Muehlenbachs, K., and Chorley, D. W., 1981, Flow-system controls of the chemical evolution of groundwater, *Developments in Water Science*, eds. W. Back and R. Letolle, Symp on Geochem. of Groundwater. New York, Else vier, pp. 225-243.

Sklash, M. G., and Farvolden, R. N., 1979. The role of groundwater in storm runoff, J. Hydrol, **43** pp. 45-65.

Sklash, M. G., Farvolden, R. N., and Fritz, P., 1976, A conceptual model of watershed response to rainfall, developed through the use of oxygen-18 as a natural tracer, Can J. Earth Sci, 13, pp. 271- 238.

Stuart, W.T., Brown, E.A., and Rhodehamel, E.C., 1954, Ground-water investigation of the Marquette iron-mining district: Michigan Department of Conservation, Geological Survey Division Technical Report,3, pp. 92.

Stumm, W., and Morgan, J. J., 1981, Aquatic Chemistry, 2nd ed. Wiley-Interscience, New York, 780.

Swain, C. J., 1974, A fortran program for irregularly spaced data using the difference equations for minimum curvature, In Computers and Geosciences, 1, pp 231-240.

Truesdell, A.H., and Jones, B.F., 1974, WATEQ, a computer program for calculating chemical equilibria of natural waters: U.S. Geological Survey Journal of Research, 2, pp. 233-248.

Twenter, F.R., 1981, Geology and hydrolgy for environmental planning in Marquette County, Michigan: U.S. Geological Survey Water-Resources Investigations Report, 80-90, pp. 44.

Wallick, E. I., 1981, Chemical evolution of groundwater in a drainage basin of holocene age, east-central Alberta, Canada, J. Hydrol, 54, pp. 245-283.

Water-Resource Data, Michigan, water year 1980: U.S. Geological Survey water-data report MI-80-I (published annually), p. 590-595.

Wiitala, S.E., Newport, T.G., and Skinner, E.L., 1967, Water resources of the Marquette Iron Range area, Michigan: U.S. Geological Survey Water-Supply Paper 1842, pp. 142.

Williams and Works, 1988, Sands Plain groundwater exploration program report. Grand Rapids, MI.

Appendix A

X-ray Diffraction

Big Creek

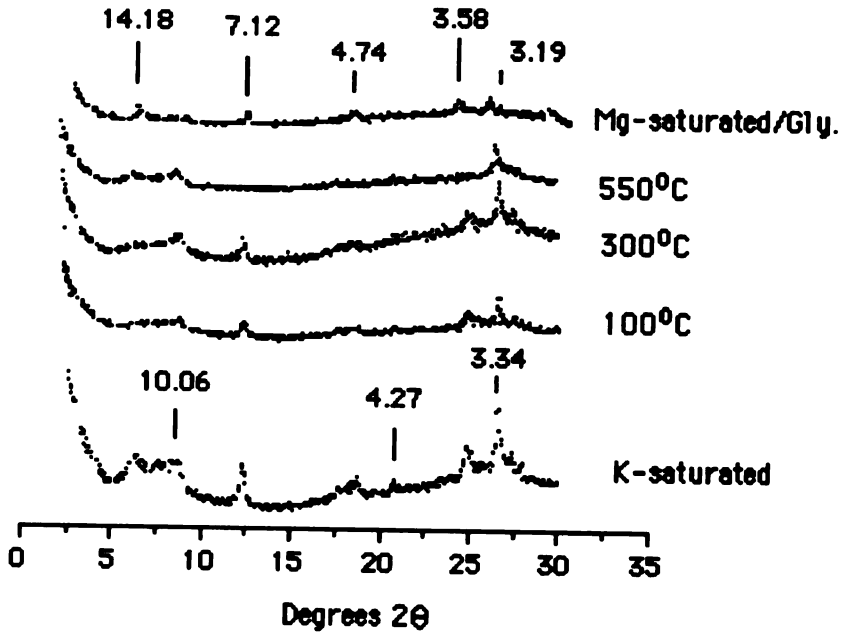

Carp River

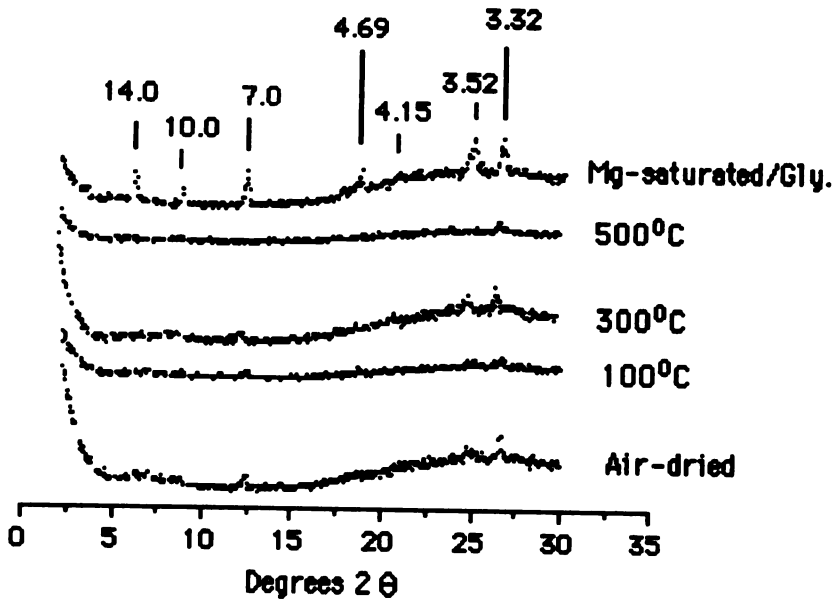

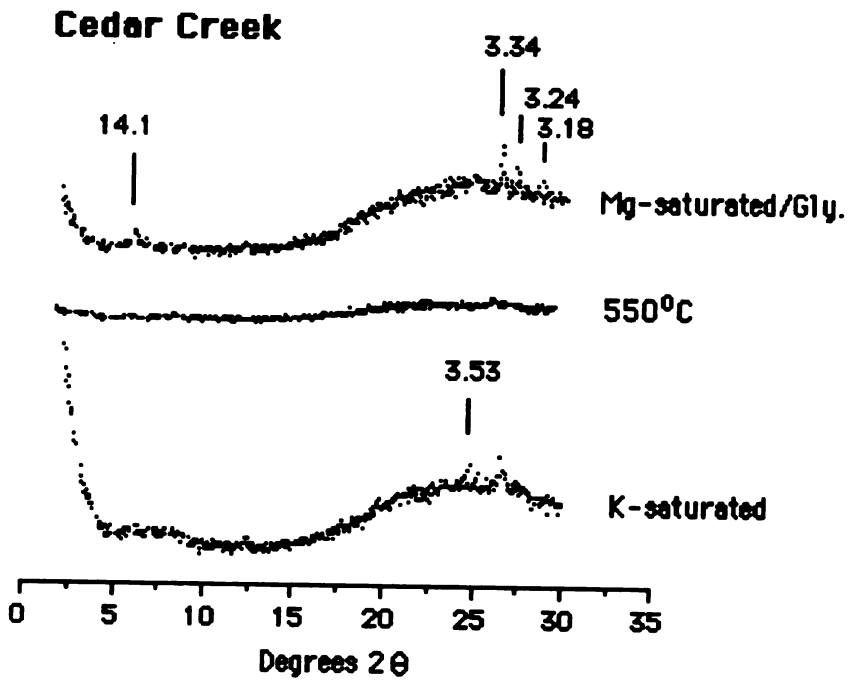
Cedar Creek
3.34
3.24
3.18
14.1
Mg-saturated/Gly.
550°C
3.53
K-saturated
0
5
10
15
20
25
30
35
Degrees 2θ

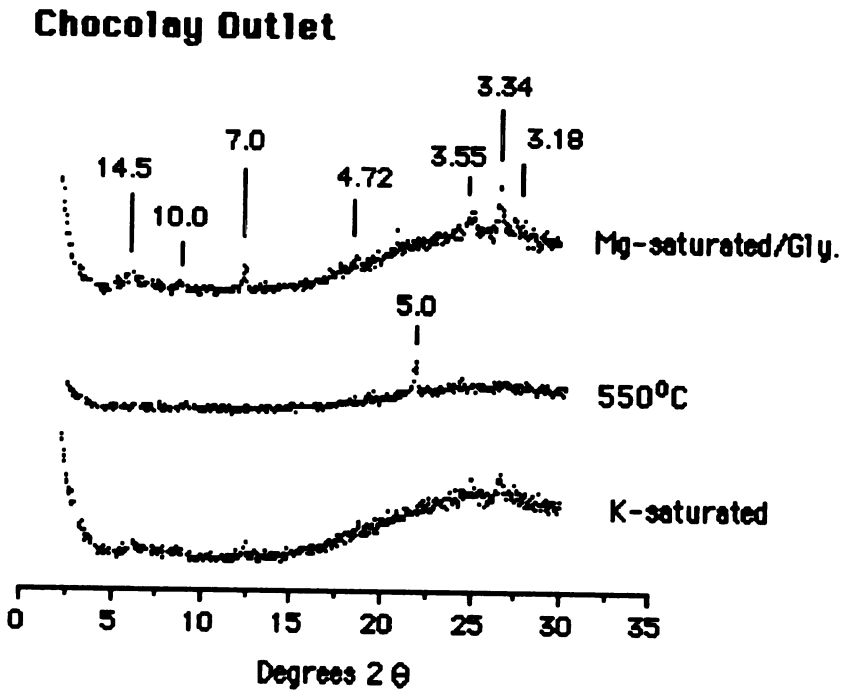
Chocolay Outlet
3.34
7.0
3.18
14.5
3.55
4.72
10.0
Mg-saturated/Gly.
5.0
550°C
K-saturated
0
5
10
15
20
25
30
35
Degrees 2θ

Cherry Creek

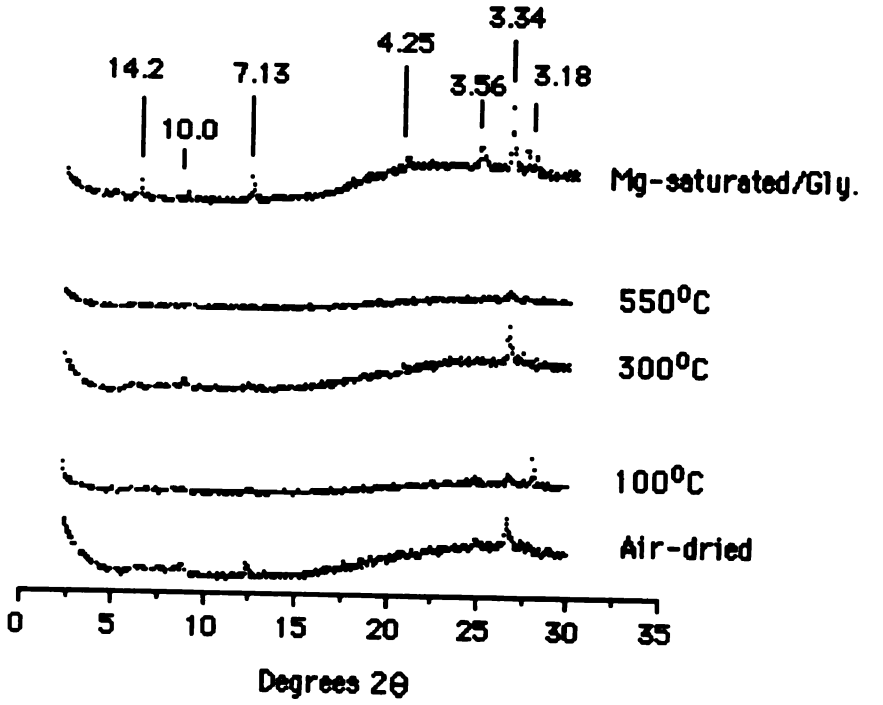

Goose Lake Tel iron removal

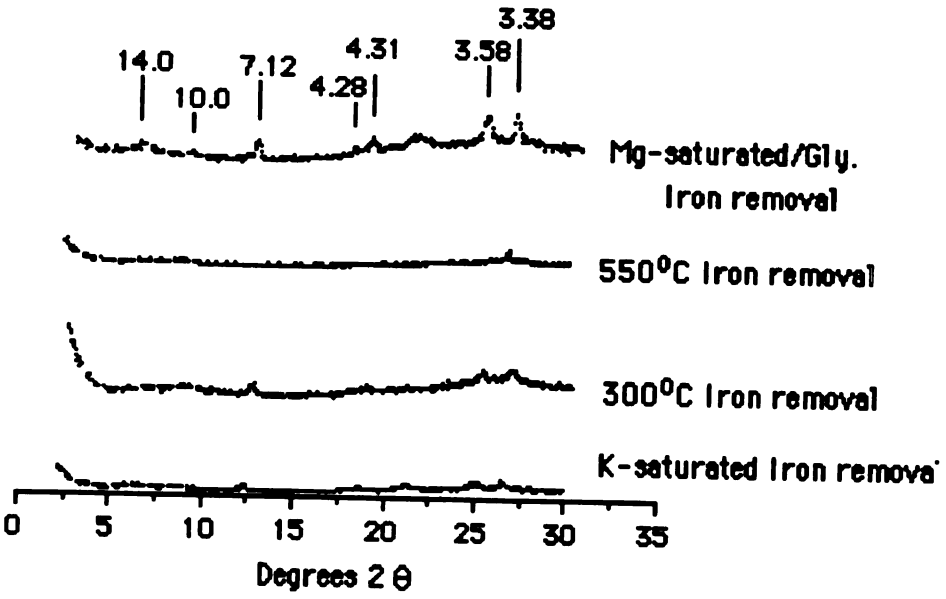

Silver Creek Midsection

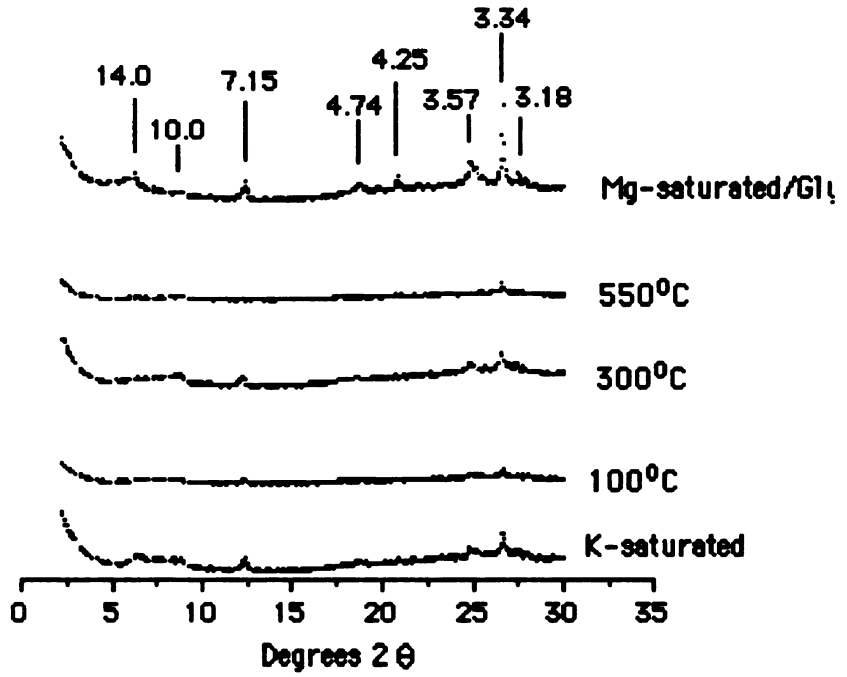

Silver Creek Mouth

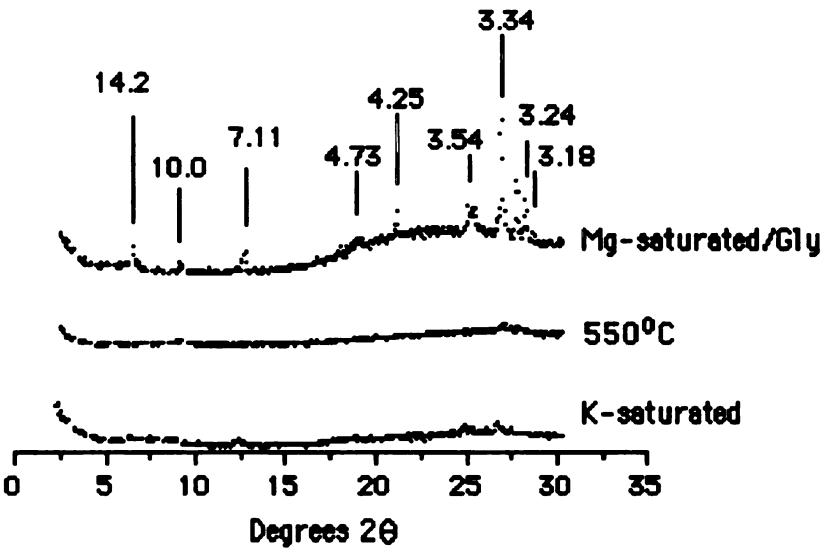

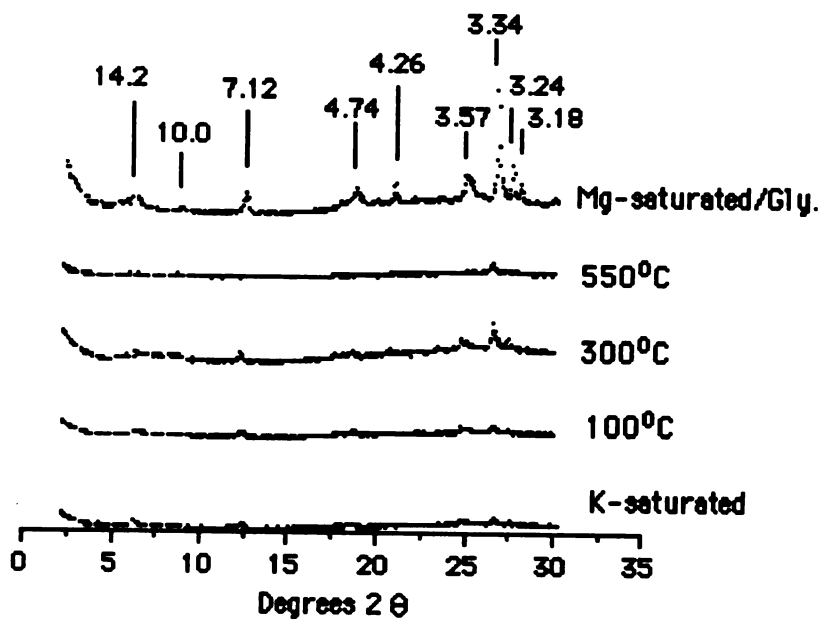
Strawberry Lake
14.2
10.0
7.12
4.74
4.26
3.57
3.34
3.24
3.18
Mg-saturated/Gly.
550°C
300°C
100°C
K-saturated
0
5
10
15
20
25
30
35
Degrees 2 θ